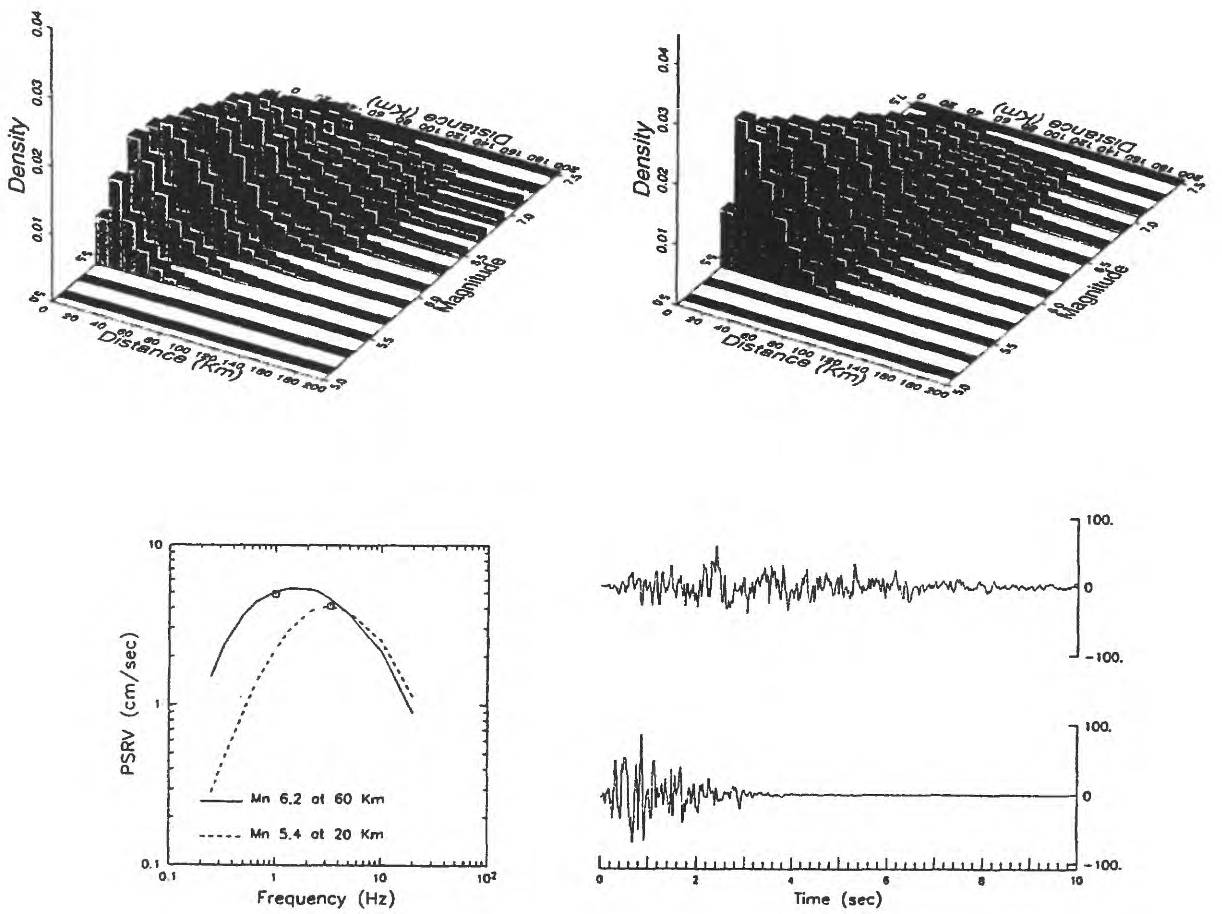

Figure 5. (*Upper*) Magnitude-distance probability density for 10% probability of exceedance in 50 years at Richmond, Virginia: *Left*: 1.0 Hz PSRV, 4.9 cm/sec from a M_N = 6.2 earthquake at a distance of 60 km; *Right*: 3.3 Hz PSRV, 4.1 cm/sec from a M_N = 5.4 earthquake at 20 km. (*Bottom Left*) Smoothed response spectra for a M_N = 6.2 earthquake at a distance of 60 km (solid) and a M_N = 5.4 earthquake at a distance of 20 km (dashed). (*Bottom Right*) Acceleration time series (cm/sec^2) for a M_N = 6.2 earthquake at a distance of 60 km (upper) and a M_N = 5.4 earthquake at a distance of 20 km (lower).

The Eastern Tennessee Seismic Zone:

Virginia Tech and UNC have been awarded a grant by the U. S. Nuclear Regulatory Commission to study the seismicity of eastern Tennessee (Figure 1). An objective of this study is the compilation and organization of over 7000 P and S wave arrival times from over 300 earthquakes which will then be used in a joint inversion for hypocenter location and velocity structure. Additionally, focal mechanism solutions will be determined for most well recorded earthquakes in the area. The velocity structure within the seismogenic region, earthquake locations, and orientation of fault planes, as well as other existing geophysical elements (e.g., potential field data, seismic lines, etc.) will be critically examined in an effort to develop plausible tectonic models for the seismic zone.

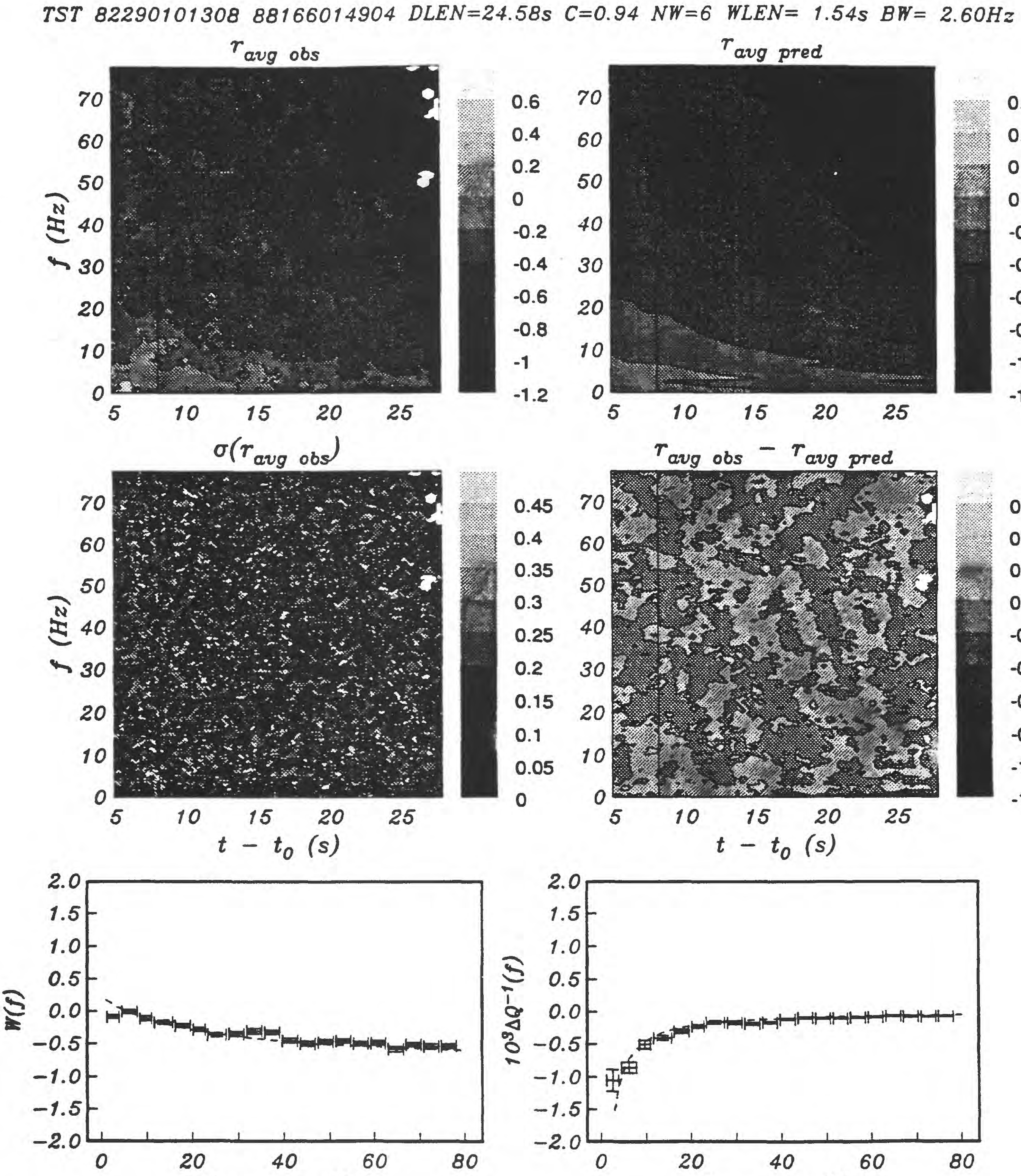

Figure 2a. Synthetic example illustrating the inversion of moving-window log spectral ratio data for the log source spectral ratio, $W(f)$, and the apparent change in inverse coda Q, $\Delta Q^{-1}(f)$. The dashed lines on the $W(f)$ and $\Delta Q^{-1}(f)$ plots are theoretical values. Error bars are 68.3% confidence intervals. Figure shows the observed spectral ratio (upper left) and its standard deviations (lower right); the spectral ratio predicted by the model (upper right); the residual (lower right); and the model parameters (bottom). The title shows the data length used (DLEN), the broadband crosscorrelation (C), the number of multitaper windows used (NW), the length of the moving 75% overlap time windows (WLEN), and the spectral bandwidth (BW).

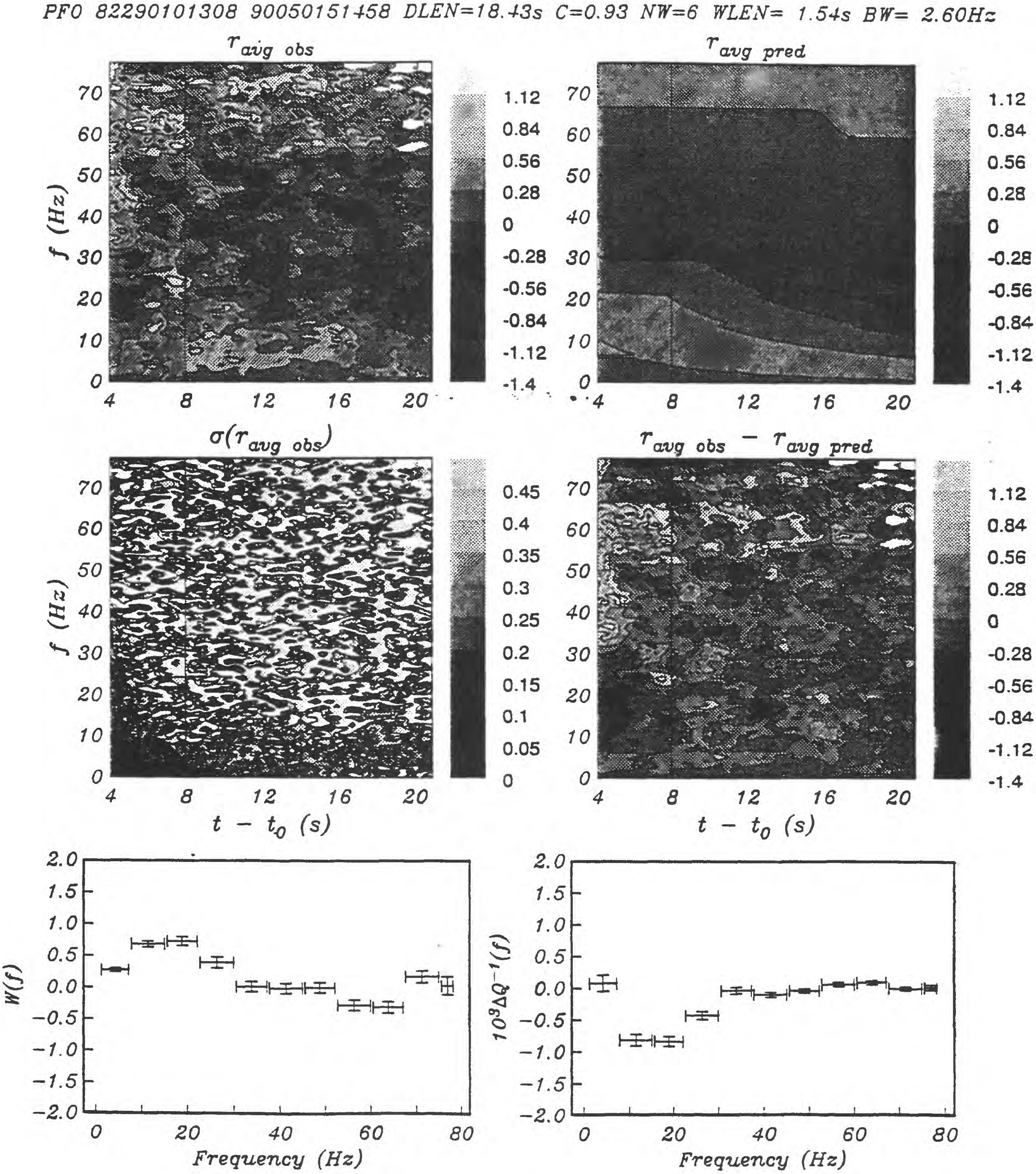

Figure 2b. Anza network example illustrating the inversion of moving-window log spectral ratio data for the log source spectral ratio, $W(f)$, and the apparent change in inverse coda Q, $\Delta Q^{-1}(f)$. As with Figure 2a, modeling is performed at times greater than twice the shear-wave arrival time, shown by the vertical line. Low signal-to-noise data (white regions) is not used in the parameter determination.

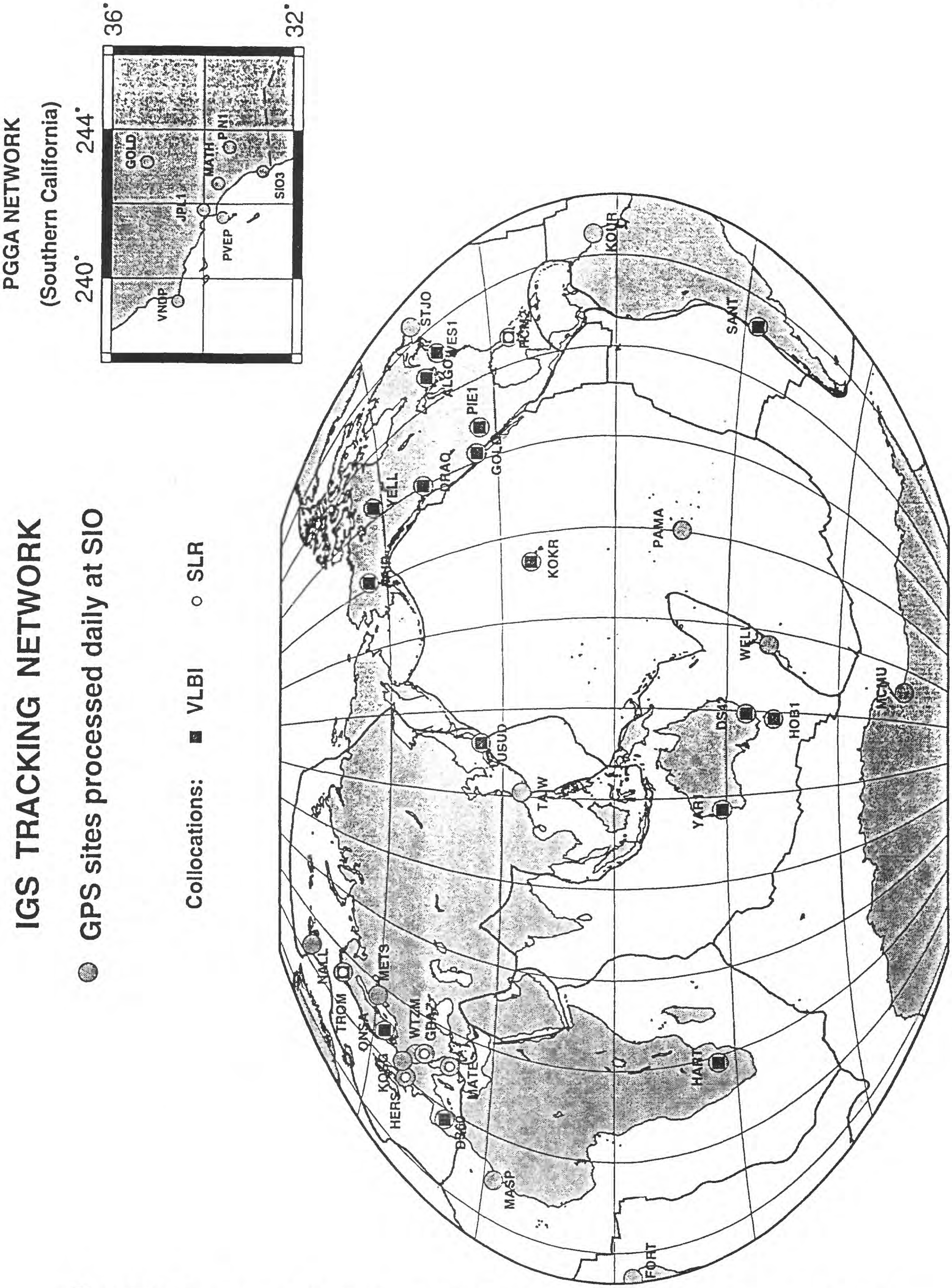

Figure 1: The current distribution of the tracking stations of the International GPS Service for Geodynamics and the PGGA sites in southern California.

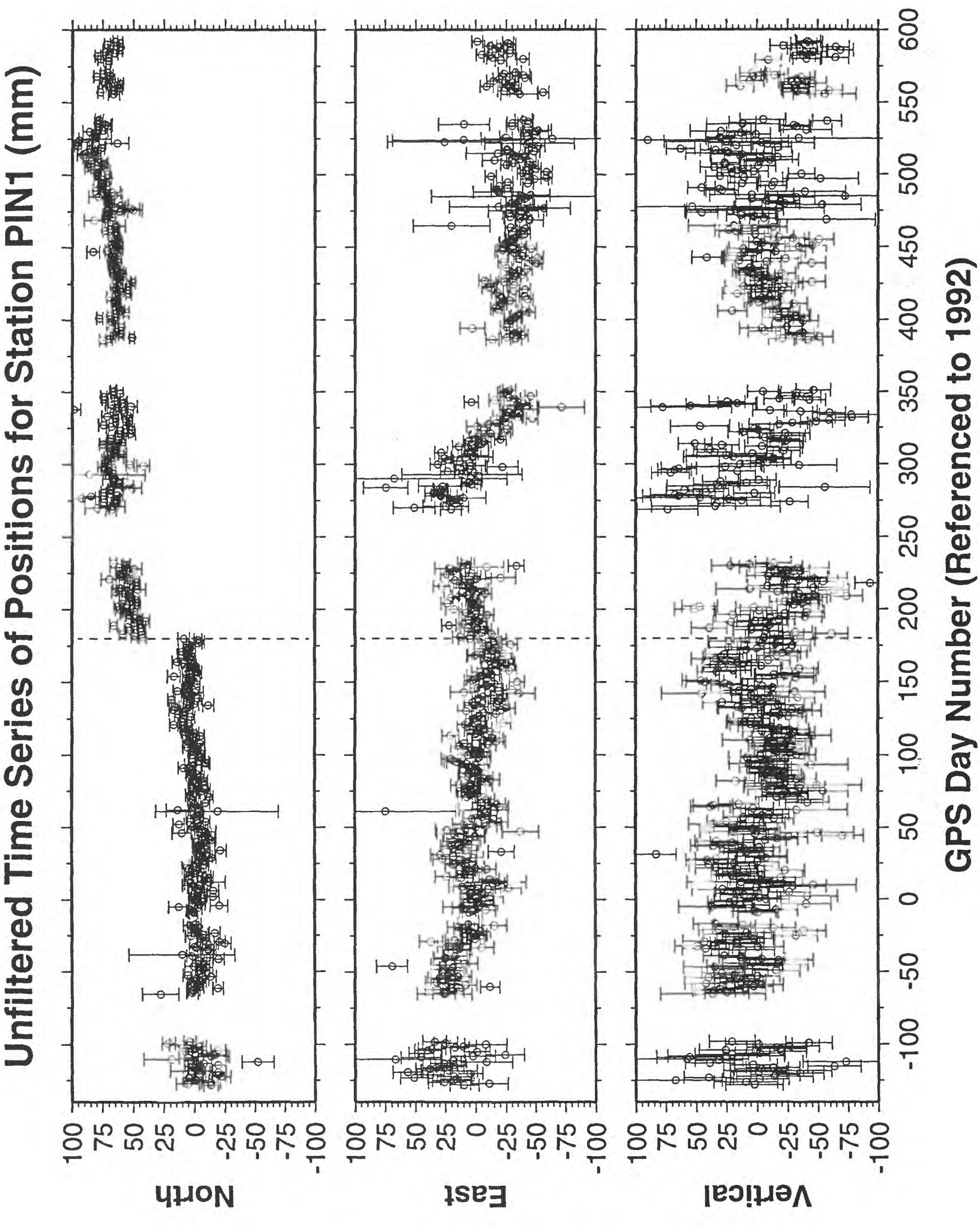
Unfiltered Time Series of Positions for Station PIN1 (mm)
North
East
Vertical
100
75
50
25
0
-25
-50
-75
-100
-100
-50
0
50
100
150
200
250
300
350
400
450
500
550
600
GPS Day Number (Referenced to 1992)

Figure 2

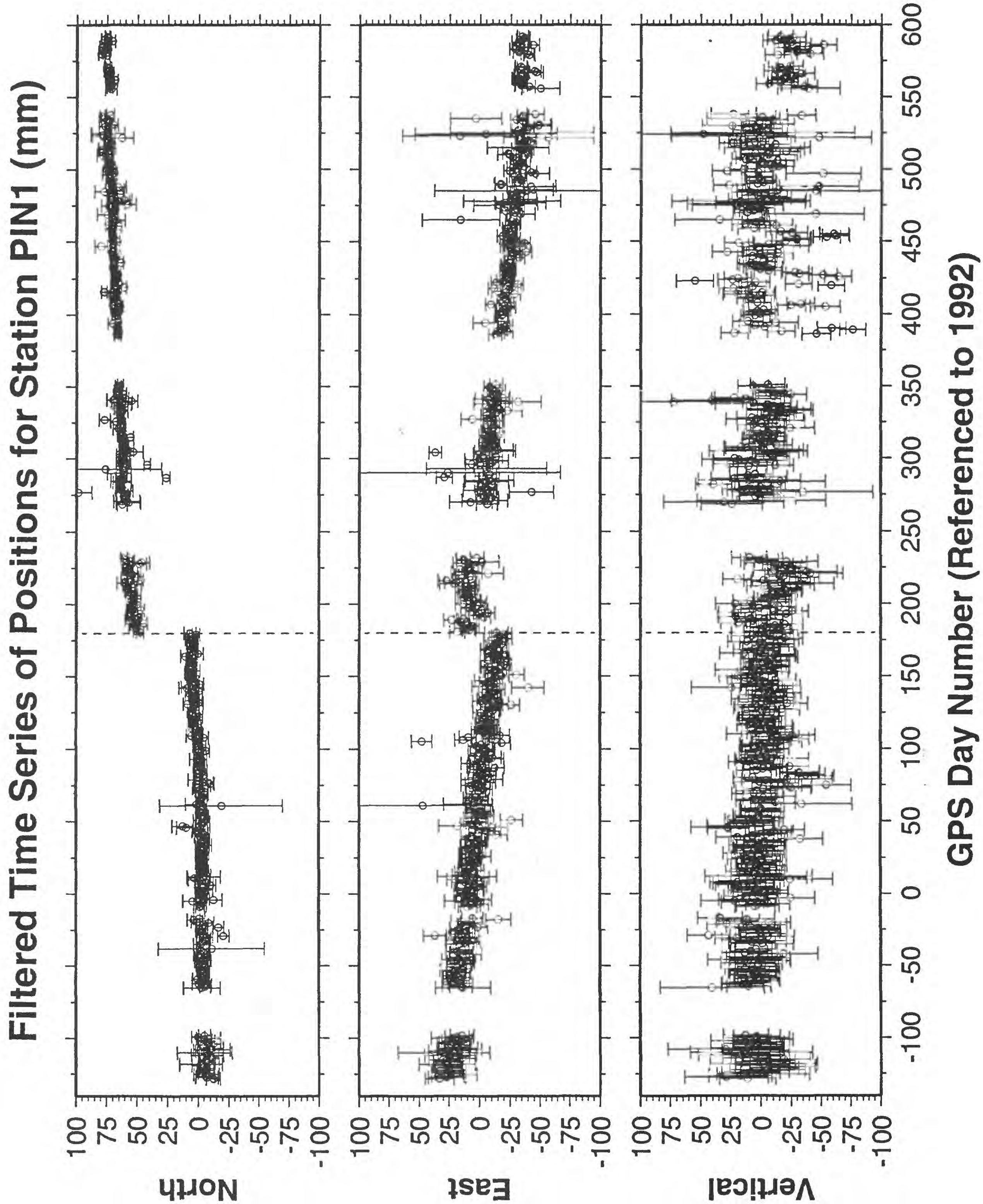
Filtered Time Series of Positions for Station PIN1 (mm)
North
East
Vertical
100 75 50 25 0 -25 -50 -75 -100
-100 -50 0 50 100 150 200 250 300 350 400 450 500 550 600
GPS Day Number (Referenced to 1992)

Figure 3

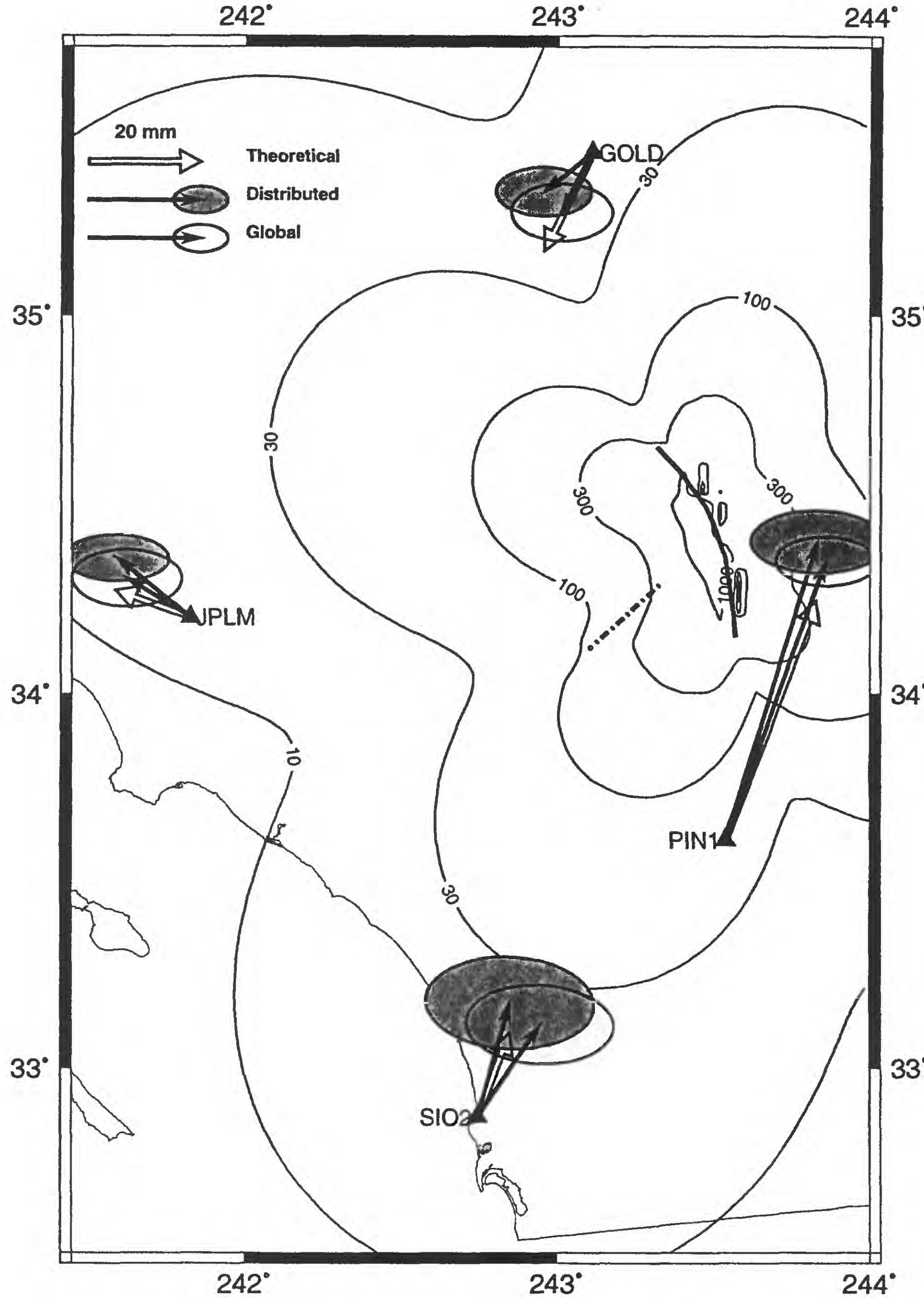

Figure 5. Observed (solid arrows) and modeled (blank arrows) displacements at four of the PGGA stations in southern California due to the Landers and Big Bear earthquakes of 28 June 1992. We show the displacements and 95% confidence ellipses computed processing the PGGA and IGS data in a simultaneous global solution (unshaded ellipses) and using the distributed processing approach explained in the text (shaded ellipses). The observed displacements are with respect to a global reference frame and, therefore, indicate absolute displacements of the California sites. The contours of displacement magnitude and the computed displacements are based on an elastic halfspace assumption for the behavior of the Earth's crust (all units mm). The surface trace of the Landers rupture is indicated by a heavy line and for the Big Bear earthquake by a dashed line.

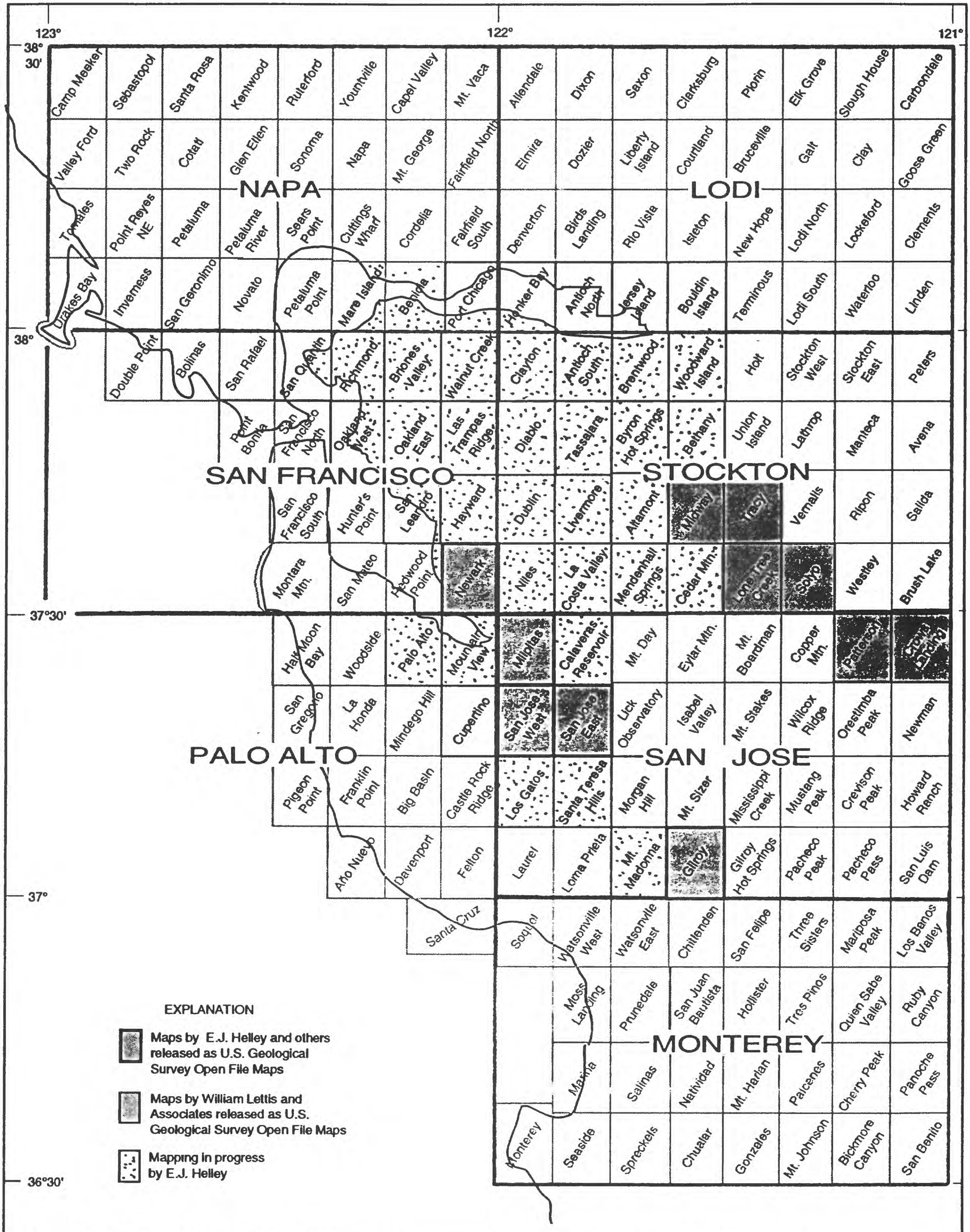

Fig. 1 Index map showing recent mapping of Quaternary deposits in the southern San Francisco Bay Region

faults. Ultra-high resolution seismic reflection profiles reveal an astonishing number of faults cutting Holocene sediments. In related work, Ed Helley, John Fitzpatrick and Jim Bischoff have dated oyster shells from terrace deposits at three localities on the shore of San Pablo Bay and one near Benicia. The dates range from 112 to 142 Kyrs, suggesting that the oysters were deposited during Sangamon time. The distribution and age of the oyster beds also suggest that the area from southern San Pablo Bay to Benicia has not undergone vertical deformation since the Sangamon.

USGS volunteers Larry Dickerson, John Parker, Mary Bowen and Neil Foley along with Ed Helley, Dick Pike, Conyn Criley and Earl Brabb have copied and organized approximately 50,000 logs of water wells in Santa Clara, San Mateo and San Francisco Counties in an attempt to determine the character of surficial materials around San Francisco Bay. The logs were obtained from the California department of Water Resources, Sacramento, and the Santa Clara Valley Water District in San Jose. Additional data in digital form were provided by John Fio, U.S. Geological Survey Water Resources Division, Sacramento. These data complement a similar task of digitizing water wells in Alameda and Contra Costa Counties underway by Rogers/Pacific under a NEHERP contract monitored by Tom Holzer. Knowledge of the engineering character of the surficial deposits described in the logs will help assess ground shaking and liquefaction during earthquakes.

USGS volunteer Walter Hensolt has completed a map showing the elevation of bedrock beneath the surficial deposits around San Francisco Bay from Golden Gate south to Coyote. The map is being edited for release in Open Files.

USGS volunteers and previous NEHRP recipients David Jones and Russ Graymer have completed a geologic map of the Niles 7.5' quadrangle showing the Mission fault in relation to several newly mapped faults from Mission San Jose to Tolman Peak. The map is being edited for release in Open Files.The map is one of the building blocks for redefining the regional structure between the Hayward, Calaveras and Greenville faults.A schematic structure section prepared by D.L. Jones for the area from the Berkeley Hills to Mount Diablo, 30 km north of Niles, is provided in Figure 2.

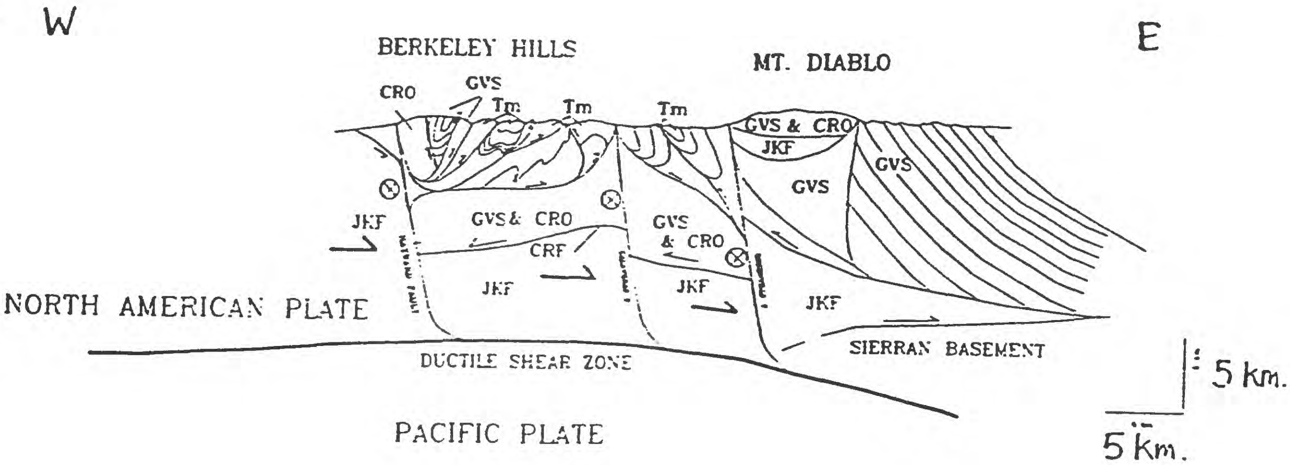

Figure 2- Schematic structure section through the East Bay hills. JKF, Franciscan complex; GVS, Great Valley sequence; CRO, Coast Range ophiolite; Tm, marine sedimentary rocks of Miocene age; CRF, Coast Range fault. From Jones (1992).

Digital compilation of new and existing geologic maps by Carl Wentworth and Chad Nelson continues to interact with the development of ALACARTE and needed digital procedures. The user interface ALACARTE for controlling the commercial geographic system ARC/INFO (Fitzgibbon and Wentworth, 1991) has been extensively revised to work with ARC 6, with the ability to hold menus open on-screen and work with both vector and raster data. The ALACARTE code can be obtained over internet from anonymous ftp sierra (130.118.4.116; look first at the most recent ALACARTE README).

Earthquake import and cross-section routines are being incorporated into ALACARTE and have been used under our guidance by Steve Walter (USGS, Menlo Park) to prepare a seismicity map for the San Jose, California 1x2 degree sheet in ARC/INFO showing earthquakes by magnitude (dot size) and depth (dot color), with focal-mechanism beachballs for larger events colored and scaled to fit the dot. Cross sections include distinguishing cluster grouping by color. This work also involves experimental (and successful) use of a raster base through the ARC module GRID (rather than the vector format now in general use in our work in ARC/INFO). Code is also in hand to allow projection of earthquakes along azimuths specified separately by earthquake or groups of earthquakes, which will permit making cross sections that include earthquakes from faults having different strikes (assign the projection azimuth to the earthquakes as a function of strike, rather than selecting an azimuth for the cross section as a function of strike).

Methods for compiling and storing data in ARC/INFO related to the Peninsula candidate site for deep San Andreas drilling are largely in hand and disk space has been obtained and installed. Experimental plotting routines exist that can be modified to fit database content.

A digital map database of the distribution of geologic materials in the southern San Francisco Bay region has been completed and submitted for open-file realease. This has been compiled at a scale of 1:125,000 from three 1970's compilations: Brabb, geologic map of Santa Cruz County, 1989; Ellen and Wentworth, hillside materials, in press; and Helley and Lajoie, flatland materials, 1979. The database consists of lines (contacts, faults, and various other boundaries) and identities of the intervening areas (polygons, identified by unit label of the source map, stratigraphic unit reported in the source, and general age and lithology). Release will be in two parts, a short text describing the database and how to obtain it, and a compressed tar file (ssfb_ml.tar.Z) of the database in ARC coverage format that can be obtained over internet from anonymous ftp on sierra (130.118.4.116) or by sending a magnetic tape to Wentworth (1/4 inch 150 MB cartridge or 8mm 2.3 or 5.0 Exabyte).

Work has begun using the San Francisco Bay region database to extend the work of Borcherdt, Wentworth, and others (1991) to a map of the whole south Bay region showing excedent potential for intensity of a 1906 earthquake on the San Andreas fault. Base intensities (on Franciscan rock) are determined using an attenuation function and the GIS buffer function to generate contours. These are so sensitive to the position and shape of the fault that use of a smoothed version of the source fault may yield misleading results near the fault and, thus, decisions must be made concerning which surface trace(s) to use and how to simplify the contours with increasing distance from the fault.

ALACARTE skills were used by Chad Nelsen to help Bob McLaughlin assemble a geologic map of the Loma Prieta, Laurel, Los Gatos and Santa Teresa Hills 7.5' quadrangles for the Loma Prieta Earthquake Professional Paper. One challenging task was to digitally contort the geology from an obsolete and geographically incorrect base map so that it would mesh with the other data.

Compilation and analysis of the bedrock geology for Contra Costa and Alameda Counties is in progress by Russ Graymer, Dave Jones, and Earl Brabb. Linework for Contra Costa is nearly complete. Linework for Alameda County is about 50 Percent complete.

REPORTS

Brabb, E.E., compiler, 1993, Preliminary geologic map of the onshore part of the Palo Alto 1:100,000 quadrangle, California: U.S. Geological Survey Open File Report 93-271, map scale 1:62,500.

Helley, E.J., 1990, Preliminary contour map showing elevation of surface of Pleistocene alluvium under Santa Clara Valley, California: U.S. Geological Survey Open-File Report 90-633.

Helley, E.J., Fitzpatrick, J.A., and Bischoff, J.L., 1993, Uranium-series dates on oyster shells from marine terraces of San Pablo Bay, California: U.S. Geological Survey Open File Report 93-286, 6 p.

Jones, D.L., 1992, Tectonics of a transpressive plate boundary: a new parodigm for the central California Coast Ranges: Northern California Geological Society Field Trip Guidebook to Late Cenozoic geology in the north Bay region, p. 33.

Jones, D.L., and Graymer, R.W., 1993, Structural significance of quaternary imbricate thrust faults in the East Bay hills south of Hayward, central California Coast Ranges: American Geophysical Union 1993 Fall Meeting, Abstract Supplement, p. 608.

Noller, J.S., Sowers, J.M., and Lettis, W.R., 1993, Preliminary maps showing Quaternary geology of the Solyo and Lone Tree Creek 7.5-minute quadrangles, California: U.S. Geological Survey Open File Report 93-224, map scale 1:24,000.

Sowers, J.M., Noller, J.S., and Lettis, W.R., 1993, Preliminary maps showing Quaternary geology of the Patterson and Crows Landing 7.5-minute quadrangles, California: U.S. Geological Survey Open File Report 93-223, map scale 1:24,000.

Sowers, J.M., Noller, J.S., and Lettis, W.R., 1993, Preliminary maps showing Quaternary geology of the Tracy and Midway 7.5-minute quadrangles, California: U.S. Geological Survey Open File Report 93-225, map scale 1:24,000.

Wang, C. Y., Cai, Y. and Jones, D. L., 1993, Stresses and block deformation in the greater San Francisco Bay area: American Geophysical Union 1993 Fall Meeting, Abstract Supplement p. 608.

Weber, J., Jones, D.L., and McEvilly, T.V., 1993, Tectonic wedges and blocks at the eastern margin of the Coast Ranges, Sacramento delta region, California: American Geophysical Union 1993 Fall Meeting, Abstract Supplement p. 609.

ANALYSIS OF WIDE-ANGLE REFLECTION/REFRACTION RECORDINGS FROM THE BAY AREA SEISMIC IMAGING EXPERIMENT (BASIX)

Seismic Reflection Crustal Studies Project: Project No. 9930-12253

T. Brocher
OEVE, Branch of Seismology
U. S. Geological Survey
345 Middlefield Road, MS/977
Menlo Park, California 94025
Telephone: (415) 329-4737
brocher@andreas.wr.usgs.gov

INVESTIGATIONS UNDERTAKEN

BASIX attempted to image the subsurface geometry of the crust in the vicinity of the major earthquake producing faults in the San Francisco Bay Area using seismic reflection and refraction methods. BASIX obtained seismic reflection lines designed to provide a picture of the crust down to the base of the crust using a large airgun source and receivers moored to buoys in the water. At the same time, temporary seismic recorders were deployed throughout the Bay Area (see Figure 1) to record these airgun signals at large distances (wide-angles).

I have analyzed wide-angle seismic data recorded by five-day and CALNET stations during the BASIX experiment. The analysis of these records has included forward modeling and inversion of travel times.

RESULTS

My work has provided preliminary velocity and structural models for the Bay Area in the following areas: 1) the block beneath SF Bay between the San Andreas and Hayward faults, 2) the San Andreas fault in the vicinity of the Golden Gate, and 3) the crust beneath the East Bay faults between the San Andreas fault and the Great Valley.

San Francisco and San Pablo Bays

My most important finding is that San Pablo and San Francisco Bays are underlain by a prominent mid-crustal reflector at a depth of about 16-18 km (Figure 2). This reflector can be mapped from nearly the San Andreas fault to east of the Hayward fault, and may serve to couple the motions of these two faults, explaining the apparent pairing of large magnitude earthquakes that have occured on the San Andreas and Hayward faults (Kerr, 1993). The reflector represents the top of a high-velocity (velocity about 7 km/s) mafic layer (Figure 3). The identity of the mafic layer is uncertain; it could represent a slab of subducted oceanic crust or a magmatically underplated unit. For reasons given below, we believe that at least the western half of the reflector originates from the top of a slab of oceanic crust.

The block bounded by the San Andreas and Hayward faults has only a thin 100-200 m sediment cover on the Franciscan basement rocks. Based on the relatively low-velocities within the crust, Franciscan rocks are thought to extend to a depth of about 16-18 km (Figure 3).

The crustal thickness underneath the bay is thought to be about 25-27 km. Near-vertical reflections from 9 s two-way travel time suggest that the crust is about 27 km thick.

San Andreas Fault

BASIX line 202 crosses the San Andreas fault in the vicinity of the Golden Gate. Prominent reflections from this line define an east dipping slab about 5 km thick which I am currently interpreting as a slab of oceanic crust (Figure 4). This oceanic slab extends to the east of the San Andreas fault and either flattens or is intersected by a west dipping slab of mafic lower crust, possibly representing the pre-Jurassic oceanic crust which floors the Great Valley. The depth to the top of the slab of oceanic crust beneath the fault is in close agreement with the maximum depth of earthquakes found along the fault in this location, and coupled with our previous work on the crustal structure in the vicinity of the Loma Prieta earthquake, suggests that the depth of the slab of oceanic crust may exert some control on the maximum depth of earthquakes found along the San Andreas fault on the San Francisco peninsula between San Francisco and Santa Cruz (Figure 5).

East Bay Faults and Crust

The Hayward and Rodgers Creek faults bound a 1.5 km deep basin filled with low velocity (2 km/s) sedimentary rocks. The Green Valley fault is also associated with a vertical offset of about 600 m, with the sense of motion being down to the east. From west to east between the Hayward to the Antioch faults, the top of the Franciscan plunges eastwards beneath younger sedimentary rocks to about 3 km depth (Figure 6). Velocities of the rocks to a depth of about 10 km are constrained by reversed Pg arrivals.

Unreversed Pn arrivals recorded by stations located in the Sierran foothills and eastern Great Valley suggest that the crust thins in the vicinity of the Antioch fault to about 24 km (Figure 6). Alternatively, these data, as well as compilations of previous refraction/reflection experiments by Fuis and Mooney (1990), suggest that the crust thickens towards the Coast Range and towards the Sierras. The crustal thinning occurs in the vicinity of deep seismicity near Antioch, and the depth to the base of seismicity can be traced to nearly the Moho near Antioch.

Reports Published

Brocher, T. M., M.J. Moses, and S.D. Lewis, Evidence for oceanic crust beneath the continental margin west of the San Andreas fault based on onshore-offshore wide-angle seismic recordings, U. S. Geological Survey Professional Paper on Loma Prieta, Vol. 1., in press, 1994.

Brocher, T.M., and M.J. Moses, Onshore-offshore wide-angle seismic recordings of the San Francisco Bay Area Seismic Imaging Experiment (BASIX): The five-day recorder data, U. S. Geological Survey Open-file Report, 93-276, 89 p., 1993.

Brocher, T.M., and D.C. Pope, Onshore-offshore wide-angle seismic recordings of the San Francisco Bay Area Seismic Imaging Experiment (BASIX): The CALNET data, U. S. Geological Survey Open-file Report, in preparation.

Page, B.M., and Brocher, T.M., Thrusting of the central California margin over the edge of the Pacific plate during the transform regime, Geology, v. 21, p. 635-638, 1993.

Kerr, R.A., Finding a piece of a California jigsaw puzzle, Science, v. 262, p. 993, 1993.

Abstracts Published

Brocher, T.M., Seismogenic and potentially seismogenic structures imaged by wide-angle onshore-offshore seismic profiling of the western margin of North America, EOS Trans. AGU, Supplement, 74, 431, 1993.

Brocher, T.M., W.S. Holbrook, U.S. ten Brink, J.A. Hole, and S.L. Klemperer, Results from wide-angle seismic reflection and refraction profiling of the San Francisco Bay Area during BASIX, Geol. Soc. Amer. Abstr. with Programs, National Meeting, v. 25, no. 6, A-310, 1993.

Hole, J.A., S.L. Klemperer, T.M. Brocher, W.S. Holbrook, and U.S. ten Brink, Data and results from BASIX wide-angle seismic reflection and refraction in the San Francisco Bay Area, Geol. Soc. Amer. Abstr. with Programs, National Meeting, v. 25, no. 6, A-418, 1993.

Hole, J.A., W.S. Holbrook, S.L. Klemperer, U.S. ten Brink, and T.M. Brocher, Crustal structure beneath San Francisco Bay and across the Bay Area faults from wide-angle seismic reflection data, EOS Trans. AGU, Supplement, 74, 445, 1993.

Pope, D.C., T.M. Brocher, J. McCarthy, E.D. Karageorgi, and W.S. Holbrook, Comparison of recording technology for onshore-offshore seismic profiling of continental margins: Examples from BASIX, EOS Trans. AGU, Supplement, 74, 445, 1993.

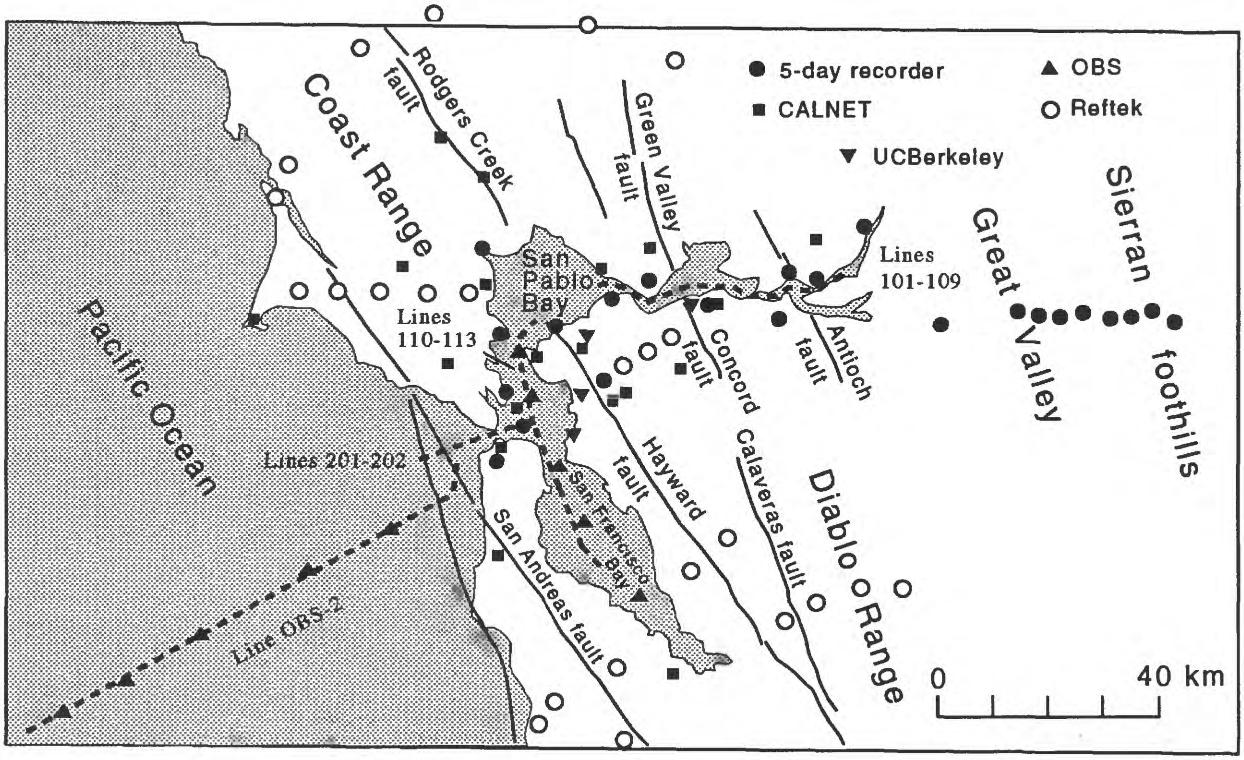

Figure 1. BASIX seismic reflection lines (dashed lines) and wide-angle recorders (various symbols).

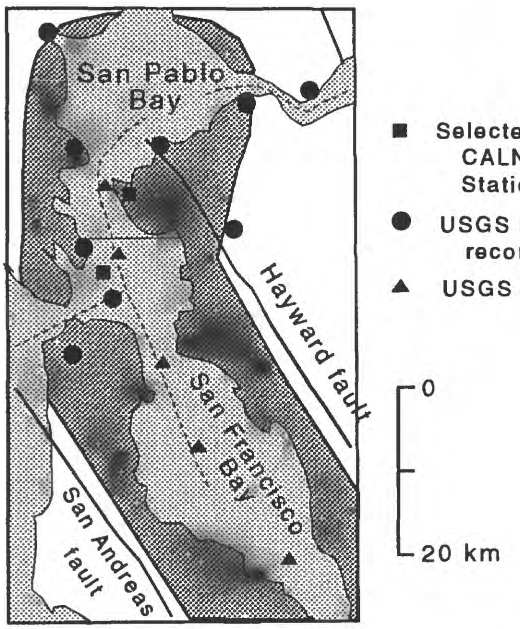

Figure 2. Map showing in dark shading the minimum geographic extent of subhorizontal mid-crustal reflections between 6 and 8 seconds two-way travel time. Reflection extents are defined by stations shown (symbols defined on side panel) from shots recorded from the BASIX lines (dashed lines).

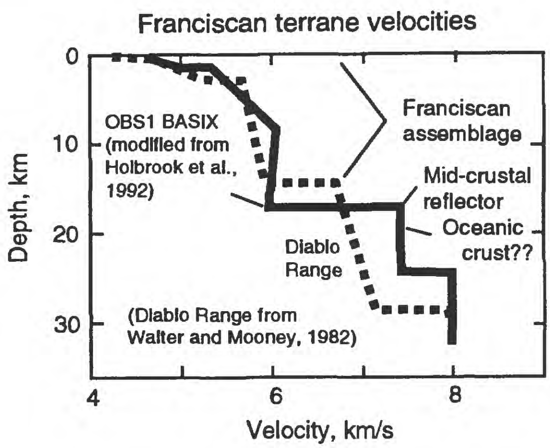

Figure 3. One-dimensional velocity models obtained by Holbrook et al. (1992) and Walter and Mooney (1982) showing relatively small differenceabove 15 km. Note the presence of a high-velocity layer (7 km/s) beneath the Franciscan assemblage which we believe produces the prominent mid-crustal reflection observed at 6 seconds two-way travel time (about 18 km depth).

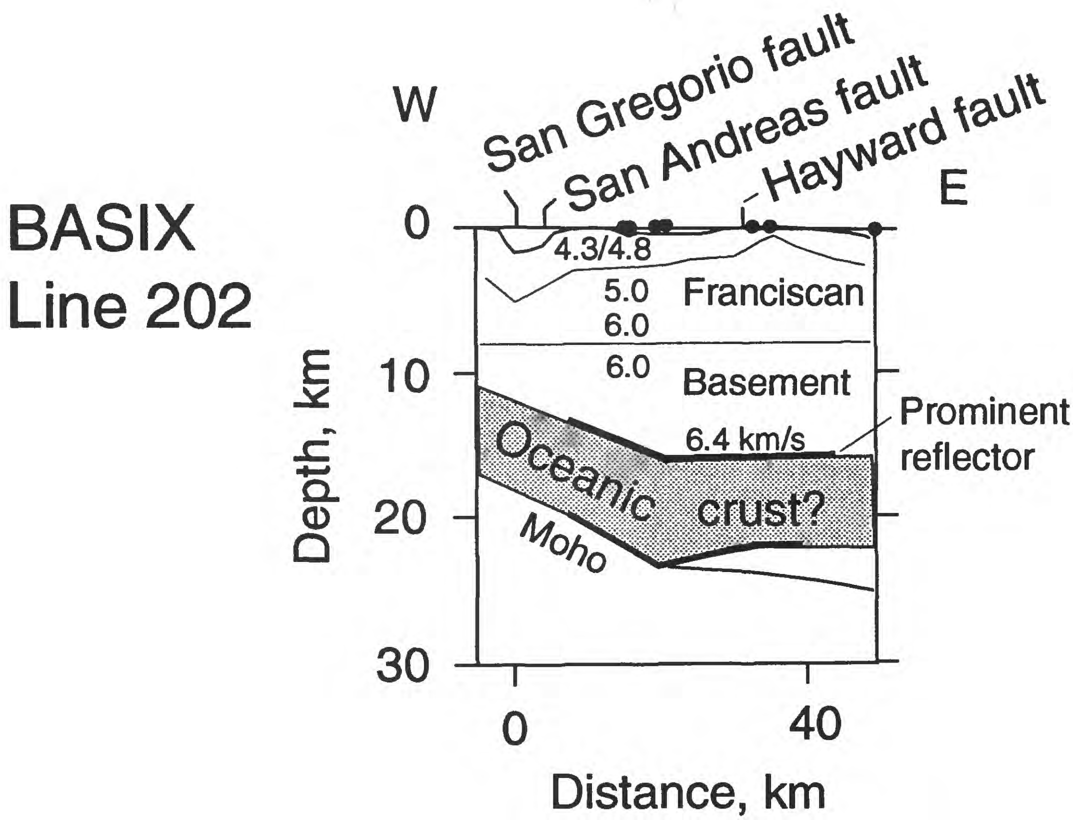

Figure 4. Preliminary velocity model for BASIX line 202, showing east dipping slab beneath San Andreas fault. We interpret this slab as a piece of oceanic crust, due to its dip and thickness, although we lack refracted arrivals within it, so its velocity is currently poorly known. The reflector shown in Figure 2 is labeled as a prominent reflector from the top of this slab.

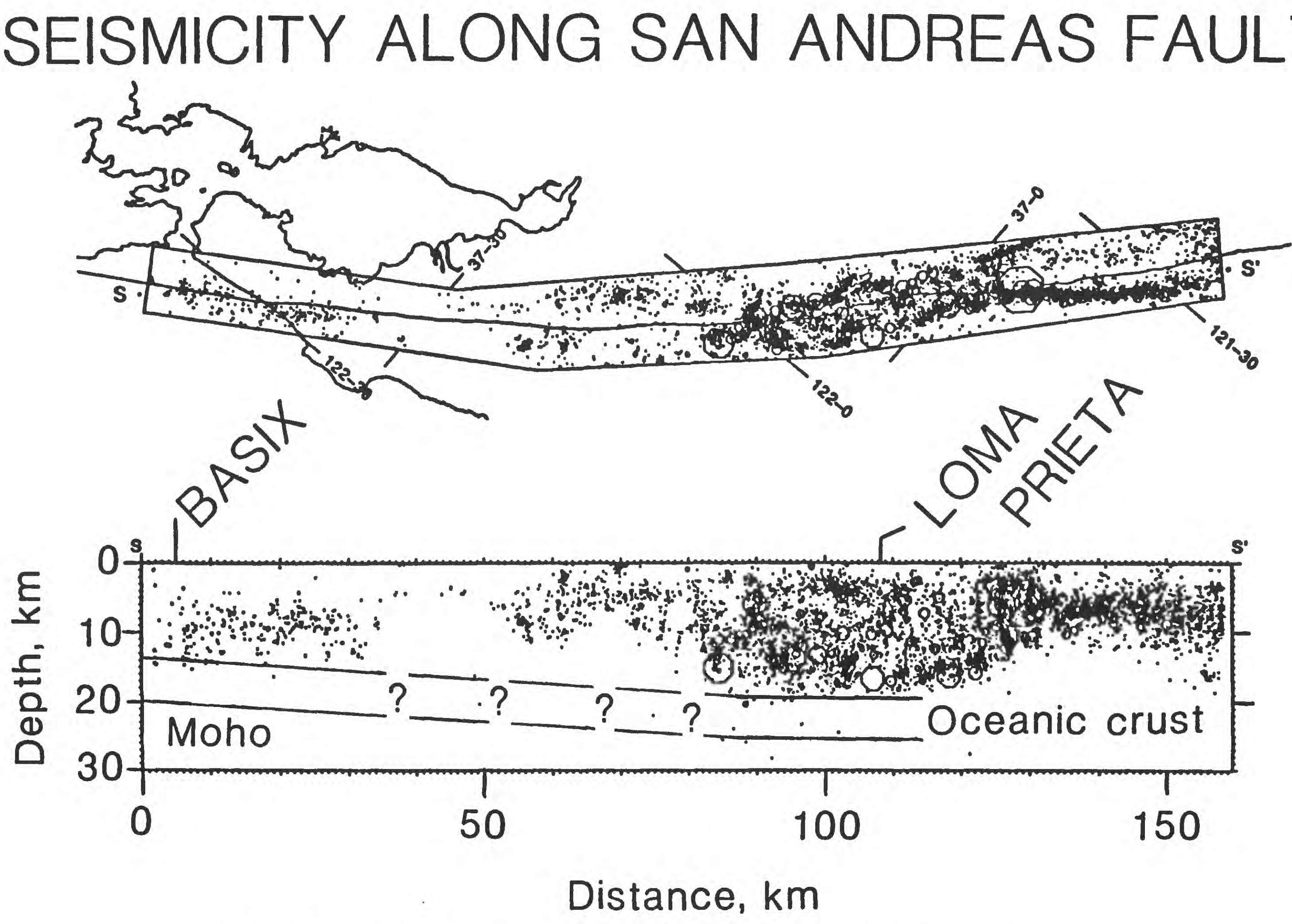

Figure 5. Seismicity along the San Andreas fault from Dietz (1992) on which we have superimposed location of slab of inferred oceanic crust determined from BASIX line 202 and from the vicinity of Loma Prieta (Page and Brocher, 1993). Note that in both cases the seismicity lies above the top of the inferred slab of oceanic crust.

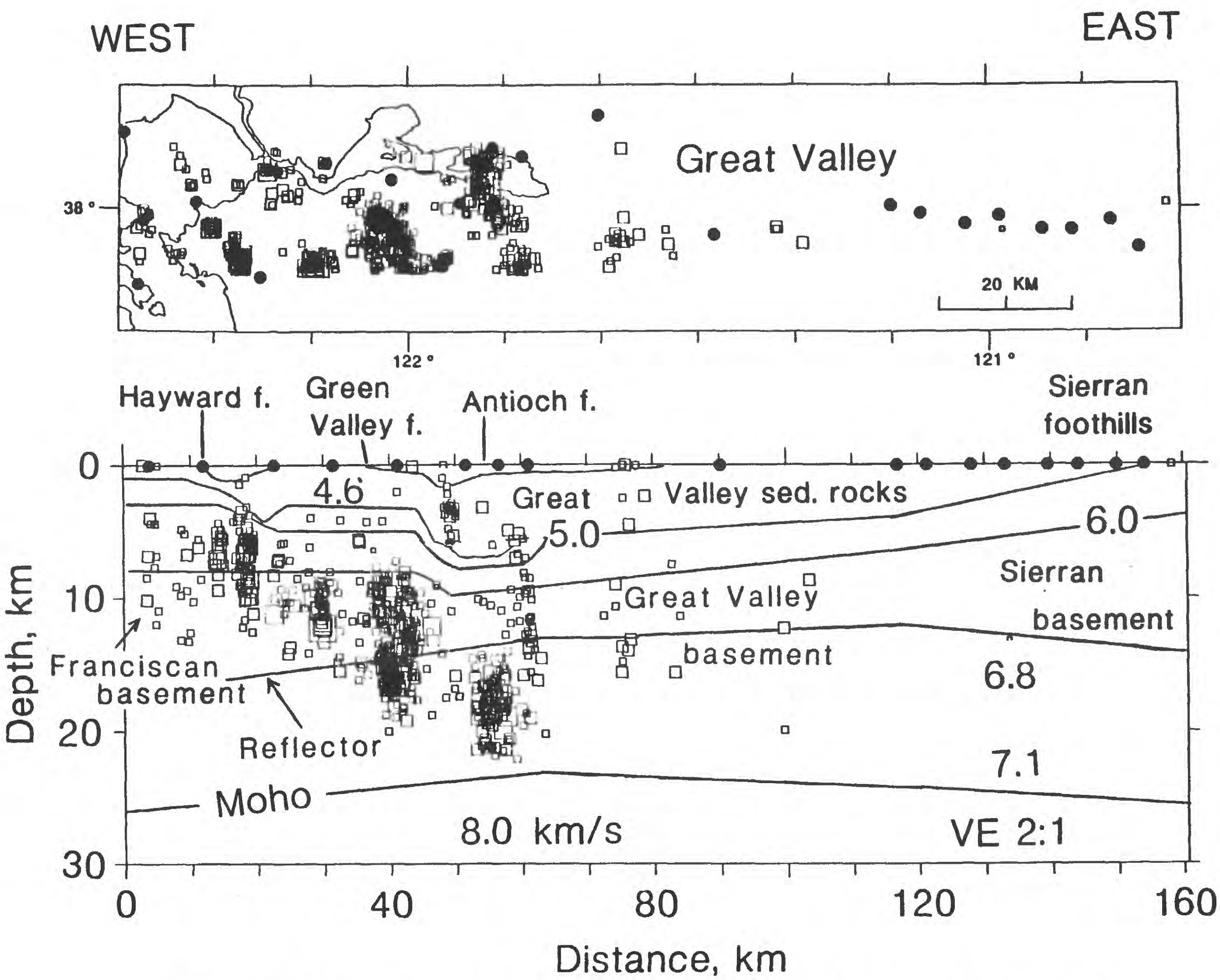

Figure 6. Preliminary velocity model for BASIX lines 101-109, showing generally thin crust beneath Bay Area and Great Valley, and that the maximum depth of seismicity (squares) increases eastward towards Antioch. BASIX wide-angle receivers (filled circles) are unreversed in the Great Valley and Sierran foothills, and the crustal structure for this region is largely from previous refraction work from these areas.

Northern San Andreas Fault System

9960-12326

Robert D. Brown
Branch of Earthquake Geology and Geophysics
U.S. Geological Survey
345 Middlefield Road, MS 977
Menlo Park, California 94025
(415) 329-5620
rbrown@isdmnl.wr.usgs.gov
Program Element II

Investigations

1. Synthesis studies of the geology, seismology, and tectonics of the San Andreas fault system, especially in northern California.

2. Advisory activities for Bay Area Regional Earthquake Preparedness Project (BAREPP) and San Francisco Bay Conservation and Development Commission (BCDC), both of which are state agencies. Similar, but intermittent and *ad hoc*, advisory activities for other state and federal agencies.

3. Research on applications of earth science-information, reviews of applications work by others, and interpretation of geologic and geophysical results for non-technical audiences.

Results

1. Completed a review of historical and field evidence concerning the location of the San Andreas fault near Shelter Cove, Humboldt County, California. This on-land location for the fault and the reported surface faulting there in 1906 have been challenged in a number of papers published since 1979. I examined archived field notes and other data from F.E. Matthes's 1906 investigation, notes from my own (1969) and M.G.Bonilla's (1965 and 1966) field work, pre-development aerial photographs, and published work by several other investigators. The evidence supports the interpretation reported in the Report of the State Earthquake Commission (Lawson, 1908): that the 1906 right-lateral strike-slip fault rupture

was expressed on land at Shelter Cove and that this rupture is a part of a major tectonic break, the San Andreas fault.

2. Compiled and analysed data on geologic structures from slide blocks and from underlying strata in the Lakes district of Point Reyes National Seashore. Steep dips and tight folding in the slide blocks contrast with low north dips below the slide plane. These relations are inconsistent with the simple rotational slope failures previously suggested as the cause of Lakes district landslides. They are consistent with failure on a northward-dipping thrust fault, reactivated in a retrogressive sense by uplift along the southwest side of the San Andreas fault. Northwestward movement, indicative of near-fault uplift, can be dated (by woody plants in basal lake deposits) at about 3400 yr BP. Lack of significant scarp degradation and the paucity of deltaic sediment in the landslide lakes characterizes most slide blocks and suggests a similar age for much of the 20 km^2 extensional terrane. Relative uplift of 0.3 to 0.6 m of was observed west of the fault at Bolinas in 1906. Although no mass movements were reported in the extensional area in 1906, uplift without major sliding may have occurred there: in beach exposures above the main thrust plane, scattered erosional remnants of iron-oxide-cemented beach gravels adhere to the base of seacliffs about 1 m above high tide level. Other evidence of oblique slip, with an uplifted block west of the (dominantly right-lateral, strike-slip) San Andreas fault occurs south of the Golden Gate on the northern San Francisco Peninsula.

3. Continued to participate in activities of BCDC's Engineering Criteria Review Board. BAREPP, however, was consolidated into the California Office of Emergency Services after its October, 1992, meeting, and at that time the BAREPP Advisory Board was dissolved. Reviewed plans, regulations, proposed legislation, and research proposals and projects for federal and state agencies, and industry or professional associations. Designed and directed preparation of an exhibit display on the San Andreas fault for a local non-profit association. Served as associate editor for Earthquakes and Volcanoes.

Reports

1. Brown, R. D., Wallace, R. E., Hill, D. P., 1992, The San Andreas fault system, California, U.S.A.: Annales Tectonicae, Special Issue, Supplement to v. VI, p. 261-284

PUGET SOUND PALEOSEISMICITY

9950-13175

Robert C. Bucknam
U.S. Geological Survey
M.S. 966, Box 25046
Denver, Colorado 80225
(303) 273-8566
bucknam@gldvxa.cr.usgs.gov

PROGRAM ELEMENT II

INVESTIGATIONS

The primary objective of this project is to document and characterize Holocene deformation in the Puget Sound, Washington, region and develop an understanding of its structural and tectonic origins. Work during the reporting period (October 1992-September 1993) focused on refining the extent and age of late Holocene uplift in central and southwest Puget Sound (Fig. 1) that has been inferred to have been the site of a large earthquake about 1000 years ago (Bucknam and others, 1992). An important component of the work is the paleoecological analysis of sites near sea level using fossils to infer changes in relative sea level during the late Holocene in the Puget Sound region. Plant macrofossil and pollen studies are being carried out by Estella Leopold at the University of Washington, assisted by Dan Ekblaw, Gengwu Liu, and Tracy Fuentes; diatom studies are being carried out by Eileen Hemphill-Haley, U.S. Geological Survey at the University of Oregon.

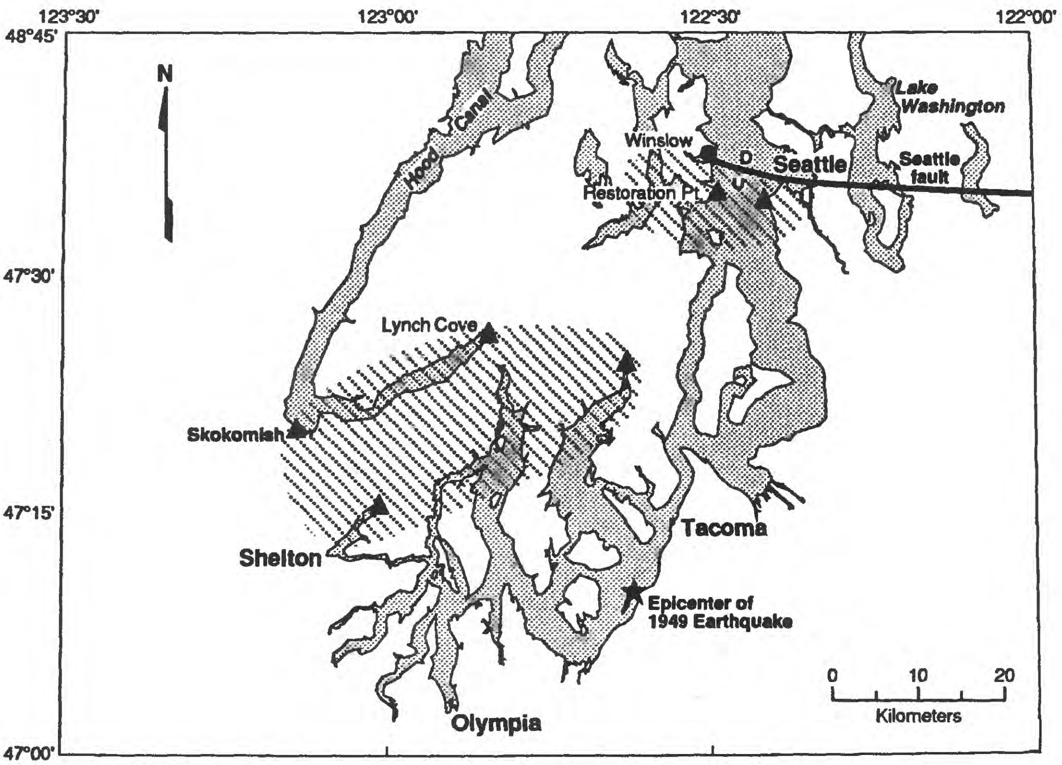

Figure 1. Diagonal ruling shows approximate extent, as presently known, of late Holocene uplift in central and southwest Puget Sound. Upward pointing arrows are sites with evidence of uplift; named sites are discussed in this report. Solid circles (Winslow) is site of several decimeters of subsidence.

case of 2 asperities in each subduction segment.

We show results for the space- and time-dependent deformation of the top of the upper plate, which might in some cases be accessible for geodetic measurements, as well as the area of the outer-rise, with its sometimes pronounced cycle-related seismicity. In particular, we observe the important influence of the presence of asperities on the cycle-related stressing and deformation. Figure 1a shows a single asperity along the thrust interface and Figures 1b and c show two cases of pairs of asperities. Figures 2a,b,c show contour plots of the the corresponding changes in surface extensional strain in directions perpendicular to the trench immediately after imposing slip on the asperity(ies). Figure 3 shows that surface strain as a function of time and position along strike for the row of elements darkened in the insert. All results shown here are for the case in which the remainder of the thrust interface, outside the asperity(ies), is allowed to freely slip.

There is strong enhancement of the cycle-related deformation in the area of the upper plate positioned over the asperity. The size and shape of the influenced area is affected obviously by the size of the asperity, but also by the mechanical behavior of the fault zone surrounding the asperity. These model results are meaningful for interpretation of geodetic data along profiles perpendicular to the trench, and show clear differences depending on where a particular profile is positioned in relation to the underlying asperity.

For the outer-rise area there is space- and time-dependence of cycle- related stressing due to the presence of asperities. This is consistent with past seismological observations (Dmowska and Lovison, 1992) that seismicity clusters along the subducting margin in association with asperities.

For the Shumagin Islands segment the matching of our 2D model results with the geodetic measurements (strains, tilts, uplift) from the Islands network requires that the average seismic coupling factor along the interplate interface (without asperities) would be rather low, equal to 0.1 (Dmowska et al., 1992). As our 3D modeling shows, similar fit would be achieved if, instead, the Shumagin segment were positioned in a corridor between two larger asperities, e.g., one to the east, where the 1938 earthquake nucleated, and one to the west, in the western part of the Shumagin Gap area (which shows higher coupling, as revealed by larger outer-rise as well as down-dip earthquakes, Dmowska et al., 1992).

Reports:

Dmowska, R., "Stress transfers during the earthquake cycle in oblique subduction segments" (abstract), *EOS, Trans. Am. Geophys. Un.*, **73**, N. 43, supplement, p. 361, 1992.

Dmowska, R. and L. C. Lovison, "Influence of asperities along subduction interfaces on the stressing and seismicity of adjacent areas", *Tectonophysics*, **211**, 23-43, 1992.

Dmowska, R., G. Zheng and J. R. Rice, "Earthquake cycles in a subduction segment with a row of asperities", (abstract) *EOS, Trans. Am. Geophys. Un.*, **74**, N. 43, supplement, p. 91, 1993.

Dmowska, R., G. Zheng, J. R. Rice and L. C. Lovison-Golob, "Stress transfer, seismic phenomena and seismic potential in the Shumagin seismic gap, Alaska" (abstract), Wadati Conference on Great Subduction Earthquakes, abstract book, 150-152, Fairbanks, Alaska, Sept. 16-19, 1992.

Zheng, G., R. Dmowska and J. R. Rice, "Modeling earthquake cycles in the Shumagins (Aleutians) subduction segment with seismic and geodetic constraints" (abstract), *EOS, Trans. Am. Geophys. Un.*, **73**, N. 43, supplement, p. 367, 1992.

Zheng, G., R. Dmowska and J. R. Rice, "Deformation during the earthquake cycle in an oblique subduction segment with asperities" (abstract), *EOS, Trans. Am. Geophys. Un.*, **74**, N. 43, supplement, p. 91, 1993.

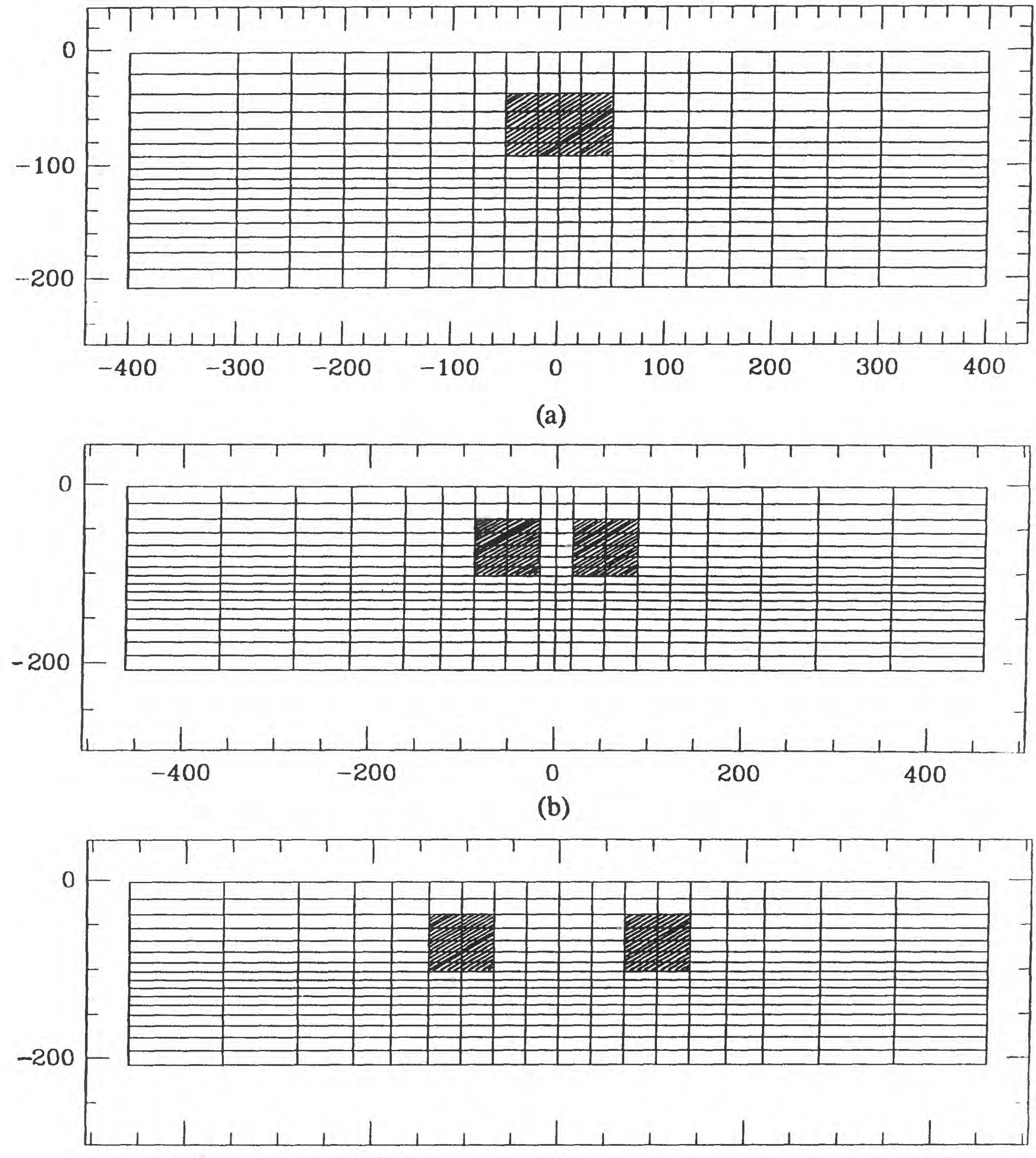

Figure 1. The thrust interface (vertical axis is distance in km from the trench, measured negative down-dip; horizontal axis is distance in km along strike). Case (a) is for a single asperity and cases (b) and (c) are for pairs of asperities. Periodic boundary conditions apply at the ends along strike. Slip is imposed on the asperities and calculated elsewhere on the thrust interface according to an assumed rheological law, taken as freely slipping in cases shown here.

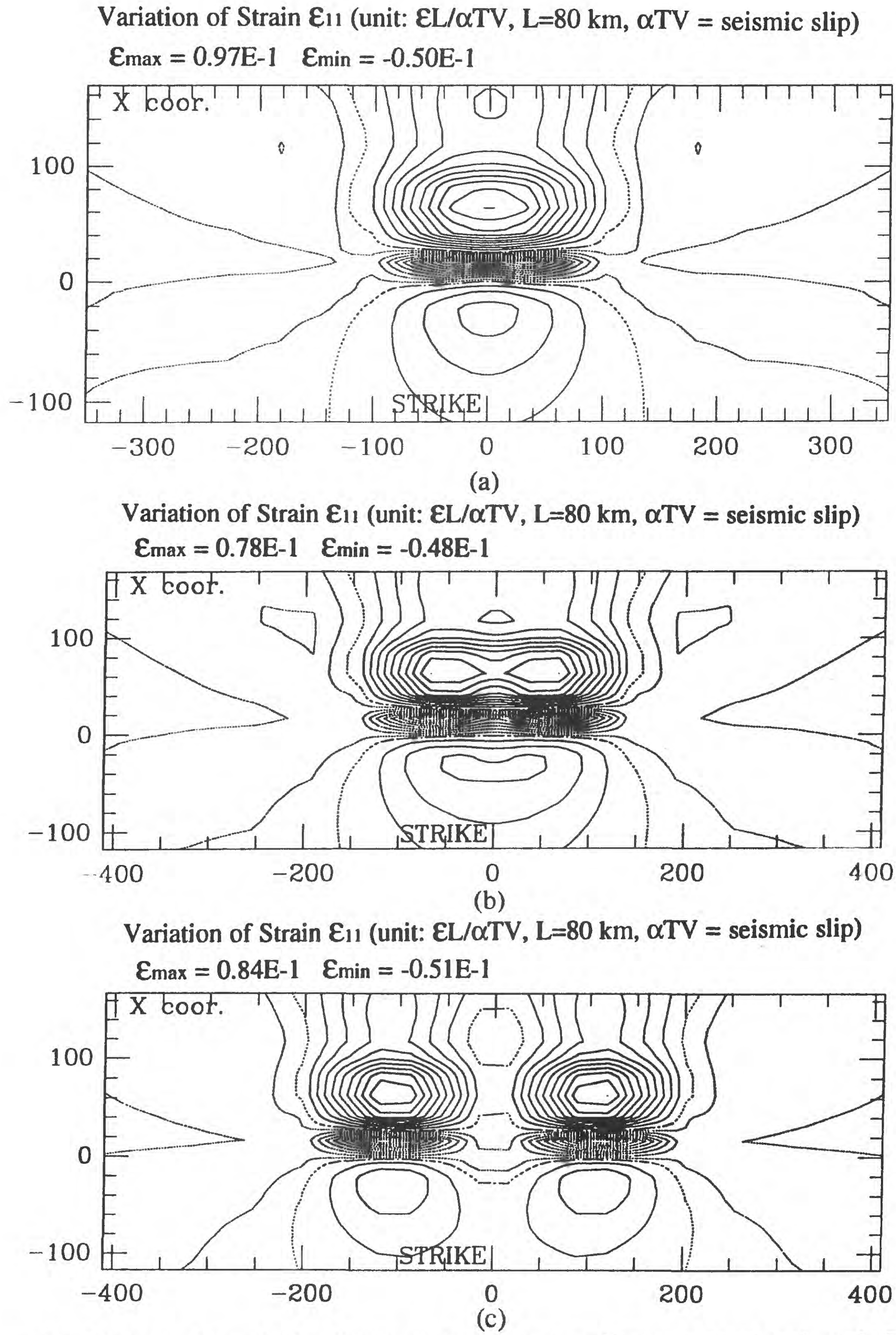

Figure 2. Contour plots of the change in trench-perpendicular extensional strain E_{11} along the surface of the earth, immediately following slip on the asperity or asperities, for the three cases shown in Figure 1. Now the positive range on the vertical axis gives distance from the trench, in km, on the overriding plate; horizontal axes give distance along strike. The dip angle has been taken as 25° here and the thrust interface outside the asperities allowed to freely slip in response to the imposed motion and deformation of surrounding material.

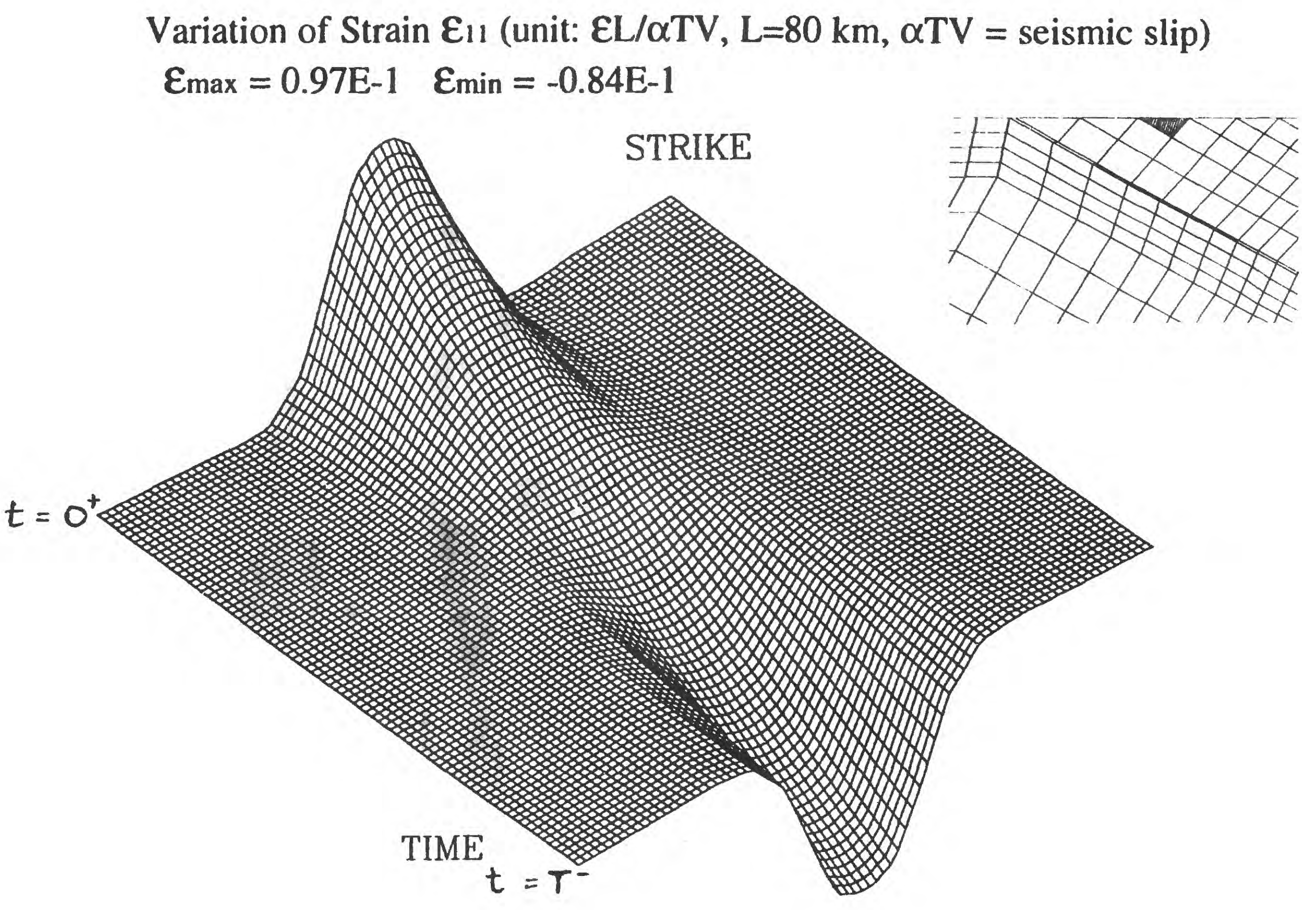

Figure 3. The inset diagram shows a section through the mesh, perpendicular to the trench, and a particular row of elements at the surface is darkened. The wireline plot shows the trench-perpendicular extensional strain E_{11} as a function of distance along strike through that element row and of time through one complete earthquake cycle. This is for case (a), a single asperity, and for a freely slipping interface outside the locked asperity.

Future Work

Further work will concentrate around the WD102-1 site as well as further afield. We are also examining liquefaction events in areas where artifacts from native Americans have been found, since these archeological deposits are proving very useful farther south (see report by E. S. Schweig, III).

Reports Published

Craven, J., Li, Y., Schweig, E. S., Ellis, M. A. and Tuttle, M. A., Paleoliquefaction Studies in the New Madrid Seismic Zone (abstract): Journal of the Tennessee Academy of Sciences, (in press).

Schweig, E. S. III, Tuttle, M. A., Li, Y., Craven, J. A., Ellis, M. A., Guccione, M. J., Lafferty, R. H. III, and Cande, R. F., Evidence for Recurrence Strong Earthquake Shaking in the Past 5,000 Years, New Madrid Region, Central U. S. (abstract): EOS, 74, p438, 1993.

Schweig, E. S. III, Ellis, M. A., and Tuttle, M. A., The Rate of Recurrence of LArge Earthquakes in the New Madrid Seismic Zone, *in* National Earthquake Conference, Post-conference Proceedings: Memphis, Tennessee, Central United States Earthquake consortium (in press).

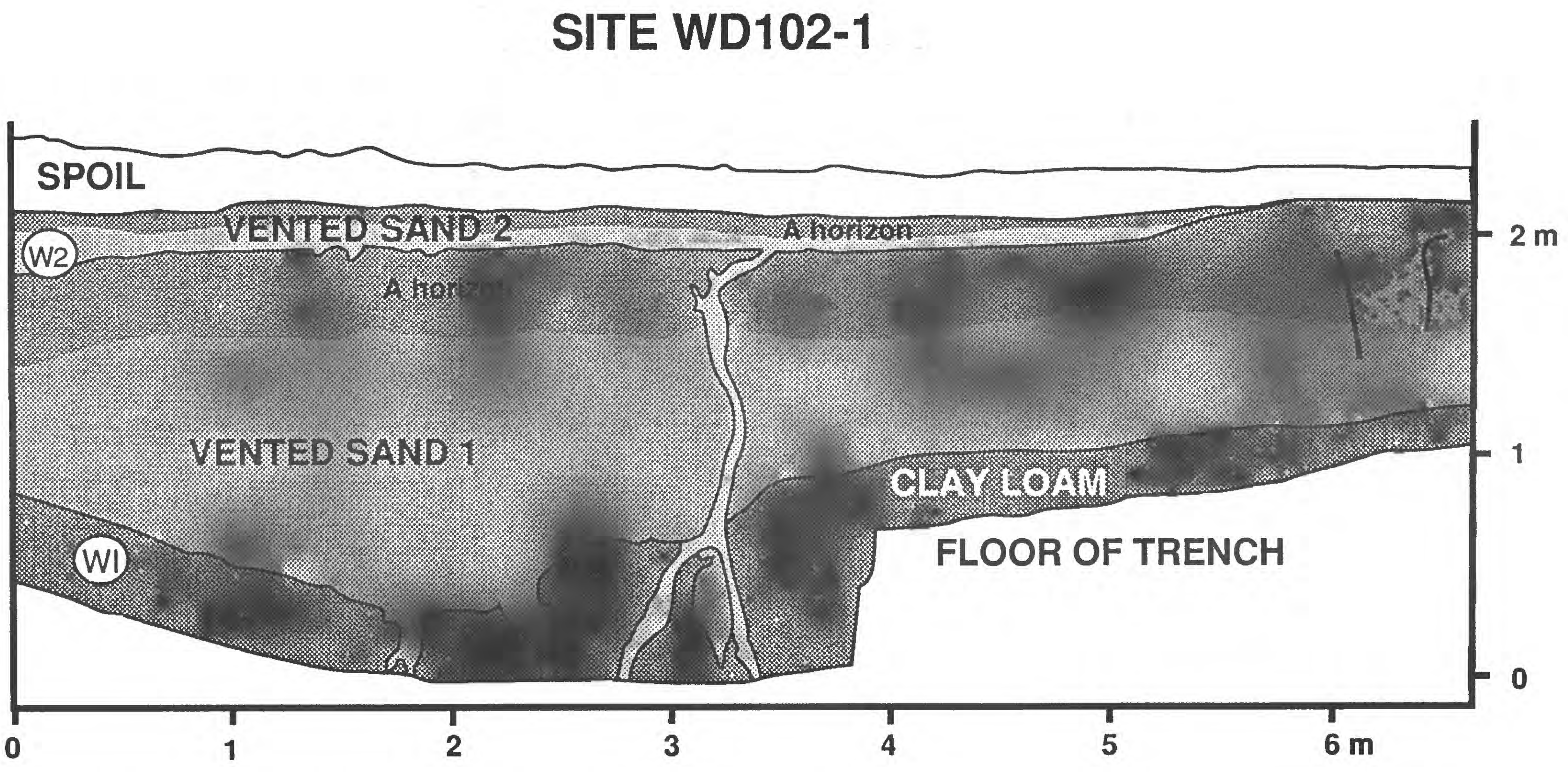

Figure 1: Simplified log of the trench wall at site WD102-1. The relative ages of the two sand blow deposits are clearly shown by the thin sand feeder dike that cuts across the lower (older) sand deposit. Note that each sand deposit is capped by a relatively well-developed soil A-horizon.

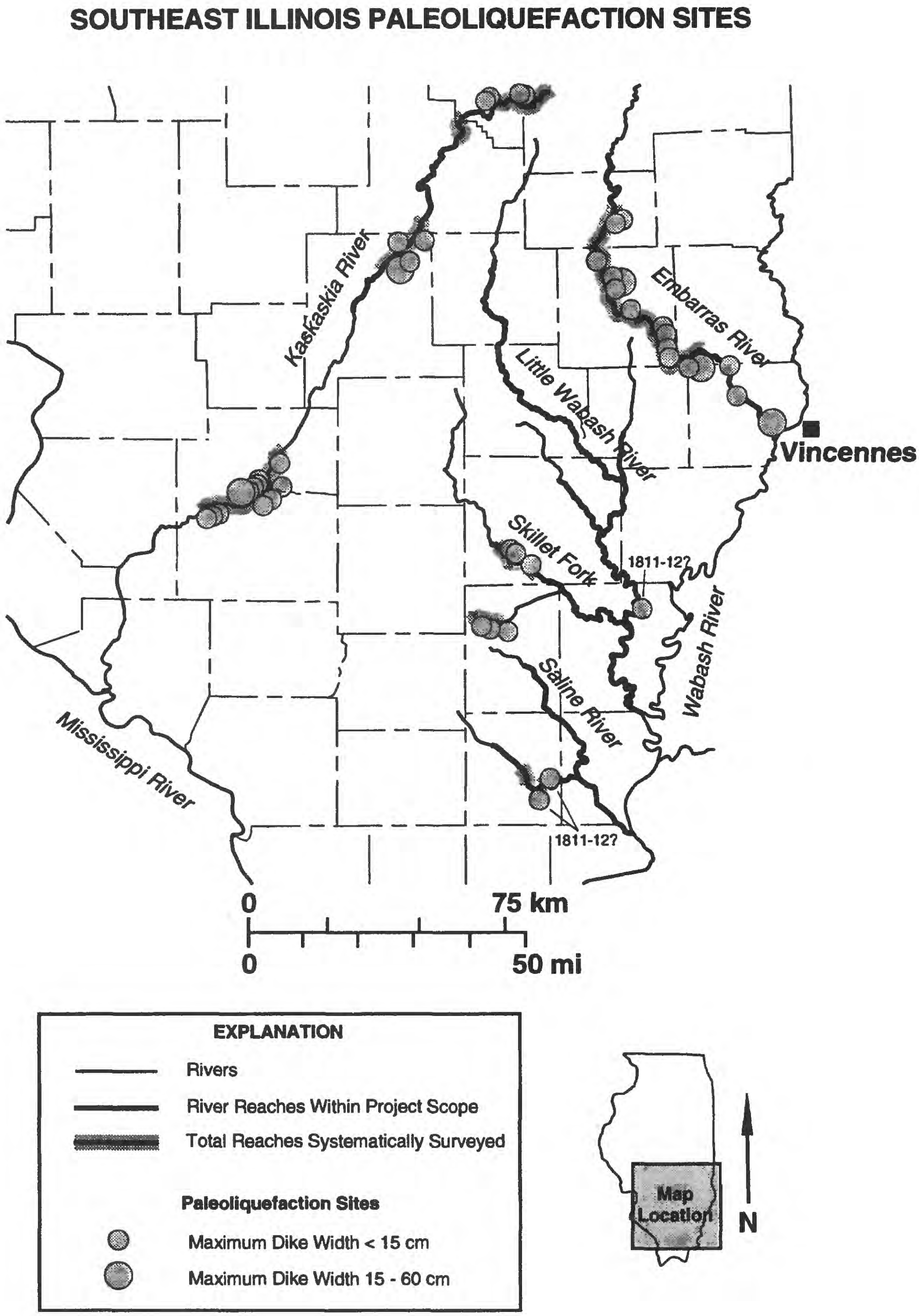

Figure 1. Location of known paleoliquefaction sites, distribution of maximum dike size, and river reaches surveyed in southeast Illinois. Survey coverage and sites represent cumulative results to date of Obermeier et al. (1993) and this ongoing research, with the exception of sites discovered along the South Fork of the Saline River by S. Obermeier (USGS) in 1993 and sites in Illinois along the Wabash reported by Munson et al. (1992).

Paleoseismic Investigations of the San Andreas Fault on the San Francisco Peninsula

Contract No. 14-08-0001-G2114
Program Element II.5

N. Timothy Hall
Geomatrix Consultants
100 Pine Street, 10th Floor
San Francisco, California 94111
(415) 434-9400

Robert H. Wright
Harlan Tait Associates
1269 Howard Street
San Francisco, California 94103
(415) 626-0765

Introduction

This report summarizes progress to date on the second phase (FY 93) of a multi-year investigation of the late Quaternary paleoseismic history of the San Andreas Peninsula reach of the San Andreas fault (SAF). The Phase I research during 1992 identified and evaluated sites along this reach of the fault that had potential for containing a decipherable and datable paleoseismic record. The Phase II research is currently focused on the most promising site, the head of an active alluvial fan cut by the fault on the Filoli Estate, which is located between Crystal Springs Reservoir and the Town of Woodside.

We have been assisted in the work by Kevin B. Clahan, a graduate student at San Jose State University, whose research and educational activities are being partially supported by funding under this contract. We are also working closely with the Center for Accelerator Mass Spectrometry at Lawrence Livermore National Laboratory which is providing radiocarbon analyses without cost.

Progress to Date

We have prepared a geomorphic map of the site that shows the deeply incised channel of Spring Creek and the locations of our backhoe trenches with respect to the active trace of the SAF (see Figure 1). We have excavated 11 backhoe trenches: 5 normal to the fault trace and 6 more that are fault-parallel. Both walls of each trench have been cleaned, sampled, and logged at a scale of 1 inch to 1 meter. At the fault, both walls of the trench, and in 3 cases the floor of the trench, have been logged at a scale of 1 inch to 0.5 meter.

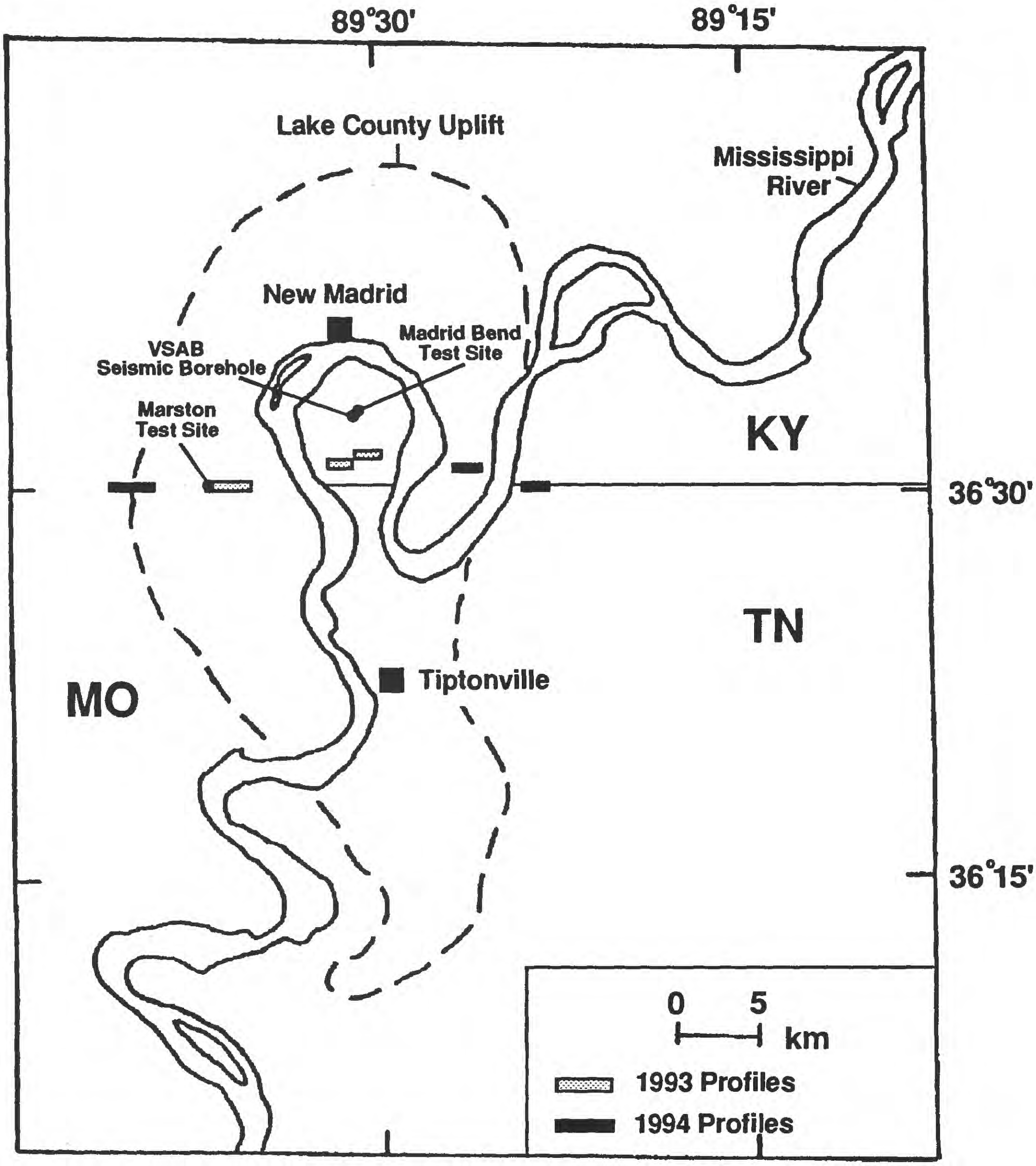

Figure 1 Map of the Lake County uplift (from Russ, 1982) showing the locations of SH-wave seismic reflection profiles to be completed in 1993 and 1994, reflection test sites, and a borehole that was used for correlation purposes.

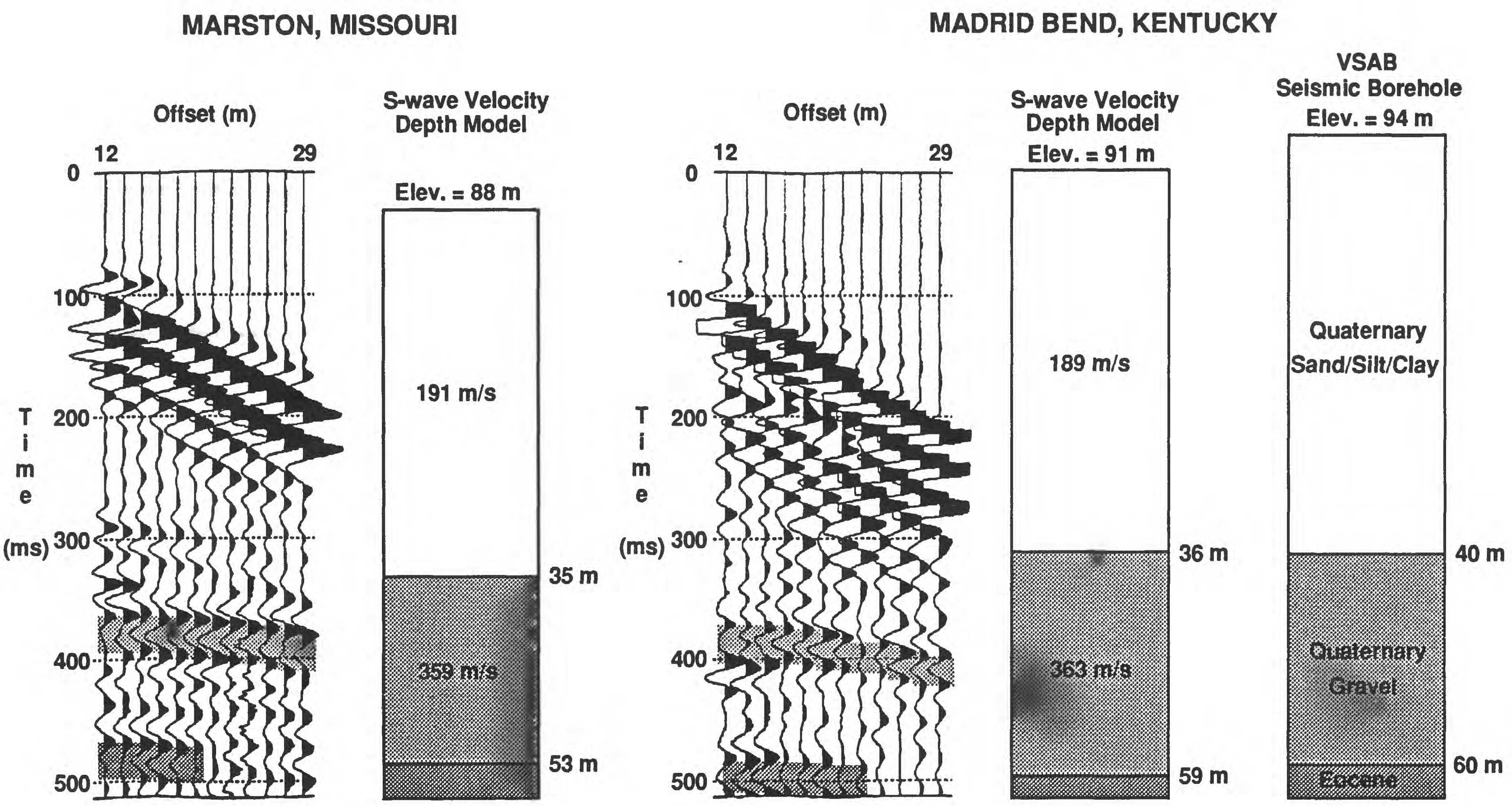

Figure 2 SH-wave walkaway tests and velocity-depth models for Marston, Missouri, and Madrid Bend, Kentucky, compared to a generalized log of the VSAB seismic borehole (see Figure 1 for locations). The shaded reflections are interpreted to represent the top and bottom of the basal Quaternary gravel.

personal communication), we see evidence for a shallow tectonic wedge under Suisun Bay, a deeper wedge of Great Valley Sequence, and an even deeper wedge of Franciscan material over magnetic basement at about 14 km depth. The pattern of deep seismicity under the town of Pittsburgh (e.g., the M 3.0 temblor of December 5, 1993 at 17.5 km depth) is indicative of deformation within the basement, though the style of deformation is as yet unclear (Figure 6a). The magnetic signature of the basement suggests it is composed of ophiolite, but outcrop evidence along the San Andreas Fault favors a metamorphic lithology. While the gross pattern of deep seismicity beneath Pittsburg gives the appearance of a single, steeply dipping continuous fault, the detailed distribution of hypocenters suggests a stacked set of wedge-related faults. Further analysis of the fault mechanisms of these deep earthquakes is in progress.

Comparisons with other tectonic wedges at Dunnigan Hills to the north and at Kettleman Hills to the south reveal the uppermost wedge in the Sacramento Delta is thinner and shallower. The wedge may originally have been thicker and was since uplifted from below by the insertion of a newer, deeper wedge, perhaps along the basement interface. Evidence for reactivation, and in some cases reversal, of faults suggests several episodes of tectonism in this region since the Late Cretaceous. We plan remapping and dip analysis of outcrops in the Vaca Mountains and the Los Medanos Hills, following the method of Lucchitta and Suneson (1993), to illuminate the tectonic history.

Identified Faults

The fault zone identified at kilometer 15 on the BASIX line is the southern extension of the Kirby Hills fault. Its location is also recorded on high-resolution uniboom data (also from BASIX) as well as on a proprietary Chevron line running parallel to BASIX, south of the river (Figures 1 and 5). Because the Kirby Hills fault does not appear to connect with the mapped fault at Antioch, we proposed to rename it the Pittsburg/Kirby Hills fault (PKHF) to distinguish it. The PKHF is seen on the CALCRUST lines 3 and 11 miles north of the river. North of Kirby Hills and south of the river, the fault changes from a steeply dipping set of faults that have a flower-structure appearance to a simple west-verging thrust that dips 30 degrees east. The deep seismicity in this area does not appear to be associated with this shallow fault (because of the interpreted intervening structures). And while the PKHF passes very near a major power plant and much recent urban development at Pittsburg, it is perhaps not displacement from this shallow fault that creates a seismic hazard here so much as more wide-spread ground-shaking due to potential larger (>M5 or 6) earthquakes in the deeper zone of seismicity (>14 km).

Another thrust fault is recognized at kilometer 25 on the BASIX line (Figure 5). This fault lines up with the mapped fault at Ryer Island and is also seen on the Chevron line south of the river. We propose to name this fault the Ryer Island fault. This fault lies subparallel to, and north of, the Los Medanos thrust (LMT), the major structure that underlies the Los Medanos Hills. South of the LMT the Montezuma Formation, a Pleistocene river gravel deposit, is involved in severe folding, and is overturned along the LMT. While some of the thrusting and shortening along the LMT zone may be older than Pleistocene, there has clearly been a great deal of post-Pleistocene action. How these structures fit together is the subject of continued investigation.

References:

Luccitta, I., and N.H. Suneson, 1993, Dips and extension, GSA Bulletin, v. 105, p. 1346-1356.

Presentations at the 1992 Fall AGU meeting:

D.L. Jones, R. Graymer, and T.V. McEvilly, Neogene Transpressive Tectonics of the Central California Coast Ranges.

P.E. Hart, J. McCarthy, E. Karageorgi, K. Williams and T.V. McEvilly, Crustal Structure of the San Francisco Bay Area: Results From the 1991 Bay Area Seismic Imaging Experiment (BASIX).

J. McCarthy, P. Hart, E. Karageorgi, K. Williams and T.V. McEvilly, Seismic Reflection Profiling in San Francisco Bay Area: The BASIX Experiment.

Presentations at the 1993 Fall AGU meeting:

Band, J.W., D.L. Jones, and T.V. McEvilly, Tectonic wedges and blocks at the eastern margin of the Coast Ranges, Sacramento Delta Area, California, EOS, 74, 609, 1993 (abs.).

Karageorgi, E.D., T.V. McEvilly, K.H. Williams, and R.W. Clymer, Land Recordings from the Bay Area Seismic Imaging Experiment (BASIX), EOS, 74, 413, 1993 (abs).

Papers in Press:

Jones, D.L., R. Graymer, C. Wang, A. Lomax and E. Brabb, Neogene transpressive evolution of the California coast ranges, Tectonics (in press), 1994.

Papers in Preparation:

J. Weber Band, et al., 1994, Tectonic Wedging and Crustal Structure in the Sacramento Delta area, California, manuscript in preparation,.

J. Weber Band, et al., 1994, The Pittsburg/Kirby Hills Fault, Sacramento Delta area, California (tentative title), manuscript in preparation.

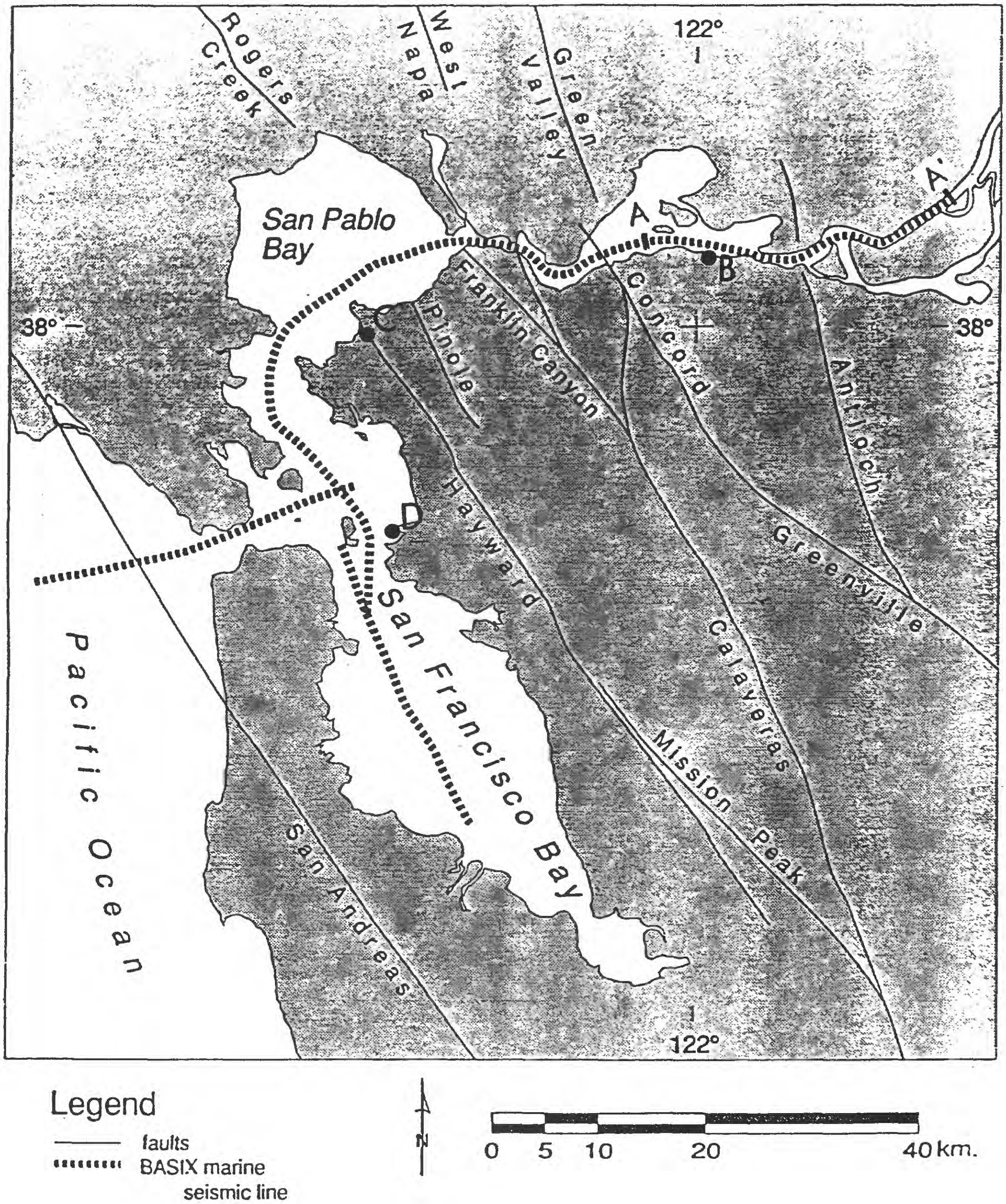

Figure 1. San Francisco Bay region with BASIX profile line. Line A-A' indicates subsurface coverage of lines 101-103 (Figure 2). Letters B, C, and D show the location of UCB land recording arrays.

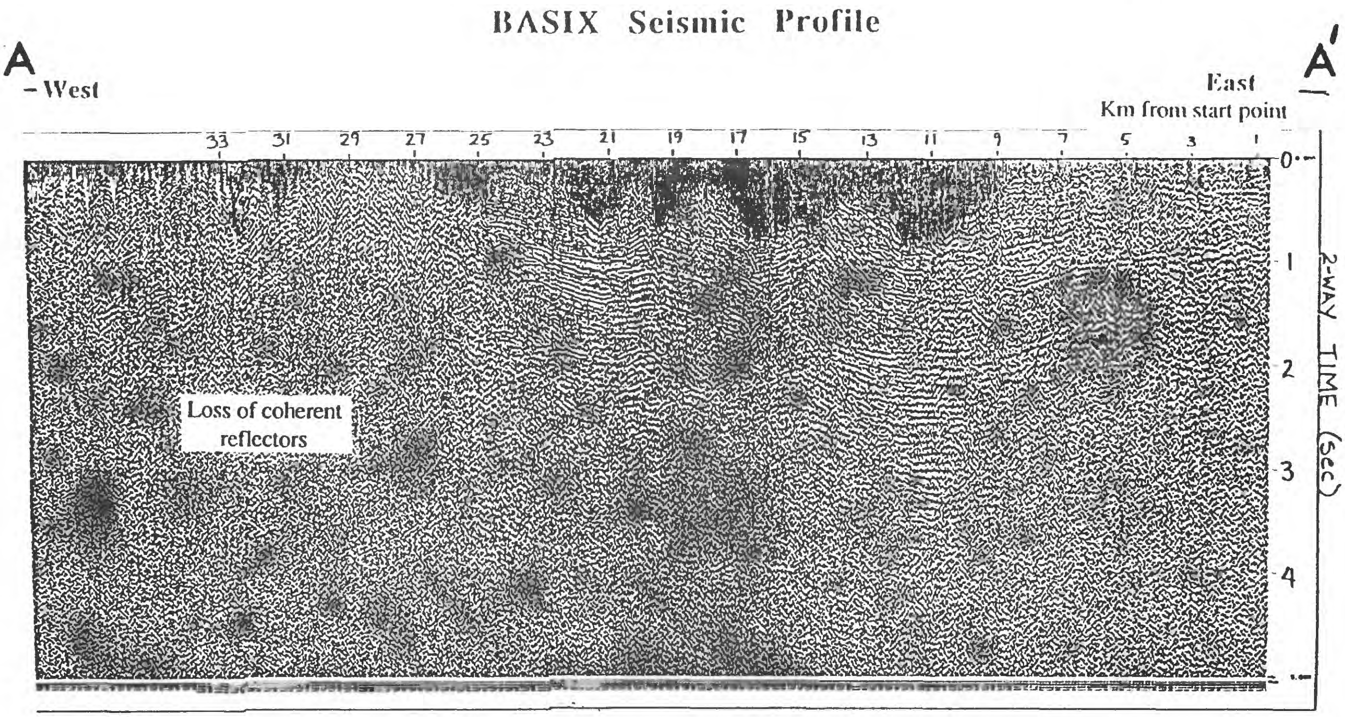

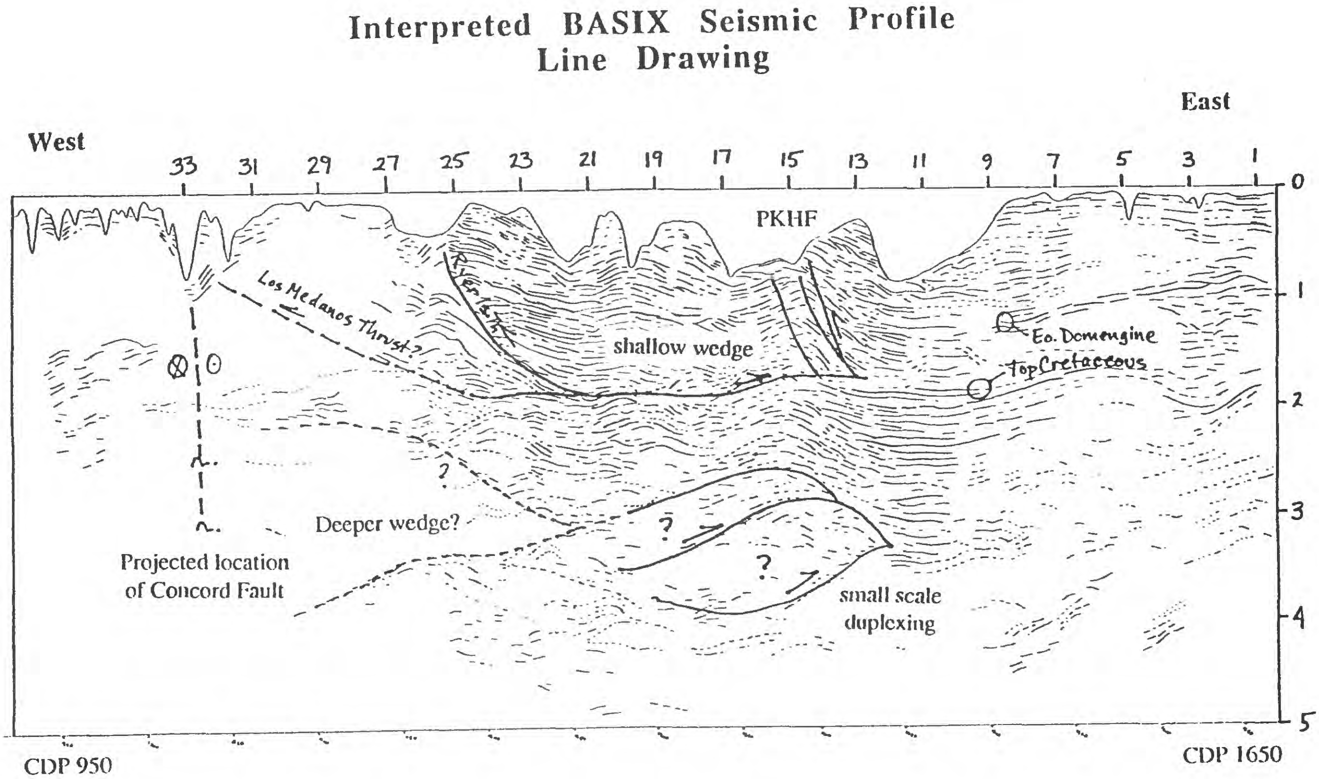

Figure 2. Final CDP stack of the eastern portion of the BASIX line in Suisun Bay (lines 101 to 103), referenced to Figure 1 (A-A'), with interpretation.

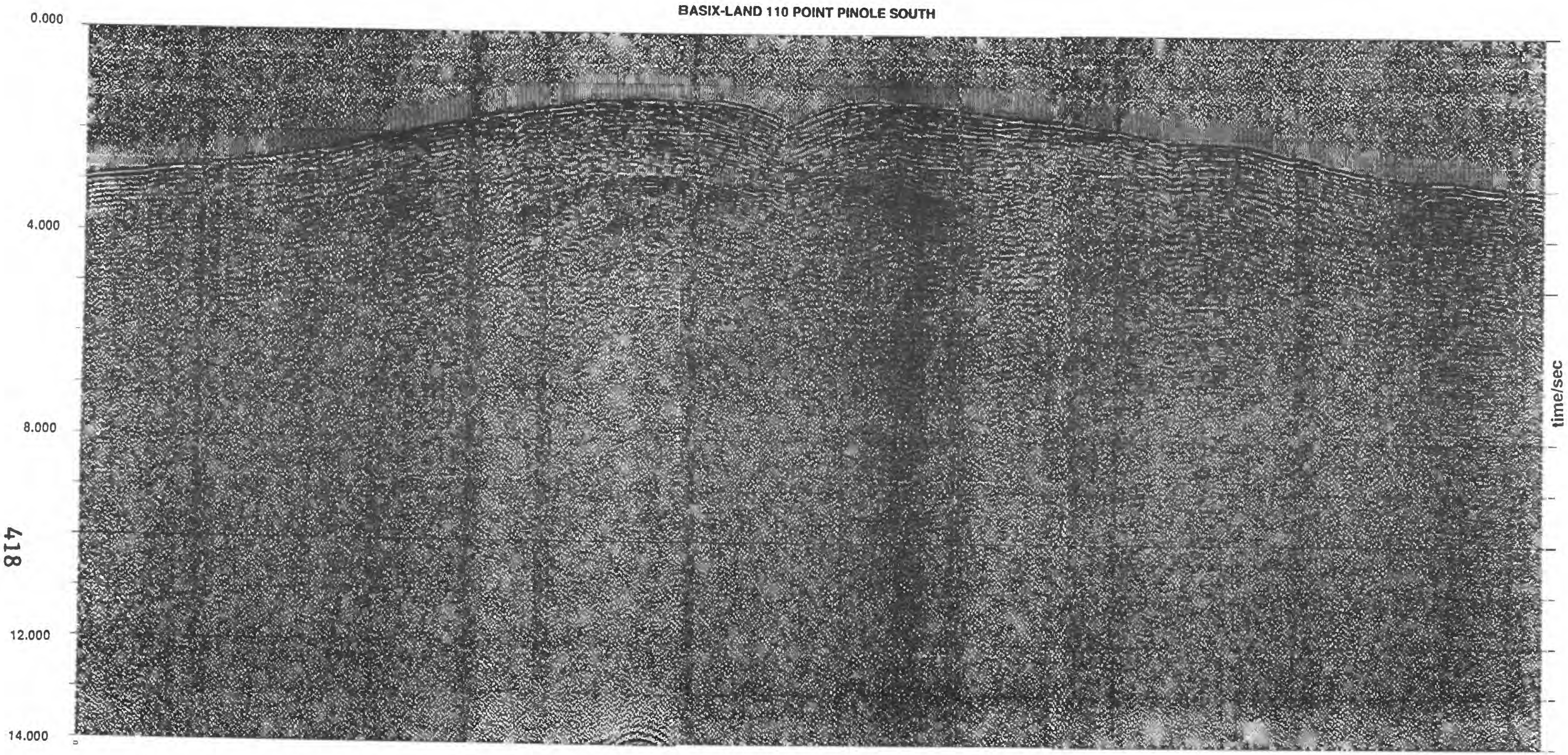

Figure 3. Receiver gather from the Point Pinole southern land array ("C" in Figure 1) for line 110 . The vertical axis is two-way travel time. The apparent mirror-imaging of the section is due to the air-gun ship making two passes of the line, first north-to-south, then south-to-north. Note the band of discontinuous reflections at 9-11 sec, also apparent on the land recordings for lines 108 and 109.

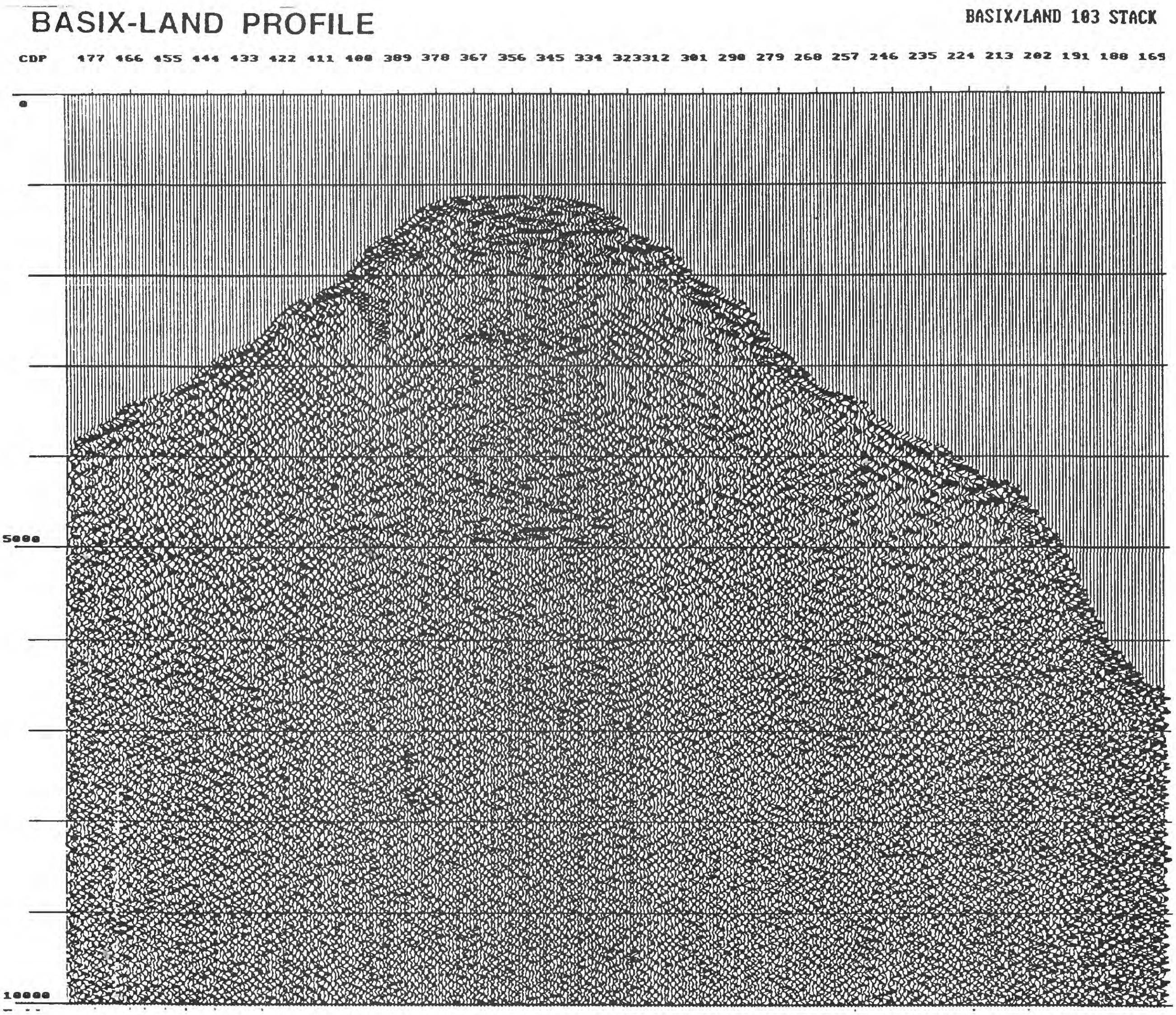

Figure 4. Preliminary CDP stack from the land recording at the Concord Naval Weapons Station ("B" in Figure 1).

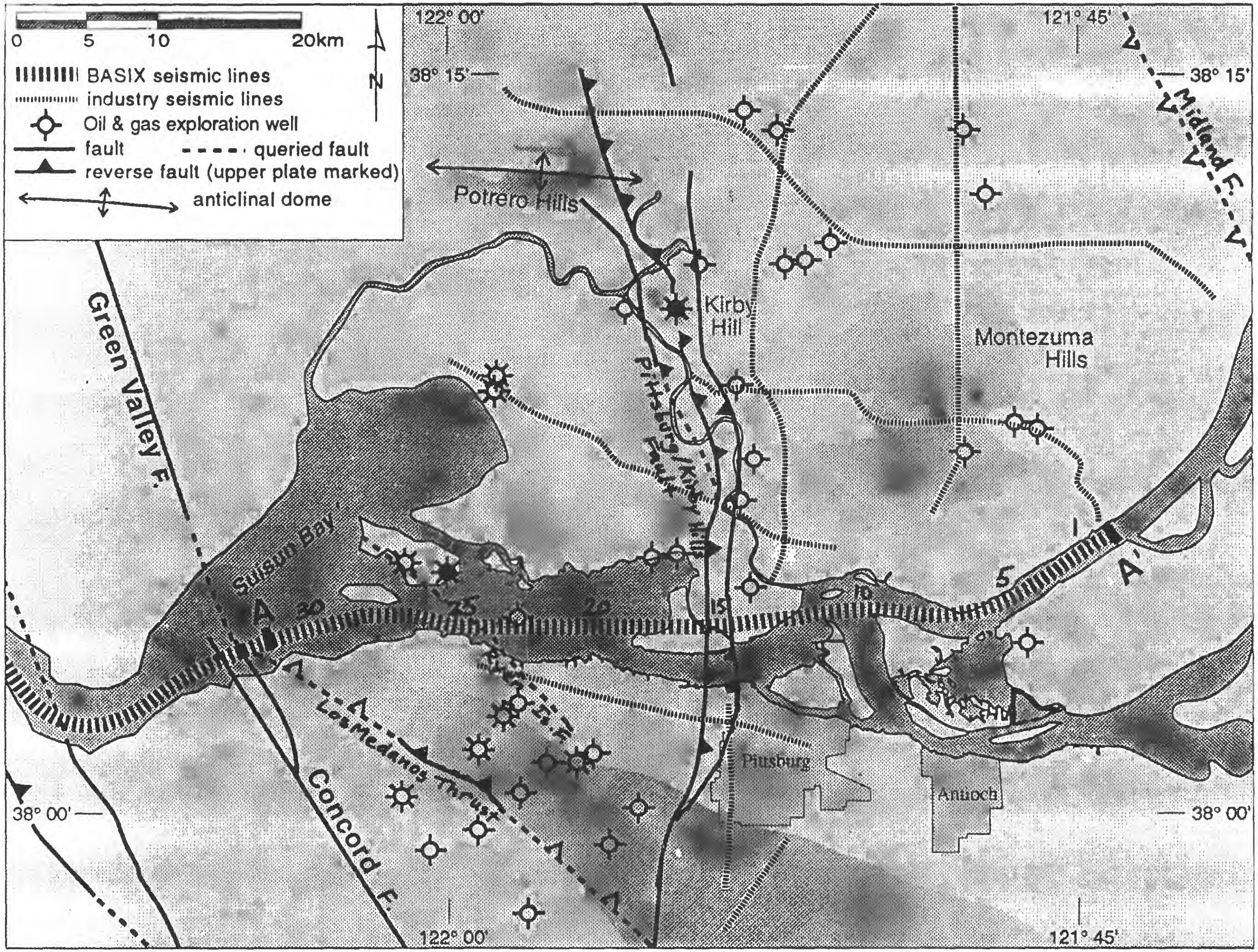

Figure 5: Map of Sacramento Delta area showing location of the BASIX line with kilometer markings, important geomorphic features, newly mapped faults, and subsidiary data sets.

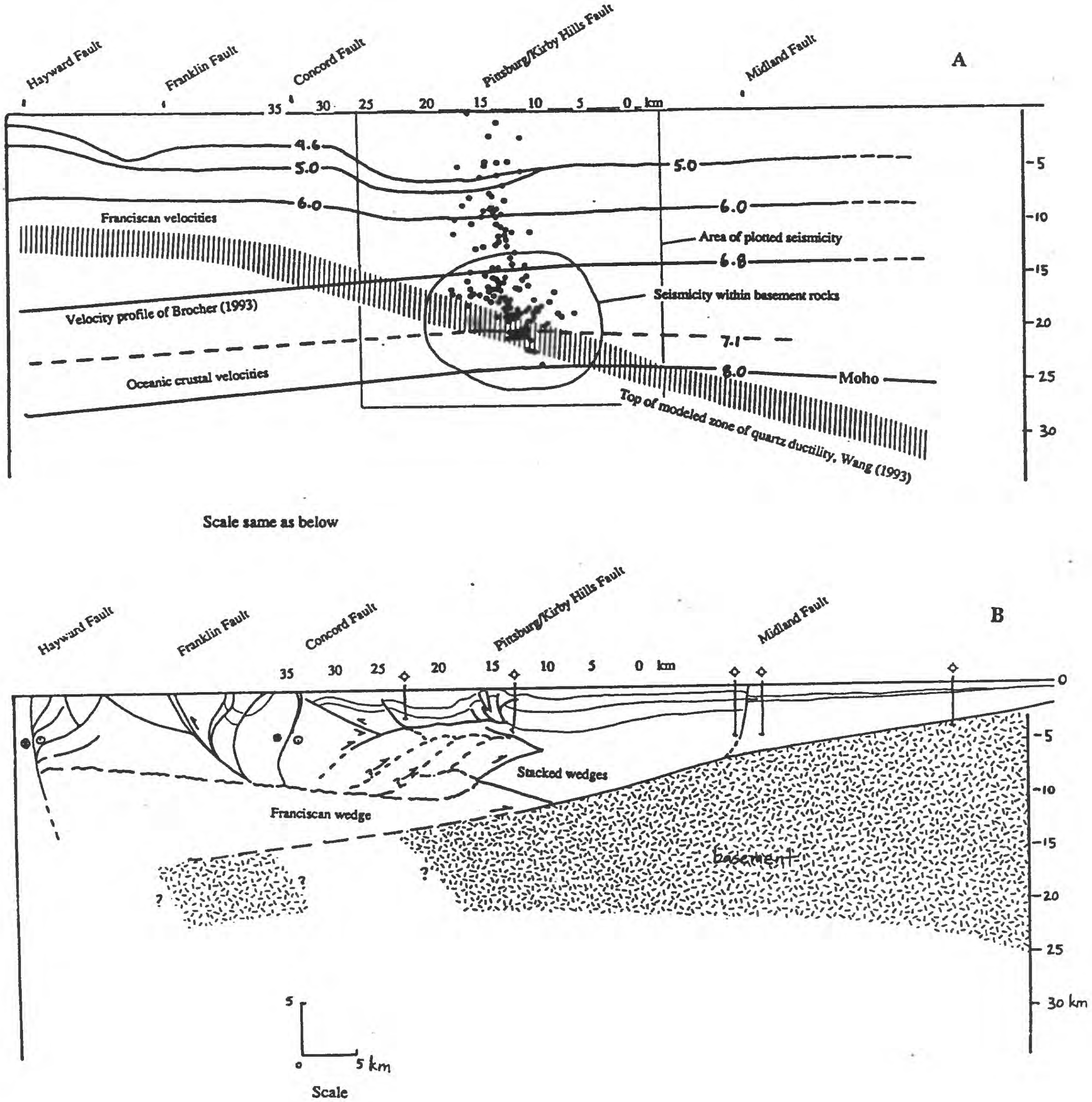

Figure 6: East-west cross sections (no vertical exageration) coinciding with the BASIX line, and extending from the Central Valley on the east to the Hayward Fault on the west. a) Seismicity in the vicinity of Pittsburgh on Suisun Bay, with the depth of onset of ductile flow (Chi Wang, personal communication), and the velocity model of Brocher, 1993, based on BASIX refraction data (personal communication), shown as contours in km/sec. b) geologic cross-section based on BASIX seismic profile, outcrop and well data, and depth to magnetic basement from Jachens (1993, pers. comm).

Annual Technical Report
USGS 1408001-G2136 Program Element II.2
Tectonics of the Mission - Chabot Faults
David L. Jones, Principal Investigator
and Russell W. Graymer
Department of Geology and Geophysics
University of California
Berkeley, CA 94720
510-642-2514
E-mail: davey@perry.berkeley.edu

Summary

This study focused on the seismically active area east of Fremont (Figure 1) that is unrelated to previously known active faults, as well as adjoining areas from Garin Regional Park in southern Hayward to an area southeast of San Jose (Plate 1). Significant new discoveries resulting from the study in fiscal year 1993 include:

1) Active seismicity is located in a band of previously unmapped transpressional faults, including the Sheridan Creek and Dresser Faults, as well as the previously mapped (Hall, 1958) segment of the Mission Fault on and northwest of Mission Peak.
2) Faults previously mapped (Crittenden, 1951, Hall, 1958, Dibblee, 1980) as unrelated fault segments (i.e. Warm Springs, Mission, Arroyo Aguague Faults) are actually part of a continuous belt of faults that runs subparallel to and between the Calaveras and Hayward Faults (Plate 1).
3) At least three phases of deformation are seen in the belt; an early transpressive stage (probably pre - Pleistocene), an attenuation stage (Pleistocene or younger), and a late transpressive stage (Pleistocene or younger, probably related to active seismicity, see above).
4) The Mission and Chabot Faults, previously mapped (Hall, 1958, Dibblee, 1980) as continuous and equivalent are actually distinct. The transpressive Mission Fault cuts the older, attenuation, Chabot Fault.
5) A large component of fault normal deformation (at least 100%) has occurred across the fault belt, as evidenced in the southern portion by the repetition of lenses of ophiolite rocks on faults there (Figure 2 A-D). Because the belt is subparallel to the Hayward and Calaveras Faults, it is unlikely that compression is due to bending or asperities on strike - slip faults. Rather, compression is probably related to movement of upper crustal blocks *and* strike - slip faults bounded below by a mid - crustal decollement.

Introduction

The initial impetus for this study was the observation that a large number of small earthquakes defined a zone of active seismicity that is unrelated to the major faults, the Hayward and Calaveras Faults, in the area southeast of the town of Hayward (Fig. 1). The seismically active zone was in the general area of a reverse fault named the Mission Fault, best mapped on

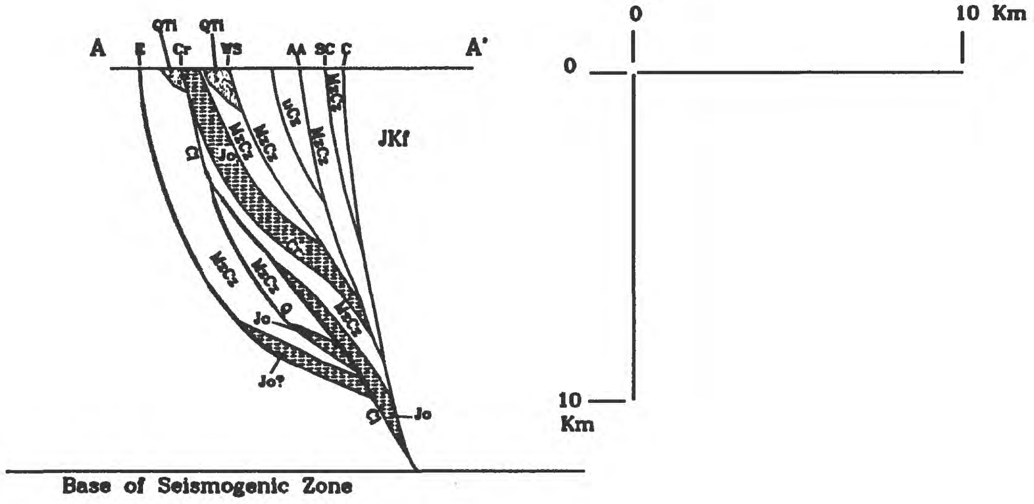

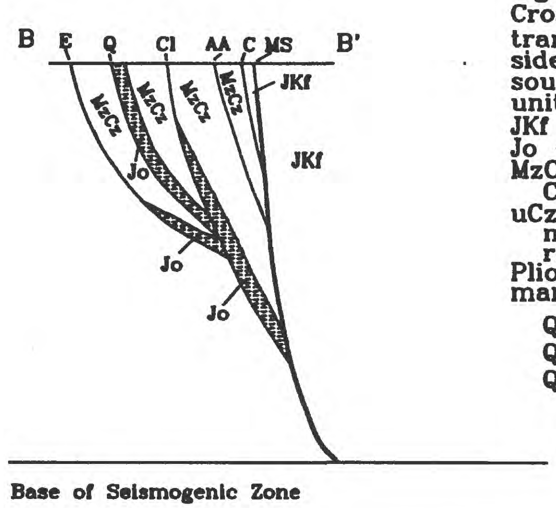

Figure 2A–C
Cross sections showing imricate transpressive faults on the west side of the Diablo Range in the southeast Bay Area. Geologic units as follows:
JKf – Franciscan rocks
Jo – Coast Range ophiolite
MzCz – Upper Mesozoic and Cenezoic marine strata
uCz – Miocene to Pliocene non – marine strata and volcanic rocks
Pliocene and Pleistocene non – marine gravels;

QTs – Silver Creek gravels
QTp – Packwood gravels
QTi – Irvington gravels.

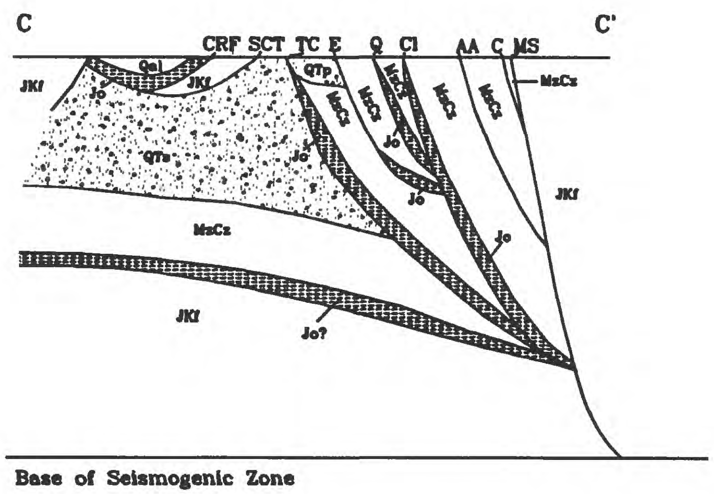

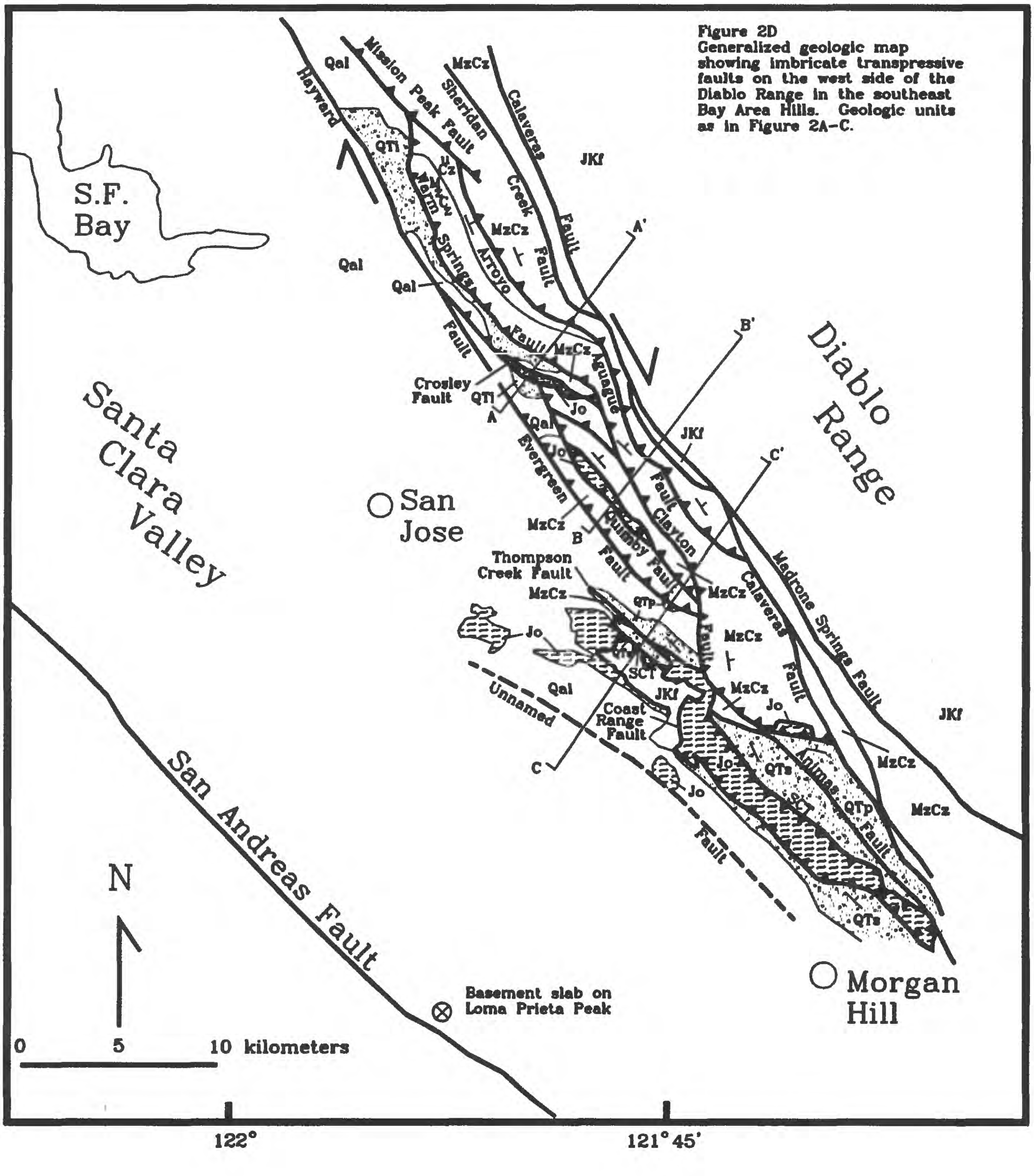
Figure 2D
Generalized geologic map showing imbricate transpressive faults on the west side of the Diablo Range in the southeast Bay Area Hills. Geologic units as in Figure 2A-C.
S.F. Bay
Santa Clara Valley
San Jose
Diablo Range
Morgan Hill
Hayward
Mission Peak Fault
Sheridan Creek Fault
Calaveras Fault
Warm Springs Fault
Arroyo Aguague Fault
Crosley Fault
Evergreen Fault
Quimby Fault
Clayton Fault
Thompson Creek Fault
Madrone Springs Fault
Calaveras Fault
Coast Range Fault
Unnamed Fault
Animas Fault
San Andreas Fault
Qal
QTl
MzCz
JKf
Jo
QTp
QTs
SCT
A
A'
B
B'
C
C'
Basement slab on Loma Prieta Peak
N
0
5
10 kilometers
122°
121° 45'

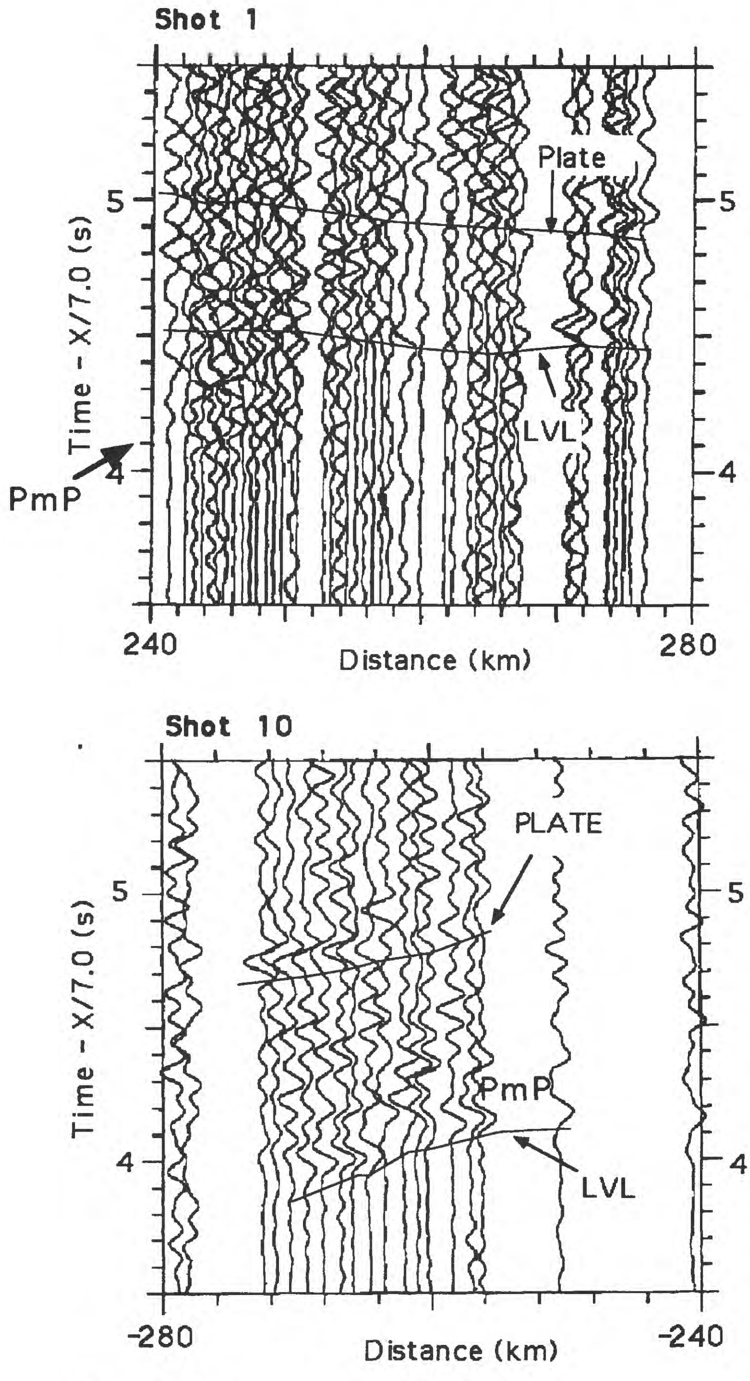

Figure 2b

Examples of Wide-Angle Relections from the Low Velocity Layer at the Top of the Plate (LVL) and the High Velocity Layer Within the Plate (Plate)

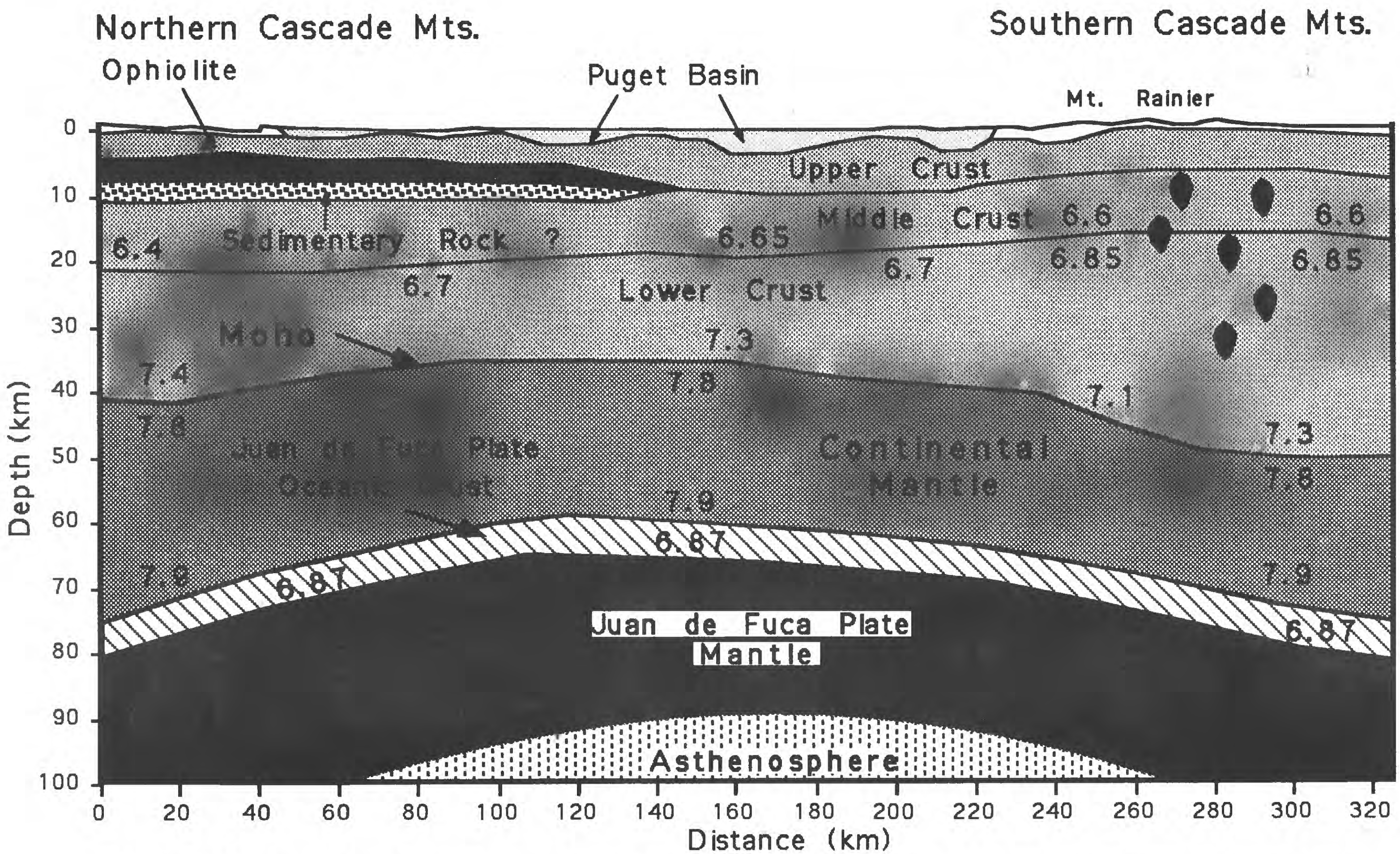

Figure 3. Interpreted geological cross section from the seismic model. Numbers are velocity values in km/s.

not reflect the long-term behavior of the fault.

The regressive Bonneville shoreline is present on both sides of the fault zone in the Pole Canyon trench. The shoreline was displaced 2.5-3.0 meters (net slip) down to the west during the most recent event; an unexpectedly large amount considering the mapped length (10 km) of surface rupture. A vertical displacement of that size is normally associated with earthquakes of magnitude 7 or greater.

REPORTS

The following brief reports and abstracts presenting preliminary results of the Oquirrh fault zone earthquake hazard evaluation have been prepared:

Olig, S.S., 1993, Prehistoric earthquakes on the Oquirrh fault zone, Tooele County: Utah Geological Survey, Survey Notes, v. 25, no. 3-4, p. 31-32.

Olig, S.S., Lund, W.R., and Black, B.D., 1993, Evidence for mid-Holocene surface rupture on the Oquirrh fault zone, Utah [abs.]: Geological Society of America Abstracts with Programs, v. 25, no. 5, p. 129.

Lund, W.R., 1993, The Oquirrh fault zone - Evidence for multiple displacements in Holocene and latest Pleistocene time: Handout for Association of Engineering Geologists field trip to the Pole Canyon trench site on the Oquirrh fault zone, September 1993.

REFERENCES

Barnhard, T.P., 1988, Fault-scarp studies of the Oquirrh Mountains, Utah, in, Machette, M.N., editor, In the footsteps of G.K. Gilbert - Lake Bonneville and neotectonics of the eastern Basin and Range Province, Utah: Utah Geological Survey Miscellaneous Publication 88-1, p. 52-54.

Barnhard, T.P., and Dodge, R.L., 1988, Map of fault scarps formed on unconsolidated sediments, Tooele 1°x2° quadrangle, northwestern Utah: U.S. Geological Survey Miscellaneous Field Studies Map MF-1990, scale 1:250,000.

Machette, M.N., Personius, S.F., and Nelson, A.R., 1992, Paleoseismology of the Wasatch fault zone - A summary of recent investigations, interpretations, and conclusions, in Gori, P.L., and Hays, W.W., editors, Assessment of regional earthquake hazard and risk along the Wasatch Front, Utah: U.S. Geological Survey Professional Paper 1500-A-J, p. A1-A71.

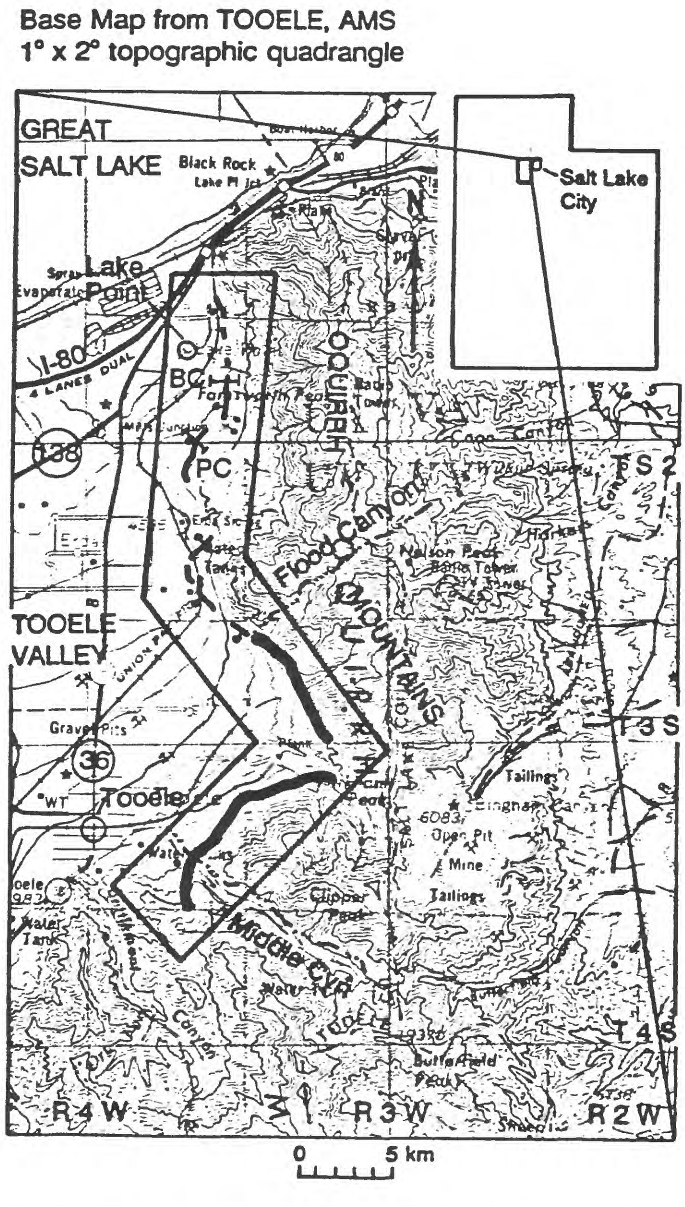

Figure 1. Location of the Big Canyon (BC) and Pole Canyon (PC) trench sites on the Oquirrh fault zone, Tooele County, Utah (after Barnhard, 1988).

Temporal and Spatial Behavior of Late Quaternary Faulting, Western United States and Map of Major Active Faults of the Western Hemisphere

9950-10215

Michael N. Machette
Branch of Earthquake and Landslide Hazards
U.S. Geological Survey, Box 25046, MS 966
Denver, CO 80225-0046
(303) 273-8612
(machette@gldvxa.cr.usgs.gov)

PURPOSE OF PROJECT

This project consists of two discrete but interrelated tasks that are combined for administrative reasons. In 1993, the bulk of activity and NEHRP funds were directed to the "World Map of Major Active Faults, Western Hemisphere", which is co-sponsored by the International Lithosphere Program (ILP). The common theme for both tasks is to define regional variations in the time-space distribution of late Quaternary paleoseismic activity as a guide to understanding the accumulation and release of strain on active faults and folds and to improve the quality of geologic input to seismic hazards analyses. Project members are Michael N. Machette, Richard L. Dart, and Kathleen M. Haller.

INVESTIGATIONS

1. The ILP sponsored map project will compile World, Continental, and United States maps of major active faults in support of their new Global Seismic Hazards Assessment Program (GSHAP). This work began in earnest in mid-1992 with a carefully chosen list of participants for the Western Hemisphere. We are still enlisting technical experts from Canada, the United States, and Mexico/Central America that are known to be both productive and knowledgeable, and which have strong national contacts. For the United States, the compilation will be supervised by the USGS in Denver, under the direction of this project. In addition, the USGS will assist compilers in the other regions with digitization and technical aspects of the data base.

Our strategy is to assemble a large body of data onQuaternary faults and folds in the U.S. Although many authors have compiled maps, few have taken the time to fully document their maps with supporting databases; thus, fault data in catalog form is relatively sparse. Overall, we suspect that there is existing catalog data for about 20% of the faults and folds in the U.S.

The customers for these products include internal (USGS) and external NEHRP scientists, as well as scientists, engineers, planners with state and local governments, universities, and consulting firms. We are using ARC/INFO on a SUN workstation for the map preparation and are compiling a relational database (FoxPro, Microsoft Corp.) of fault and fold data on Macintosh computers. However because most of the intended users do not have Macintosh computers, we also intend to distribute the data in DOS and/or Windows versions of the database. CD-ROM verions will come with a run-time version of the program and digital map files to for easy access at low user cost.

2. Machette, Haller, and Kelvin Berryman (visiting scientist from New Zealand Geological Survey) completed the description, mapping, and sampling of six large exploratory trenches that were excavated in Pleasant Valley, south of Winnemucca, Nevada in 1992. Four of the trenches were placed across surface ruptures of the 1915 Pleasant Valley earthquake (estimated Richter magnitude $7^3/_4$) in order to investigate the timing of prehistoric faulting. Two additional trenches were located on nearby pre-1915 fault scarps; one on a valleyward strand of the Tobin Scarp and a second that is to the north along the frontal fault of the Sonoma Range in Grass Valley. Samples for thermolumines-

cence dating (at The University of Ohio) were submitted in the spring of 1993, and results should be available in the spring of 1994. Results of this trenching study are being prepared for a U.S. Geological Survey-sponsored Redbook Conference on Paleoseismology in September 1994 (organized by Yeats, Schwartz, and Prentice).

3. Crone and Machette published two comprehensive manuscripts (USGS Bulletins) that describe the results of their 1991 Gilbert Fellowship field studies of the 1988 earthquakes at Tennant Creek, Australia (Crone and others, 1992) and Marryat Creek, Australia (Machette and others, 1993). In addition, they prepared several abstracts and a paper that summarize their work. These manuscripts discuss the implications of long-recurrence intervals for intraplate faulting. In addition, they continued dating studies using thermoluminescence (cooperatives with J. Hutton and J. Prescott, University of Adelaide; and H. Millard, USGS) and electron-spin resonance (cooperative with K. Tanaka, CRIEPI, Tokyo, Japan) to better define the minimum time for the penultimate faulting events and for stratigraphic control on rates of deposition.

RESULTS

1. During FY 93, we conducted a number to planning and progress meetings for the active fault map portion of the project. These are described briefly as follows:

South America: ILP meeting Feb. 11-14, 1993 in Quito, Ecuador. National representatives from Argentina (H. Basitas, S.A. Coordinator), Chile (R. Thiele), Columbia (J. Romero), Ecuador (H. Yepes and A. Eguez), Peru (J. Machare), and Venezuela (C. Giraldo) presented plans for completing a preliminary draft of their respective maps by August 1994. Commitments for Bolivia and western Brazil are still lacking.

Central America: Commitments have been obtained for compilation of San Salvador and Guatemala (G. Dengo), Honduras (M. Gordon), Panama (P. Mann), and Costa Rica (W. Montero); although little actual compilation has occurred to date.

Caribbean: A coordinating meeting was held at AGU in San Francisco on Dec. 7, 1993, to further formulate plans for this region. We currently hold commitments for Puerto Rico (B. McCann), Hispanola (P. Mann and C. Prentice), and part of Cuba (M. Gordon). Further commitments should be made in late 1993. We discussed plans with P. Mann and M. Gordon to hold a special session at the 1994 AGU meeting on Active Faulting in the Caribbean.

Mexico: Our first Mexico meeting was held in conjunction with the International Conference on Exotic Terranes in Guanajuato on Nov. 12, 1993. F. Ortega (national representative) invited about 25 scientists to participate and about 20 of these attended. Although no responsibilities were assigned, Ortega will select 6-8 scientists to lead the compilation in specific regions. There appears to be a high-level of interest and commitment to this project from the Mexican scientific community. A draft map of Mexico might be completed in about a year, and a progress meeting will probably occur at one of their national earth science meetings in the fall of 1994.

United States: We conducted project business at two meetings this year. At the GSA meeting in Reno in May, we had an opportunity to discuss the status of compilation for most of the western states, and to gain further commitments. At AGU in San Francisco, we held our first meeting concerning the California map of active faults, and were partially successful in gaining commitments. The main problems with California are the large number of faults and folds and the overwhelming amount of data that must be compiled.

By the end of FY 93, we had obtained digital data for Quaternary faults in California, Nevada, Utah, Colorado, the west half of Montana, and parts of New Mexico. The California faults were scanned in Menlo Park using a specially prepared version of Jennings' 1992 fault map. This file has been edited, but needs to be revised to reflect changes made on the upcoming (1994) version of Jenning's map. In addition, there is concern of the part of the CDMG about release of digital data. The USGS and CDMG are currently discussing how and when such data can be released. The files for most other states come from sources within the USGS or from state geological surveys which do not hold copyrights to their products (Table 1).

In May, we released a comprehensive list of guidelines for the compilation of the digital map and database. This report includes definition of terms, examples from compiled faults, extensive notes for the data comment fields, and sample forms. The guidelines have been distributed widely, and are being used by many of those listed in Table 1.

We have been testing our methods of digitization and data compilation on an area of western Montana and eastern Idaho, where we had previous experience with Quaternary faulting. The results of this pilot study were presented at the GSA meeting in Reno, and we received many favorable comments. The product is nearly complete, and we intend to submit the map and text data for USGS review in early 1994. In addition, a preliminary version of the California and Nevada fault maps were presented at the AGU meeting in San Francisco. The response to these poster sessions indicates a high demand for the digital products.

TABLE 1. Status of Quaternary fault data for selected regions of the United States
*[Data quality: **A**, good; **B**, adequate; **C**, poor or nonexistent]*

State/region	Map and Type	Database and Type	Main Contacts
Alaska	*A.* Digital, 1994	*A.* Text, unpublished	Plafker
Arizona	*B.* Nondigital, ca. 1987	*B.* Partial, text; ca. 1987	Pearthree
California	*A.* Digital, 1992; needs further revision	*B.* Partial, text;1984, 1992	Consortium (USGS, CDMG, others)
Colorado	*B.* Digital, ca. 1987	*B.* Partial, text; ca. 1987	Colman, Kirkham
Eastern U.S.	*C.* Uncompiled	*C.* Uncompiled	Talwani, Prowell, Tuttle (?)
Idaho	*C.* Digital for north half, 1993	*C.* Partial; text, 1993	Haller, Pierce, Breckenridge
Mid-Continent	*C.* Uncompiled	*C.* Uncompiled	Crone, Obermeier, Schweig, others
Montana	*B.* Part digital, 1993	*C.* Partial, text; 1993	Haller, Machette, Stickney
Oregon	*B.* Non-digital and digital (offshore), 1992	*B.* Partial, text; 1992	Pezzopane, Yeats, Wells
Nevada	*A.* Digital, 1991; needs revision	*C.* Partial, text; 1993	Dohrenwend, Piety, Haller, Machette
New Mexico	*B.* Part digital, ca. 1987	*B.* Partial; text, ca. 1987	Machette, Kelson
Texas (West)	*B.* Nondigital, 1993	*C.* Uncompiled	Collins
Utah	*A.* Digital, 1993	*A.* R-base, 1993	Hecker, Jarva
Washington	*B.* Non-digital, 1991	*C.* Uncompiled	Walsh
Wyoming	*B.* Non-digital, 1991	*C.* Partial, text; 1991	Case, McCalpin, Pierce

2. Preliminary interpretation of results from our Pleasant Valley trenching study were presented at GSA in Reno. Our early interpretation emphasized long recurrence intervals and no evidence of Holocene faulting had been found. However, preliminary identification of an ash found in the Sheep Creek trench suggested a probable correlation with a 1-2 ka eruption in the Mono Craters area (A.M. Sarna-Wojcicki). This new data forced us to interpret the penultimate faulting event as late Holocene, a conclusion that seemed unlikely from geologic and geomorphic considerations. Further field studies at several sites along the Pearce scarp revealed no geologic evidence for a late Holocene faulting event. Also, further examination of the ash by Sarna-Wojcicki showed only 3% tephra in the sample; thus, the sample cannot be correlated with any source with confidence. Final interpretation of results are pending the completion of thermoluminescence dating of 10 samples from a number of the trench sites. Preliminary dates suggest that an interpretation of long average recurrence intervals (tens of thousands of years) is correct.

3. The results from our Gilbert Fellowship research on intraplate faulting in Australia (see reports listed below) show that historic intraplate earthquakes typically reactivate ancient faults, but are characterized by long recurrence intervals. On September 29th of 1993 another historic surface-rupturing earthquake was added to the international catalog, bring the total to 11 events. The Latur, Southern India earthquake only had a magnitude of 6.3 (M_S), but it proved to be devastating—causing more than 10,000 deaths, and hundreds of thousands of injuries. The earthquake reportedly had at least 1 km (and possibly as much as 3 km) of rupture, which places it well above the lower threshold for rupture events in intraplate regions. In Australia, the 1970 Calingiri (M_S 5.7) and 1986 Marryat Creek (M_S 5.8) earthquakes caused 3 and 13 km of surface rupture (respectively), whereas the Tennant Creek sequence (M_S 6.3-6.7) formed three scarps with 34 km of surface rupture.

REPORTS

Crone, A.J., and Machette, M.N., 1993, A paleoseismic view of seismic hazards in eastern and central North America—With a comparison to earthquakes in Australia: Geological Society of America Abstracts with Program, v. 25, no. 7, p. A-132.

Crone, A.J., and Machette, M.N., 1993, A paleoseismic view of seismic hazards in stable continental regions—Similarities between the 1993 Latur, Southern India earthquake and Australian and North American intraplate earthquakes [abs.]: EOS, 1993 Fall Meeting Program, p. 218 and 222.

Crone, A.J., Machette, M.N., Bowman, J.R., 1992, Geologic investigations of the 1988 Tennant Creek, Australia, earthquakes—Implications for paleoseismicity in stable continental regions: U.S. Geological Survey Bulletin 2032-A, 51 p., 2 plates.

Haller, K.M., Dart, R.L., and Stickney, M.C., 1993, A compilation of major active faults for parts of Montana and Idaho: Geological Society of America Abstracts with Program, v. 25, no. 5, p. 46.

Haller, K.M., Dart, R.L., and Machette, M.N., 1993, Guidelines for U.S. Database and Map, June 1993 (prepared for Maps of major active faults, Western Hemisphere, International Lithosphere Program (ILP) Project II-2): U.S. Geological Survey Open-File Report 93-338, 35 p.

Hutton, J.T., Prescott, J.R., Bowman, J.R., Crone, A.J., Machette, M.N., and Twidale, C.R., Thermoluminescence dating of Australian paleoearthquakes: Quat. Geochronology (in press).

Machette, M.N., and Crone, A.J., Geologic investigations of Australian earthquakes—Paleoseismicity and the recurrence of surface faulting in stable regions of continents: Submitted to Earthquakes and Volcanoes, 12 ms. p., 6 figs. (in press).

Machette, M.N., Crone, A.J., Bowman, J.R., 1993, Geologic investigations of the 1986 Marryat Creek, Australia, earthquake—Implications for paleoseismicity in stable continental regions: U.S. Geological Survey Bulletin 2032-B, 29 p., 2 plates.

Machette, M.N., Haller, K.M., and Berryman, K.R., 1993, Prehistoric movement along the 1915 Pleasant Valley fault zone and implications for the Central Nevada Seismic Belt: Geological Society of America Abstracts with Program, v. 25, no. 5, p. 112-113.

Machette, M.N., Haller, K.M., and Dart, R.L., 1993, The United States map of major active faults: Geological Society of America Abstracts with Program, v. 25, no. 5, p. 112.

Machette, M.N., Haller, K.M., and Dart, R.L., 1993, A new digital map and database of major active faults in the United States: EOS, Supplement to v. 74, no. 23, p. 66.

Collaborative Research (Arizona State University and San Diego State University): Fault Structures and Earthquake Potential of the San Jacinto and San Andreas Fault Zones Near San Bernardino, California, from the Analysis of Seismic Data
Project Number 1434-93-G-2303
Element II

Harold Magistrale
San Diego State University
Department of Geological Sciences
San Diego, California 92182
(619) 594-6741
harold@hal.sdsu.edu

Christopher Sanders
Arizona State University
Department of Geology
Tempe, Arizona 85287-1404
(602) 965-3071
csanders@seisnext.la.asu.edu

Investigations undertaken:

The San Bernardino, California, area lies across the northern portion of the seismically active San Jacinto fault zone and is bounded to the north by the San Andreas fault zone. We obtained high quality hypocenters to investigate the seismic characteristics of the San Jacinto and San Andreas fault zones to identify seismological and geological features which may bound individual fault segments, which will help estimate the probable extent of fault rupture in individual earthquakes.

Sanders [1989] proposed a tentative segmentation model of the northern San Jacinto fault zone based on fault geometry observed at the surface (here we use his segment names). We can examine the seismicity patterns along and between each segment to determine if the surface fault geometries extend to seismogenic depths. A throughgoing fault that connects the aligned San Bernardino strand of the San Andreas fault zone and the Coachella Valley segment of the Banning fault can be hypothesized. Here we use microseismicity patterns to test for the presence or absence of a throughgoing fault.

To get high quality hypocenters we invert 560000 arrival times of 23000 earthquakes in a 1° by 2° area surrounding San Bernardino, California for hypocenters and 3-D P-wave velocity structure.

Results:

The boundary between the Lytle Creek-Glen Helen and San Bernardino segments is marked by a 3 km right step in the surface trace of the faults that is also defined by the hypocenters (Fig. 1, cross section BB'). This boundary is the location of a sharp 5 km step (shallower to the north) in the maximum depth of hypocenters (cross section AA').

At the surface the boundary between the San Bernardino and San Jacinto Valley segments is a 2 km left step between the fault traces. This step is not seen in the hypocenters (cross section CC'). Hypocenter depths gradually shallow southward by 2 km across the boundary. This boundary is also the site of the intersection of the Banning-Crafton Hills fault zones. The San Jacinto Valley segment lacks shallow (<8 km depth) earthquakes that are common along the San Bernardino segment (cross section AA').

The San Jacinto Valley segment has relatively few earthquakes but its location and near vertical attitude can be defined with hypocenters (cross section DD'). This segment is on strike with the hypocenter lineation defining the Anza segment (cross section EE'). Earthquakes are deeper on the Anza segment. In cross section FF' the hypocenters define a slight right bend as the Anza segment bends to the more northerly strike of the San Jacinto Valley segment. It appears that the large right step between the San Jacinto Valley and Casa Loma segments (occupied by San Jacinto Valley) does not exist at depth. The south end of the Hot Springs segment is well defined by hypocenters. An east dipping hypocenter plane connects the Anza and Hot Springs segments (cross section FF').

The hypocenters image two features along the San Andreas fault zone in the study area. One is an abrupt 6 km shallowing of the maximum depth of earthquakes going from south to north. The other is the north dipping Banning fault zone (including the Garnet Hill fault and Crafton Hills fault zone). In places the two features are coincident.

In the east part of the study area the step in maximum hypocenter depth is vertical to steeply southwest dipping and its position appears to be controlled by the Mission Creek fault (cross sections GG', HH' and II'). Further west the step changes attitude to north dipping (cross sections JJ', KK', and LL') and it appears to be the down dip continuation of the Banning fault zone until it intersects the San Jacinto fault zone.

The Banning fault is best expressed in the seismicity pattern as aftershocks of the North Palm Springs earthquake (cross sections GG' and HH'). The depth extent of these aftershocks appear to be controlled by the tread or riser of the depth step. Further west the north dipping Banning fault zone is defined by the hypocenters in cross sections II', KK', and LL' until the Banning fault zone intersects the San Jacinto fault zone.

Two of the three examined segment boundaries along the northern San Jacinto fault zone do not appear as significant at seismogenic depths as they do at the surface. The Anza segment appears to connect directly with the San Jacinto Valley segment which in turn appears to connect directly to the San Bernardino segment. This is notable in light of the identification of the Anza segment as a slip gap where future earthquakes may originate.

Near the San Andreas fault zone the step in maximum hypocenter depth reflects fundamental differences in rock properties between each side of the step. We interpret the step as a result of juxtaposition of different rock types by large scale displacement along the San Andreas fault zone. The presence of the step may have controlled the location of the western part of the Banning fault zone as it formed. The step may be offset by the San Jacinto fault zone. The depth step between the Lytle Creek-Glen Helen and San Bernardino segments of the San Jacinto fault zone (cross section AA') is similar in character to the step in maximum hypocenter depth along the San Andreas fault zone. The offset between the depth steps is 20 to 25 km, comparable to the total offset along the San Jacinto fault zone (24 km). This may support the idea that San Andreas slip is transferred to the San Jacinto fault zone via the Banning fault.

The step in maximum hypocenter depth along the San Andreas fault zone strikes obliquely to a hypothetical throughgoing fault that connects the aligned San Bernardino strand of the San Andreas fault zone and the Coachella Valley segment of the Banning fault. The depth step crosses such a fault without any apparent offset. We conclude there is not such a throughgoing San Andreas fault in the study area.

Reference:

Sanders, C. O. (1989). Fault segmentation and earthquake occurrence in the strike-slip San Jacinto fault zone, California, *U. S. Geol. Surv. Open-File Rept., 89-315*, 324-349.

Report published:

Magistrale, H. and C. Sanders (1993). Seismotectonics and segmentation of the San Andreas and San Jacinto fault zones near San Bernardino, CA. (abstr.), *EOS Trans. AGU* **74**, p.420.

Figure 1. Relocated earthquakes and cross section locations. Heavy line indicates location of the step in maximum depth of earthquakes along the San Andreas fault zone. Symbol size scales to earthquake magnitude.

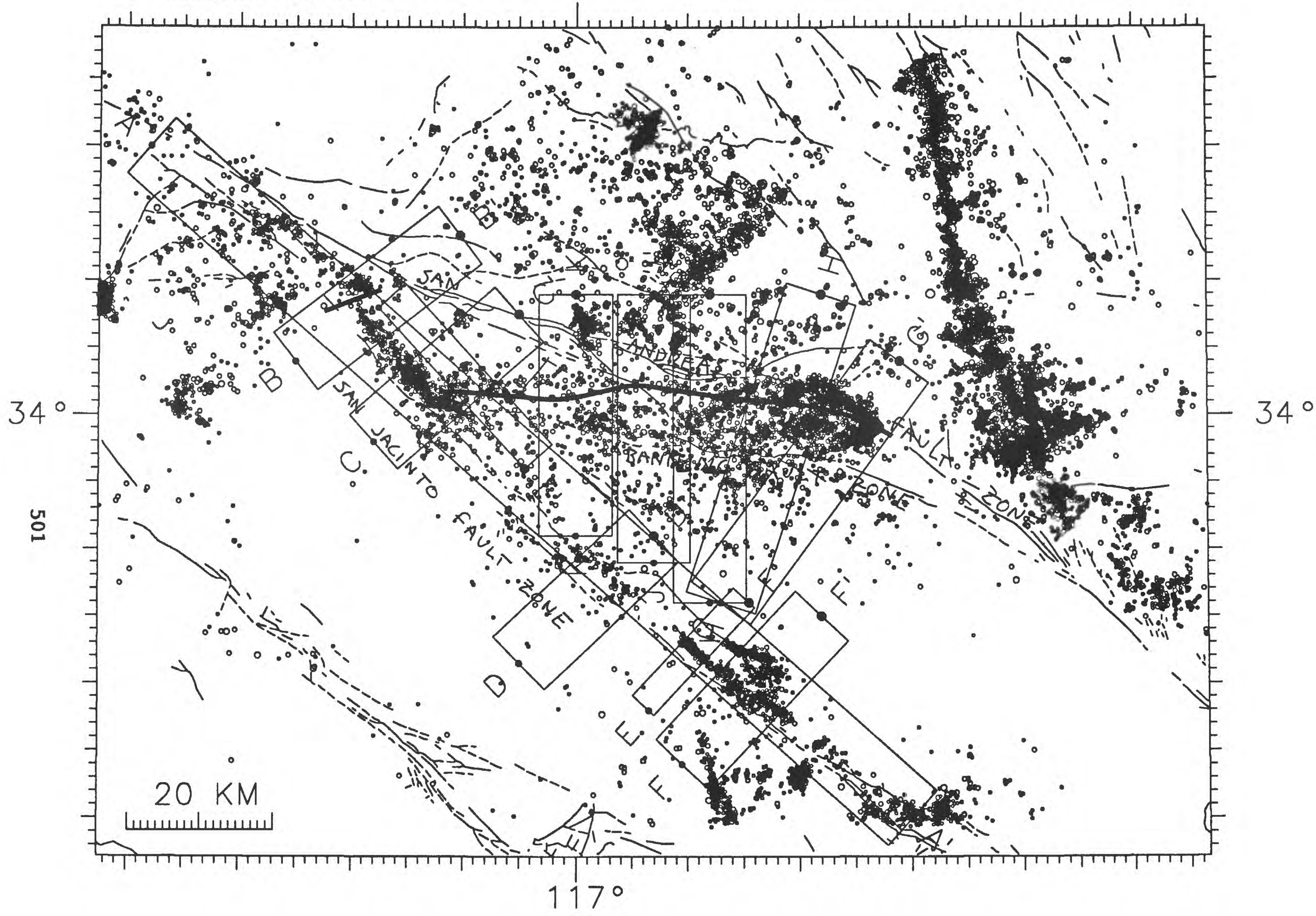

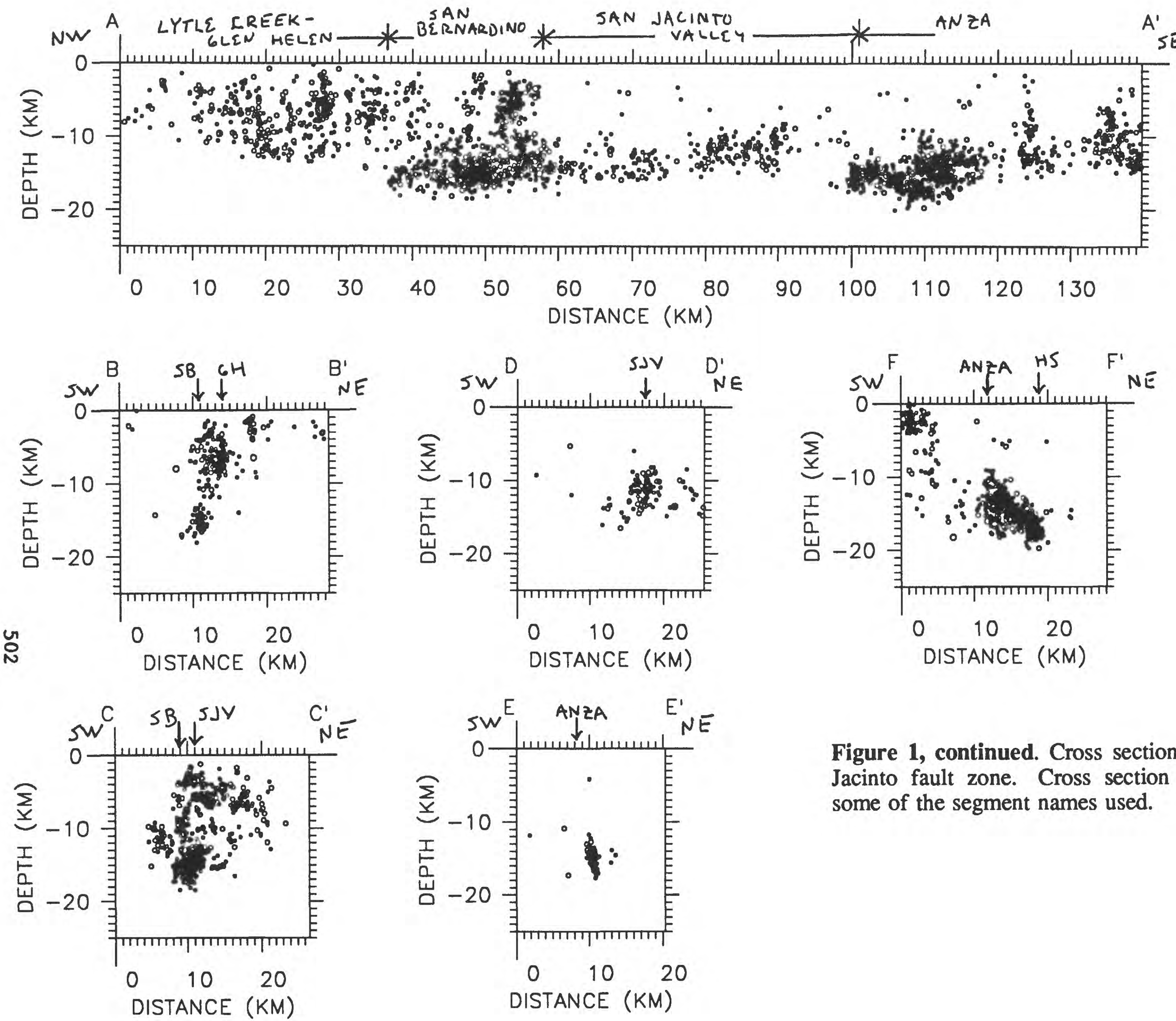

Figure 1, continued. Cross sections near the San Jacinto fault zone. Cross section AA' indicates some of the segment names used.

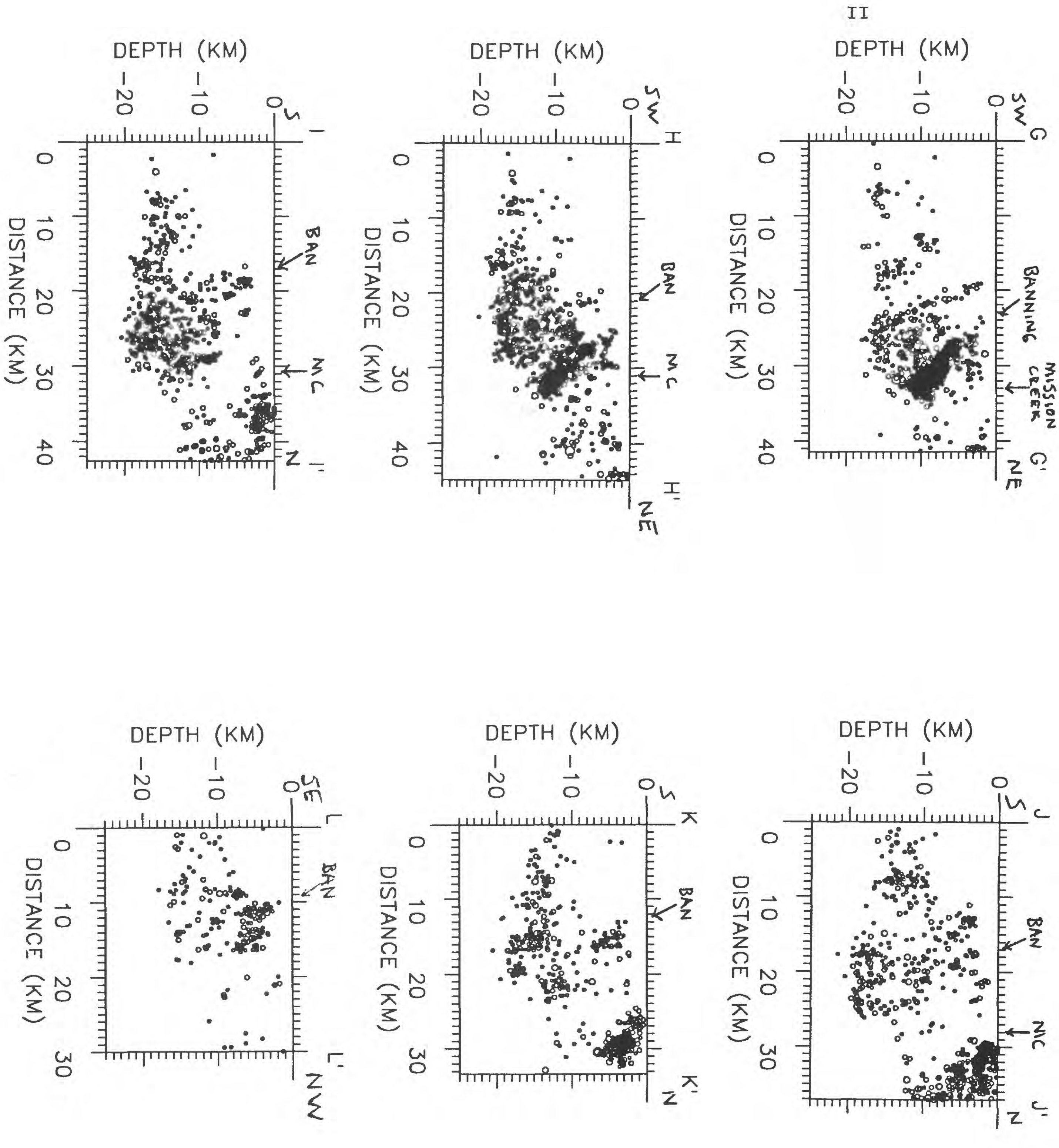

Figure 1, continued. Cross sections near the San Andreas fault zone. Note the step in maximum depth of earthquakes.

A Friction-Feedback Model for Seismicity at Parkfield, California

Award No. 1808 Program Element II.7

P. E. Malin [1], V. G. Oancea [2], and E. Shalev
[1] Department of Geology,
[2] Department of Civil & Environmental Engineering,
Duke University,
Durham, NC ,
27706.

ABSTRACT. Between mid-1989 and mid-1991, the San Andreas fault at Parkfield, California, experienced a major change in the number and size of microearthquakes taking place there. Parts of this activity are organized into a migrating earthquake sequence with a propagation speed much slower than possible in models of fault interactions based on simple elasticity and frictional sliding. Instead, this sequence can be modeled by a coupled, 2 layer, block-slider system governed by interacting velocity-weakening and velocity-strengthening frictional forces. The coupling between the two layers is assumed to be viscoelastic, accounting for aseismic slip on ductile portions of the fault. To represent the Parkfield asperity, a set of blocks in the velocity-weakening layer were given greater frictional resistance. This friction-feedback model shows how the asperity forms a barrier to a migrating sequence and how one aspect of plate motion redistributes its slip along a weak fault zone.

REPORT. The San Andreas fault at Parkfield, California, continues to be an important focus of the US program in earthquake prediction (1; Figure 1). In fact, over the past year or so this area has experienced a notable increase in earthquake activity, including m=4.7 and m=4.8 events that triggered public earthquake warnings (2). In this paper, using microearthquake data we have collected at Parkfield (3, 4), we demonstrate that a significant, episodic, change in microeathquake activity occurred several years prior to these events. We also provide a simple "friction-feedback" model for the observed space-time pattern of the microearthquakes. These patterns show rates and distances of earthquake migration that can not be explained in terms of redistribution of fault slip by elastic loading of asperities held together by simple friction. Instead, the seismicity suggests an interactive process of seismic and aseismic slip within and below the seismogenic portion of the fault.

A time- and distance-dependent sum of earthquake numbers, magnitudes, and moments can be used to demonstrate the existence of the migrating earthquake sequence (5, 6). Such a sum can be visulized from a latitude verses origin-time plot of the microeathquake data in Figure 1 (as we show and discuss later in Figure 4). By taking strips of data oriented in different ways on such a plot, and summing, for example, the number of event within a given strip, a moving increase or decrease in activity can be detected. For equal weighting of each oriention, or migration velocity, the areas of the strips must be kept constant. This is so that in the case of a homogeneious space-time distribution of microearthquakes, the sums of numbers, magnitudes, and moments are also constants, independent of migration velocity.

The results of this analysis for Parkfield microearthquakes are shown in Figure 2. In this plot, cumulative number, magnitudes, and moments are displayed as functions of migration velocity and arrival time at latitude $36^{o}59.5'$, which is the latitude of Middle Mountain (Fig. 1). Migration velocities representing changes traveling both from the north and south were include in the analysis, with the center of the velocity axis representing a 100 day wide strip moving at infinite velocity. The cumulative numbers of events, magnitudes, and moments have been contoured to show the regions of significant changes. Examples of such changes are the earthquakes and aftershocks that have occurred since late 1992, which show up as regions of tightly spaced contours of high values moving at large velocities. The specific feature we focus on here is an increase in microearthquake numbers that arrived at Middle Mountain in the last half of 1990 and traveled from the north wtih a velocity between 21 and 78 km/yr (Fig. 2). Because the earthquakes in this event were all very small, it did not result in significant increases in cummulative magnitude and moments.

We have studied the statistical significance of the features seen in Figure 2 using a jack-knife approach to finding the standard deviation of the values shown (7, 8). At the time of the 1990 southward-migrating seismicity increase, the maximum number of events in the analysis strips was at least 180 $\pm$13, as compared to a before and after background of 100 $\pm$10 or so. Thus the number of migrating earthquakes during this episode was on the order of 7 to 8 times the jackknife error of our analysis. The of this event being random can also be crudely estimated by noting that it is the only one of its kind in our data. Partitioning the velocity-date diagram into cells the size of the 1990 event (0.5 yr long and traveling N-S, S-N, or at infinite velocity) , it seems that this type of event could occur randomly at most 1 time in 40 or so.

We propose that the migrating earthquake sequences at Parkfield are due to the interaction of brittle and ductile failure, in large part near the base of the mostly brittle, or seismogenic zone (9-11). The model we propose assumes a weak San Andreas fault that is strongest near this base, below which the fault is mostly ductile and weakens relatively slowly with further depth, as illustrated in Figure 3a. Both the brittle and ductile zones are subject to the strike-slip forces of plate motion, with failure of both zones tending to occur near their boundary, where this system is the strongest. At Parkfield this picture is supported by the fact that the largest microearthquakes with the largest stress drops tend to occur at this depth (4, 12).

To show how this model accounts for the migrating earthquake sequences, we have reduced it to a system of simple block-sliders, shown schematically in Figures 3b and 3c (13-15). The model consists of two, coupled, one-dimensional layers of spring-connected block-sliders with different frictional properties. In this representation, after being loaded to failure, the upper layer of blocks resists sliding with a velocity-weaking friction law. In the lower layer, the frictional resistance is assumed to increasing with the velocity of the blocks. The blocks of each layer are coupled together by a system of dashpot-spring units (Maxwell bodies). The dashpot-spring units represents the viscoelastic character of the two crustal layers, accounting not only for their elastic connection, but their relaxation properties as well..

The specific system of blocks for our Parkfield model consists of 100 blocks: 50 brittle and 50 ductile, numbered from south to north. One end of the 2 layer system was assumed to represent the creeping San Andreas fault north of Middle Mountain. The steady pull of the lithospheric plates was applied to the ductile layer at this end. The southern end of the system was assumed to extend south of the Gold Hill area. The static friction of the entire system was randomly varied by a maximum of 10%. To account for the presumably stronger, aseismic Parkfield "asperity" near Middle Mountain where the previous M=6 earthquakes nucleated (16), the static friction of brittle blocks 15 to 22 was increased by an average of 60%.

The equations of motion in non-dimensional form were derived from Lagrange's equation. These were numerically integrated for many thousands of time steps and hundreds of cases of relative strength, stiffness, relaxation time, and velocity weakening and hardening rates (15). Failure and rapid slip of the blocks in the brittle layer were identified as microearthquake events, whose total area and slip were used to calculate relative magnitudes. The location and size of the events were then displayed in the same fashion as the latitude-magnitude-origin time plot of the Parkfield events, as shown in Figure 4. In the case shown in Figure 4b., the dashpot-spring unit had a relaxation time of 0.5 time units and an instantaneous stiffness approximately an order of magnitude large than that of the 2 layers.

The main feature of our block-slider simulation of Parkfield seismicity is the appearance of event sequences with migration speeds below simple brittle redistribution of the plate slip. The differing speeds result from the damped feedback between the frictional properties of the brittle and ductile layers. Evidently, parts of this 2 layer, friction-feedback system can hang up, producing a period of low activity followed by a slow, southward migrating seismicity front. Rapidly moving fronts also appear, in both the north and south directions, as in recent Parkfield seismicity. The different migration speeds are a consequence of slip-energy snaking back and forth between the brittle and ductile layers.

The blocks that model the Parkfield asperity form a barrier to the southward migrating sequences: events either terminate or propagate northward from there. Presumably a simultaneous failure of the asperity blocks would represent a repeat of the Parkfield earthquake. Some activity does take place within the asperity and to its south, as slip in the ductile zone passes it by. Either the strength of the brittle zone is too high or the load too slow and small. Moreover, both the system of block-slider and method for calculating event size have natural limits that may not cover this case.

References and Notes.

1. A. Michael and J. Langbein, *EOS* **74**, 145, 153-155 (1993).
2. J. Langbein et al., *ibid* **74**, 152-153 (1993); the second warning was issued by the USGS Parkfield Working Group, Menlo Park, J. Langbein, Chief Scientist, after the m=4.8 on November 14, 1993.
3. P. E. Malin and M. G. Alvarez, *Science* **256**, 1005-1007. (1992).
4. P. E. Malin et al., *ibid* **244**, 557. (1989).
5. This general approach was suggested to us in various stages by, T. McEvilly, A.J. Michael (e.g., A.J. Michael, *EOS* **74**, 43, 447, 1993), and one of our past reviewers. Its implimenation here is our own.
6. The moments and corner frequencies were determined from the S-wave frequency spectra using the methods of D. J. Andrews, in *Earthquake Source Mechanics*, K. Aki and P. Richards, Eds., *American Geophysical Union Monograph 37*, American Geophysical Union, Washington, D. C., (1986). The largest earthquake in 1990 was a local magnitude 3.3; the m=4.7 took place on Oct 20, 1992, rupturing a few kilometers of fault and producing a more typical aftershock sequence (2).
7. B. Efron, The Jackknife, the Bootstrap and other Resampling Plans, Society for Industrial and Applied Mathematics, Philadelphia, PA., 1982.
8. The estimates of the statistical errors in velocity-time analysis were found by 3 jackknife studies of the data. For the 3 tests, the data were randomly assigned to one of 15, then 30, and finally 60 different groups. Jackknife errors were then calculated for each set of groups.
9. J. Savage, *J. Geophys. Res* 76, 1954 (1971).
10. F. K. Lehner, V. C. Li, J. R. Rice, *J. Geophys. Res* **86**, 6155 (1981).
11. R. Wesson, *EOS* **65**, (1985)
12. M. E. O'Neill, *BSSA* **74**, 27 (1984);
13. Haung and Turcotte, *Nature*, **348**, 234-236 (1990).
14. Shaw et al., *J. Geophys. Res.*, 97, 479-488 (1992).
15. Malin and Oancea, ms in preparation, 1993.
16. W. H. Bakun and T. V. McEvilly, *J. Geophys. Res.* **89**, 3051 (1984).

17. We thank colleagues at the University of California at Berkeley and the United States Geological Survey for sharing the effort of keeping the Parkfield downhole seismology project alive. This work was support by DOI-USGS grant #14-08-0001- G1375.

Figure Captions.

Fig. 1. Part (a). Map of the seismicity along the San Andreas fault at Parkfield, California. The downhole seismic stations used in this study are shown as triangles, the Middle Mountain station at MM and the Gold Hill station at GH. Part (b). Cross section along the San Andreas fault at Parkfield, California, showing the hypocenters of the microearthquake in the study time period. A total of 2,700 events are show in both plots.

Fig. 2. A migration velocity verses arrival time analysis of the Parkfield microearthquake data shown in Fig. 1. The velocity are for events coming from both the north and south and the arrival time is that at Middle Mountain. The effects of aftershocks have been supressed by removing days with more than 4 nearby earthquakes. Three analysis are shown: (a) cummulative number of earthquakes, (b) cummulative magnitudes, and (c) cummulative moments. The larger earthquakes and their aftershocks are visible on the right, in late 1992 and 1993. The N-S migrating increase in numbers of earthquakes discussed here arrived at Middle Mountain in the last half of 1990, moving southward at roughly 36 km/yr.

Fig. 3. Part (a). A hypothetical strength verses depth curve for the San Andreas fault at Parkfield. The curve is based in part on numerous events and higher stress drops near the bottom of the seismogenic zone (4, 9). Below this level the fault begins to weaken at a relatively slow rate. Part (b). The velocity weakening and velocity hardening friction laws assumed for the brittle and ductile layers of the model (10, 12). Part (c). A schematic representation of the brittle and ductile layers at Parkfield in terms of a block-slider system of springs, dashpots, and masses.

Fig. 4. Part (a). Earthquake magnitudes along the San Andreas fault as a function of latitude and time. The magnitudes of the events are represented by circles of different sizes, with the October M~4.7 earthquake being the largest and M~0 the smallest. Arrows point out the proposed slow (#2) and rapid earthquake migration sequences (#1, #3, #4). Part (b). Results of the friction-feedback model of Parkfield seismicity. As in Part (a), the sizes of the ellipses represent the relative sizes of the events. As indicated by the arrows, both slow, regional and rapid, local earthquake sequences can be simulated with this type of model.

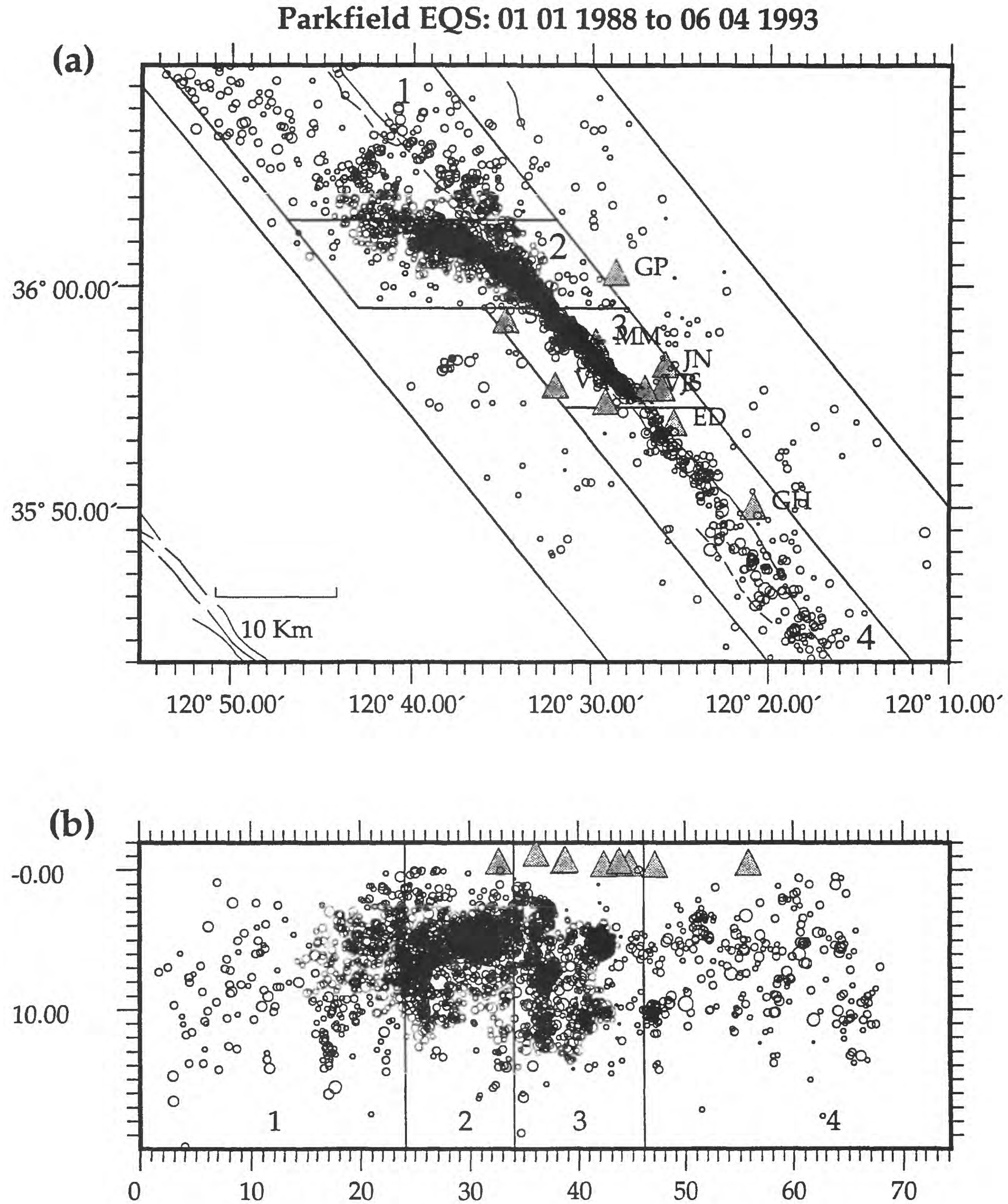
Parkfield EQS: 01 01 1988 to 06 04 1993
(a)
1
2
3
4
GP
MM
JN
VC
VR
ED
GH
10 Km
36° 00.00′
35° 50.00′
120° 50.00′
120° 40.00′
120° 30.00′
120° 20.00′
120° 10.00′
(b)
-0.00
10.00
1
2
3
4
0
10
20
30
40
50
60
70

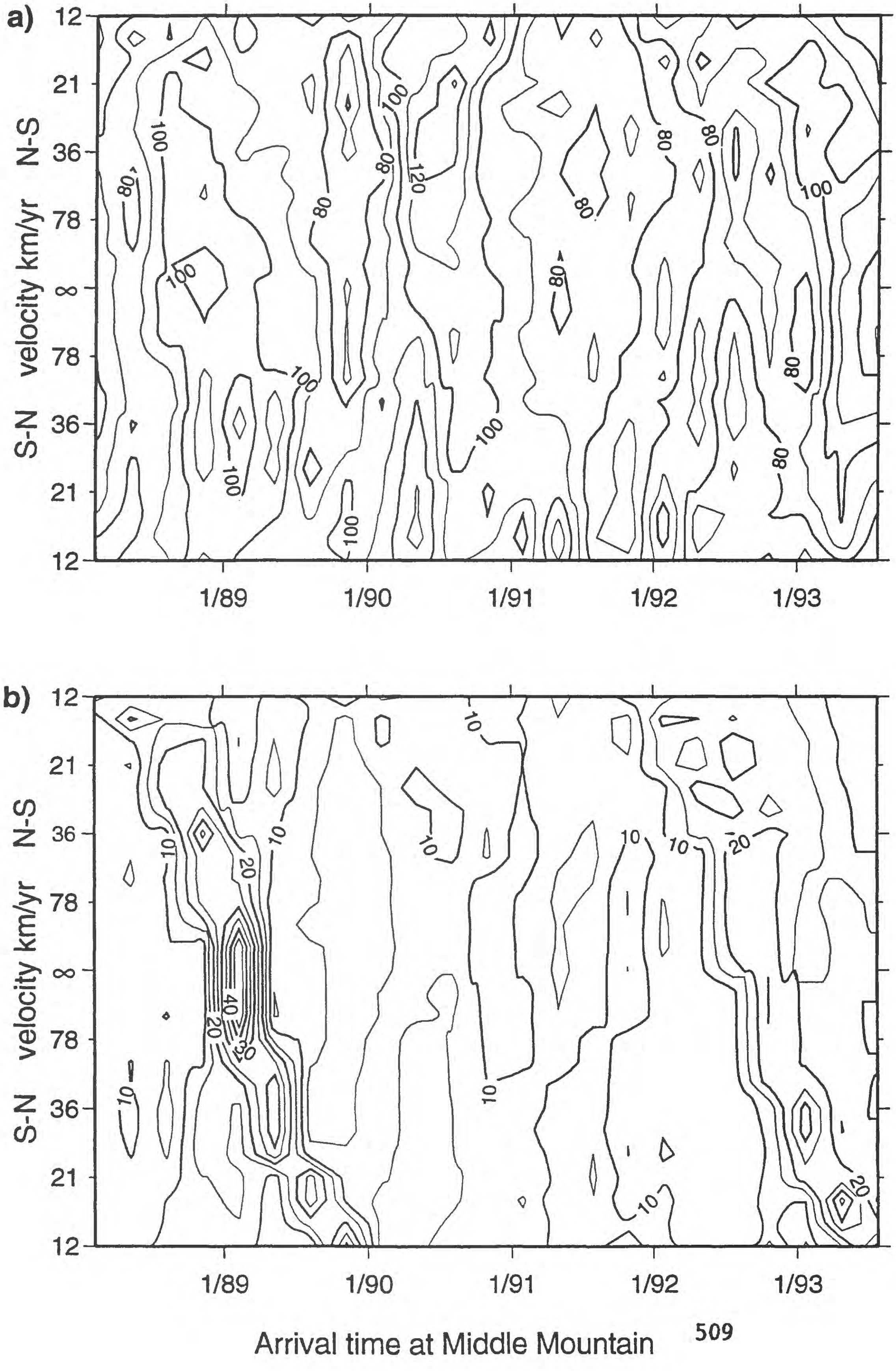
a)
b)
S-N velocity km/yr N-S
12
21
36
78
∞
78
36
21
12
1/89
1/90
1/91
1/92
1/93
Arrival time at Middle Mountain

Figure 4.

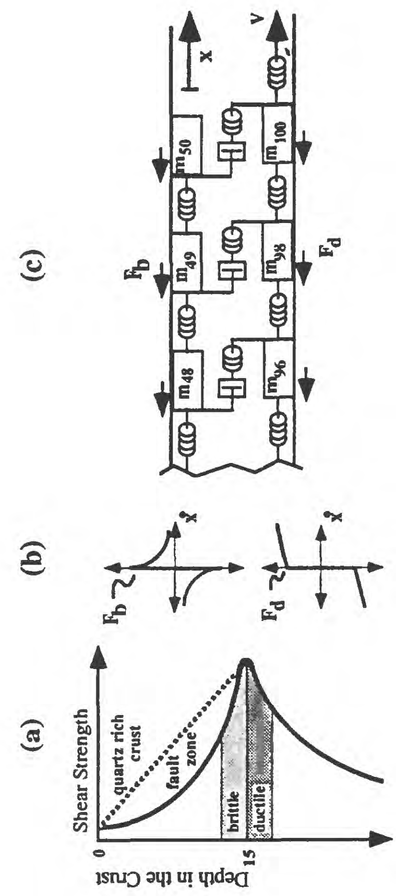
(a)
Shear Strength
quartz rich crust
fault zone
brittle
ductile
0
15
Depth in the Crust
(b)
F_b
$\dot{x}$
F_d
$\dot{x}$
(c)
F_b
m_{48}
m_{49}
m_{50}
m_{96}
m_{98}
m_{100}
F_d
x
v

(a)

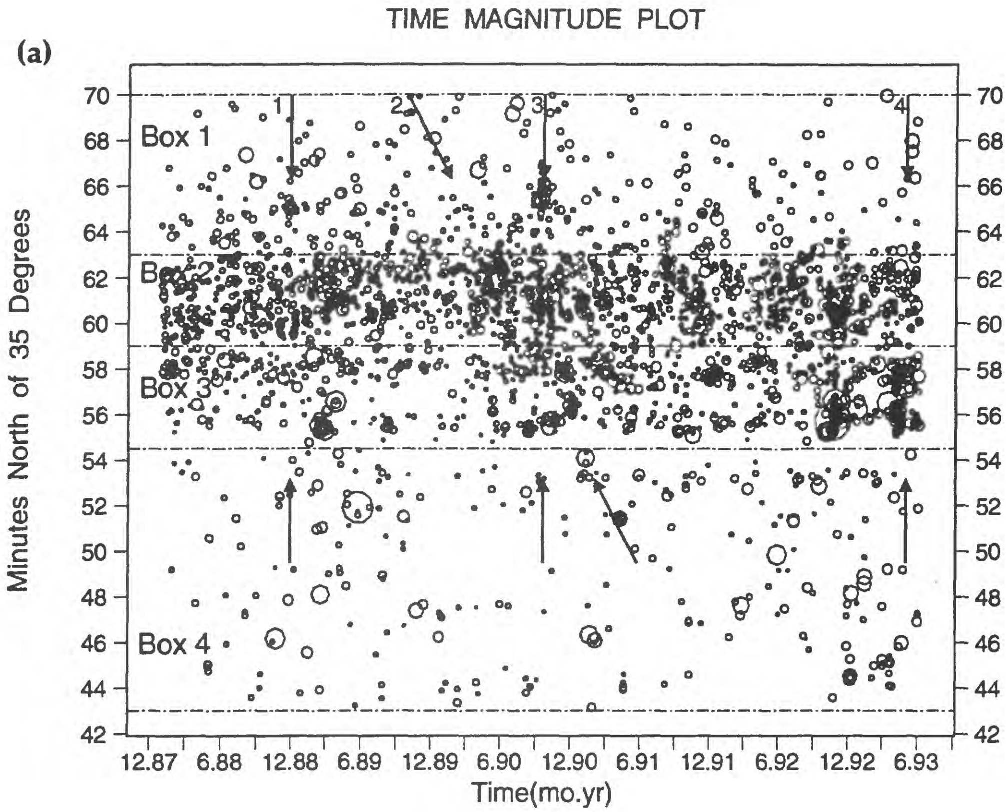
TIME MAGNITUDE PLOT
Box 1
Box 2
Box 3
Box 4
1
2
3
4
Minutes North of 35 Degrees
70
68
66
64
62
60
58
56
54
52
50
48
46
44
42
12.87 6.88 12.88 6.89 12.89 6.90 12.90 6.91 12.91 6.92 12.92 6.93
Time(mo.yr)

(b)

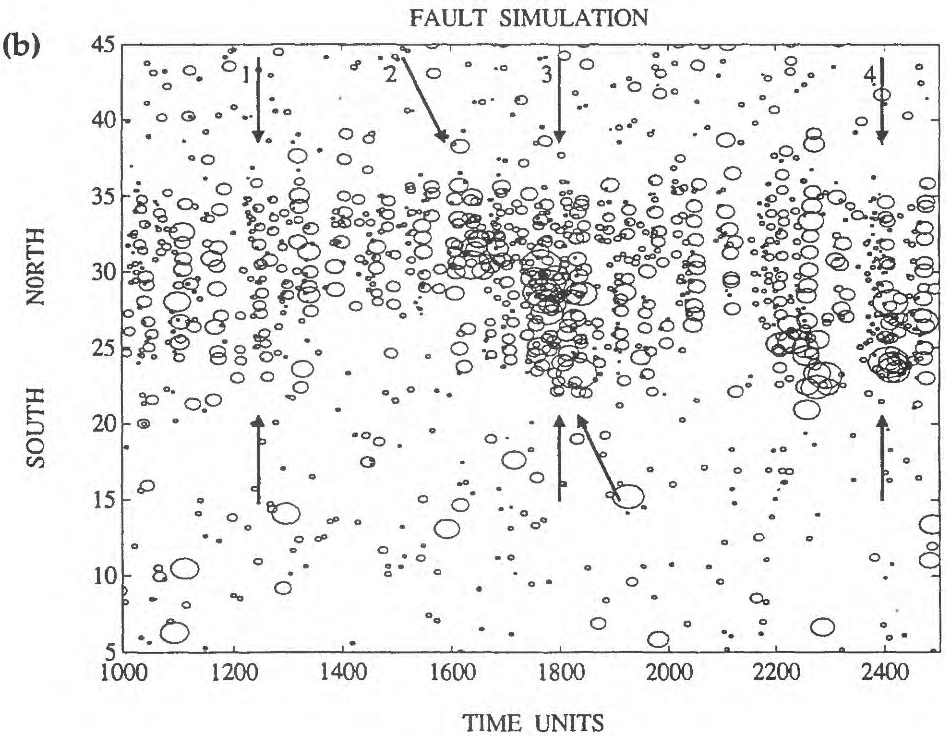
FAULT SIMULATION
1
2
3
4
NORTH
SOUTH
45
40
35
30
25
20
15
10
5
1000 1200 1400 1600 1800 2000 2200 2400
TIME UNITS

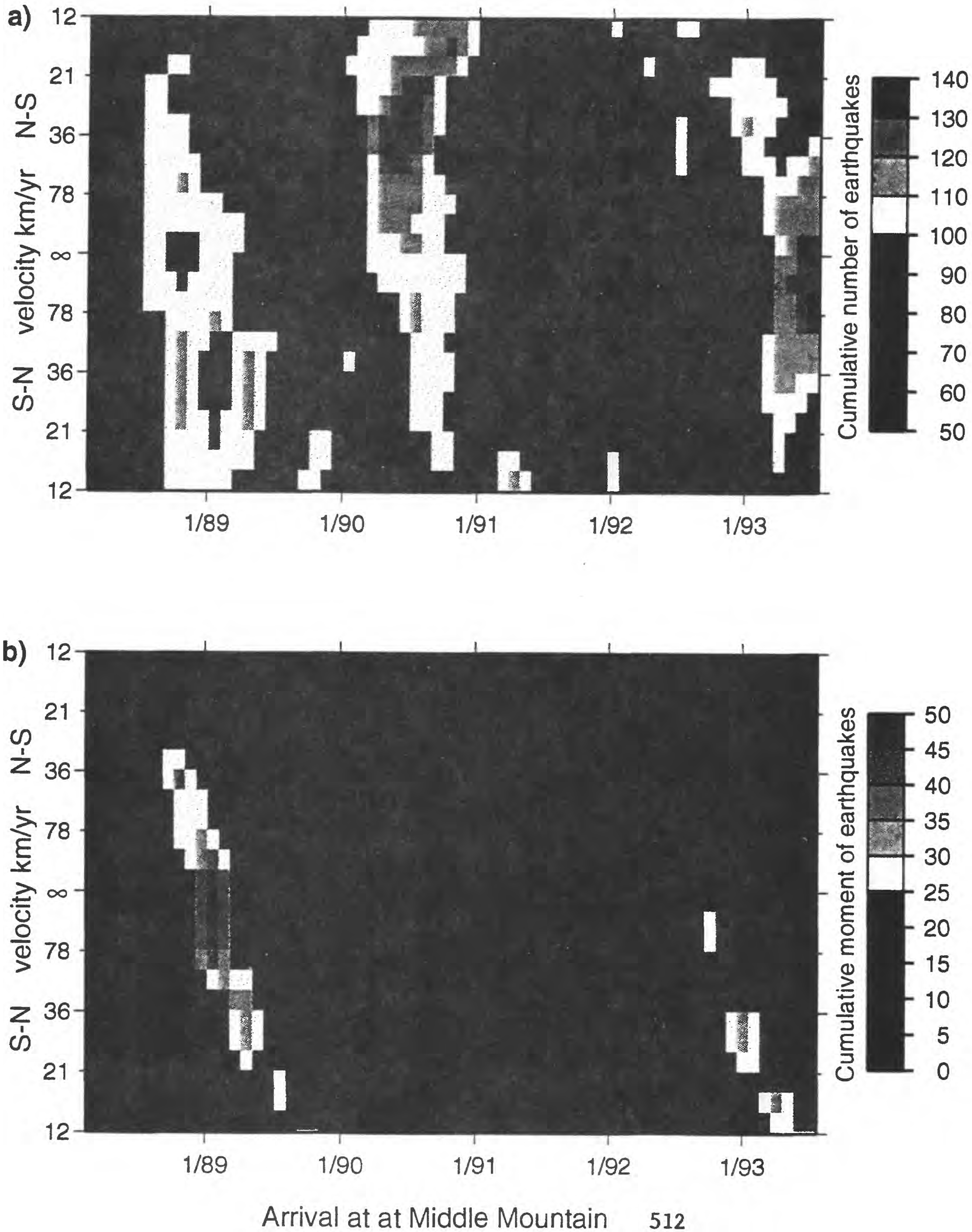
a)
12
21
36
78
∞
78
36
21
12
N-S
velocity km/yr
S-N
1/89
1/90
1/91
1/92
1/93
Cumulative number of earthquakes
140
130
120
110
100
90
80
70
60
50
b)
12
21
36
78
∞
78
36
21
12
N-S
velocity km/yr
S-N
1/89
1/90
1/91
1/92
1/93
Cumulative moment of earthquakes
50
45
40
35
30
25
20
15
10
5
0
Arrival at at Middle Mountain

Instrumentation to Improve the Washington Regional Seismograph Network
1434-92-G-2195 S.D. Malone and R.S. Crosson, P.I.s

Program Element II.2

Geophysics Program
University of Washington
Seattle, WA 98195
(206) 543-8020
e-mail: steve or bob@geophys.washington.edu
Oct. 1, 1992 - Sept. 30, 1993

Introduction

This contract is for the purchase and installation of four new, high quality broad-band digital seismograph stations as an addition to the Washington Regional Seismograph Network (WRSN). It also includes funding for the development of the data acquisition process and integration of these data into the routine data collection and analysis procedures. In addition to the four stations supported under this contract, a prototype station (LON), situated on the same pier as the DWWSSN station at Longmire WA (near Mount Rainier), has been operating for the entire contract period. By the end of the contract period, there will be a total of 7 high quality seismograph stations operating in the Pacific Northwest (5 operated by the WRSN, one by USNSN; NEW and one by IRIS-USGS; COR).

Progress

During this contract period, we completed installation of three new broad-band three-component stations. Two of these (LTY at Liberty, WA and SSW at Satsop, WA) time-stamp, digitize, and record data on-site. Data of interest are periodically retrieved from each site to the UW over phone lines. Station SSW has the highest dynamic range, since it has 24 bits/sample as compared to 16 bits/sample at LTY and LON. We are evaluating recordings from these instruments to determine how to optimize the recovery of useful data. The third station, near Tolt, Washington (TTW), also uses a 3-component broadband sensor and digitizes and time-stamps data on-site, but all of the digital data is continuously telemetered to the UW Seismology Lab by radio and recorded there. Eventually, the data from this site will be reformatted into USNSN format and transmitted to the National Seismic Network in Golden, CO via satellite. Station TTW is currently being operated in a test mode. Figure 1 shows the current network configuration. Table 1 gives the locations of the installed broad-band stations. Selection of an additional broad-band site near Port Townsend in Puget Sound is still pending.

Using an adaptation of the IRIS *GOPHER* dial-up system, we are routinely recovering broad-band data from Liberty, Satsop, and Longmire (LON) and archiving it with our short-period network data. We are working towards closer integration of the two data types. One of our students, Gia Khazaradze, has developed a technique to generate synthetic Wood-Anderson records from the broad-band data. This will allow us to determine local magnitudes from the broad-band data.

TABLE 1
WRSN 3-component Broadband Stations Operating as of 9/30/93

STA	LAT	LONG	EL	NAME
LON	46 45 00.0	121 48 36.0	0.853	Longmire
LTY	47 15 21.2	120 39 53.4	0.970	Liberty
SSW	46 58 20.4	123 26 01.8	0.120	Satsop
TTW	47 41 40.7	121 41 20.0	0.542	Tolt Reservoir, WA

In the previous contract period, we developed and tested a SEED writer for trace data from our analog telemetry network. Because all of the analog data is digitized and time-stamped simultaneously, header information is minimized. During this contract period, we expanded the SEED writer to incorporate data from both broad band and short-period stations. The broadband data, digitized and time stamped at each individual station, is combined with data from our analog stations (digitized and time stamped at the UW) to form a single SEED file. These SEED files will eventually be stored at the IRIS Data Management Center where they will be easily available.

We have completed all hardware requirements for installation of the VSAT communications link from Seattle to the USNSN; through which we plan to receive data from the USNSN station at Newport, WA (NEW) and possibly other stations. NEW is a high-quality, low-noise site and is the only station in Washington east of 118° N longitude. It provided valuable short-period information to the WRSN via telephone lines for many years until the phone line to the UW was terminated in 1987 (data is now telemetered to the NEIC).

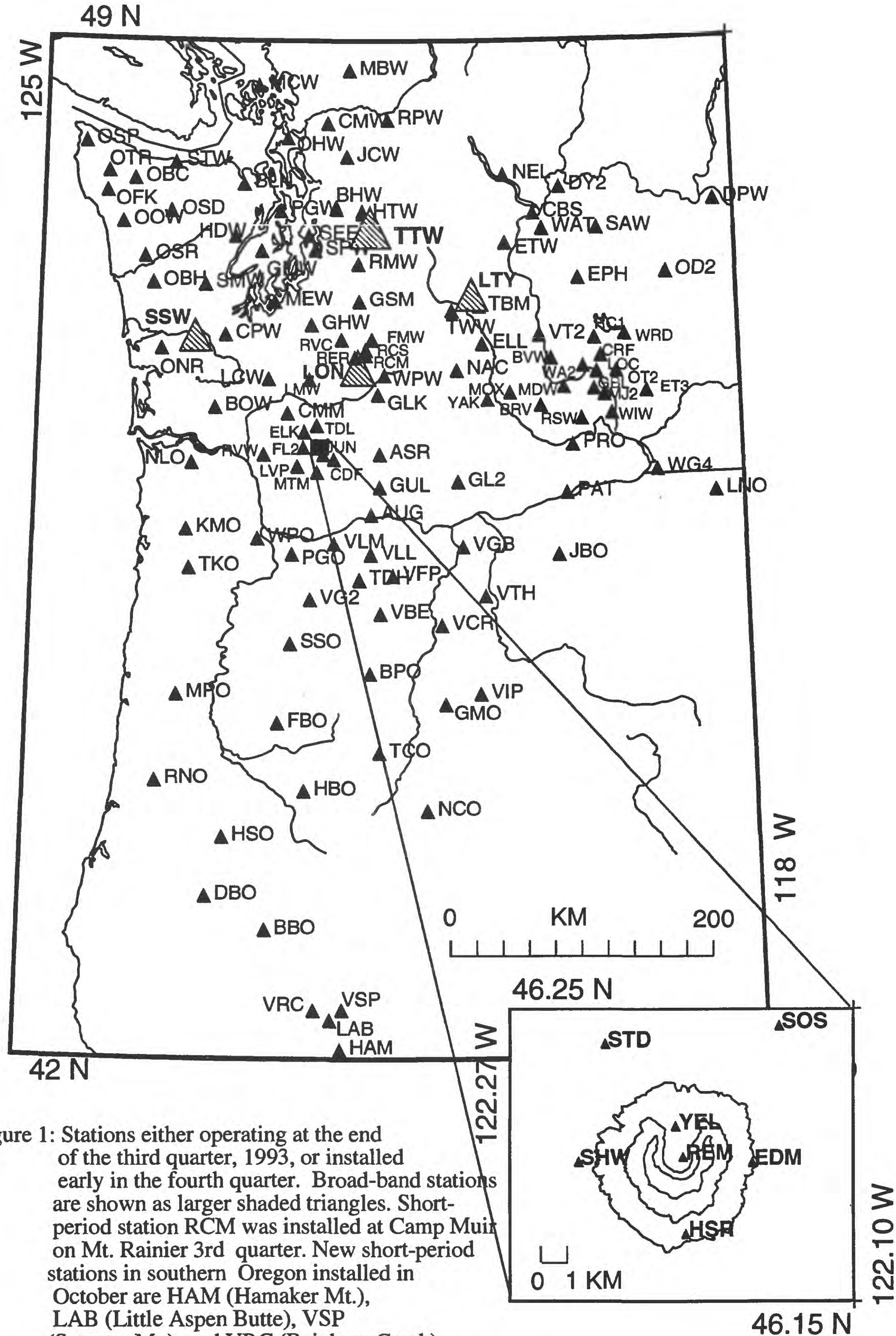

Figure 1: Stations either operating at the end of the third quarter, 1993, or installed early in the fourth quarter. Broad-band stations are shown as larger shaded triangles. Short-period station RCM was installed at Camp Muir on Mt. Rainier 3rd quarter. New short-period stations in southern Oregon installed in October are HAM (Hamaker Mt.), LAB (Little Aspen Butte), VSP (Spencer Mt.), and VRC (Rainbow Creek).

GEOMENSOR MEASUREMENTS IN THE IMPERIAL VALLEY MEKOMETER NETWORK, 1993

1434-93-0-2299
Program Element II.3

Ronald G. Mason
Department of Geology
Imperial College
London, SW7 2AZ, England
(011-44-71) 589 5111

Investigation

In 1991, we initiated a program for leveling our network, starting with the central block of stations, which we extended northwards to provide better coverage of the Imperial fault and the Brawley seismic zone north of their junction. The principal objective of the 1993 fieldwork was to make a trilateration survey of the 1991 extension, with a suitable overlap of the main block. We also planned to tie in a small number of NGS benchmarks used by IGPP, La Jolla, in a 1991 kinematic GPS survey of the network, and to re-measure such lines on and around the fault as time permitted.

Results

The fieldwork, started early in March, was completed by early May. It involved the construction of 18 stations to strengthen the otherwise weak (for trilateration surveys) northern part of the network, and the measurement of 432 lengths, involving 345 lines (Figure 1). About half the lines measured were lines first leveled in 1991, but not previously connected horizontally. The remainder were on and around the Imperial fault, intended to assess movements since the last complete trilateration survey, in 1987. We also tied in four NGS benchmarks that had been occupied repeatedly by GPS during recent years. The standard error of the measurements was about 1 ppm.

It was not part of the 1993 plan to do any leveling. However, we did re-level a 9 km length of the most northerly east-west line (Keystone Road), first leveled in 1991. We also measured vertical angles to all new stations, to enable slope lengths to be reduced to horizontal.

Preliminary analysis of 14 fault-crossing lines spanning a 12 km length of the Imperial fault south of Ferguson Road indicated a mean creep of about 70 mm between the Springs of 1987 and 1993. This compares with a predicted 57 mm based on measurements made up to 1987, the 13 mm excess being approximately equal to the creep induced on the fault by the November 1987 Superstition Hills earthquake sequence.

Re-leveling of the Keystone Road line, which spans the Mesquite basin and includes the Imperial fault and the Brawley seismic zone, revealed a sag of about 20 mm across the basin between 1991 and 1993, but no significant changes associated with either the fault or the seismic zone.

Following completion of our work, IGPP conducted a kinematic GPS survey of the network which will make use of the present measurements and the 1991 leveling data.

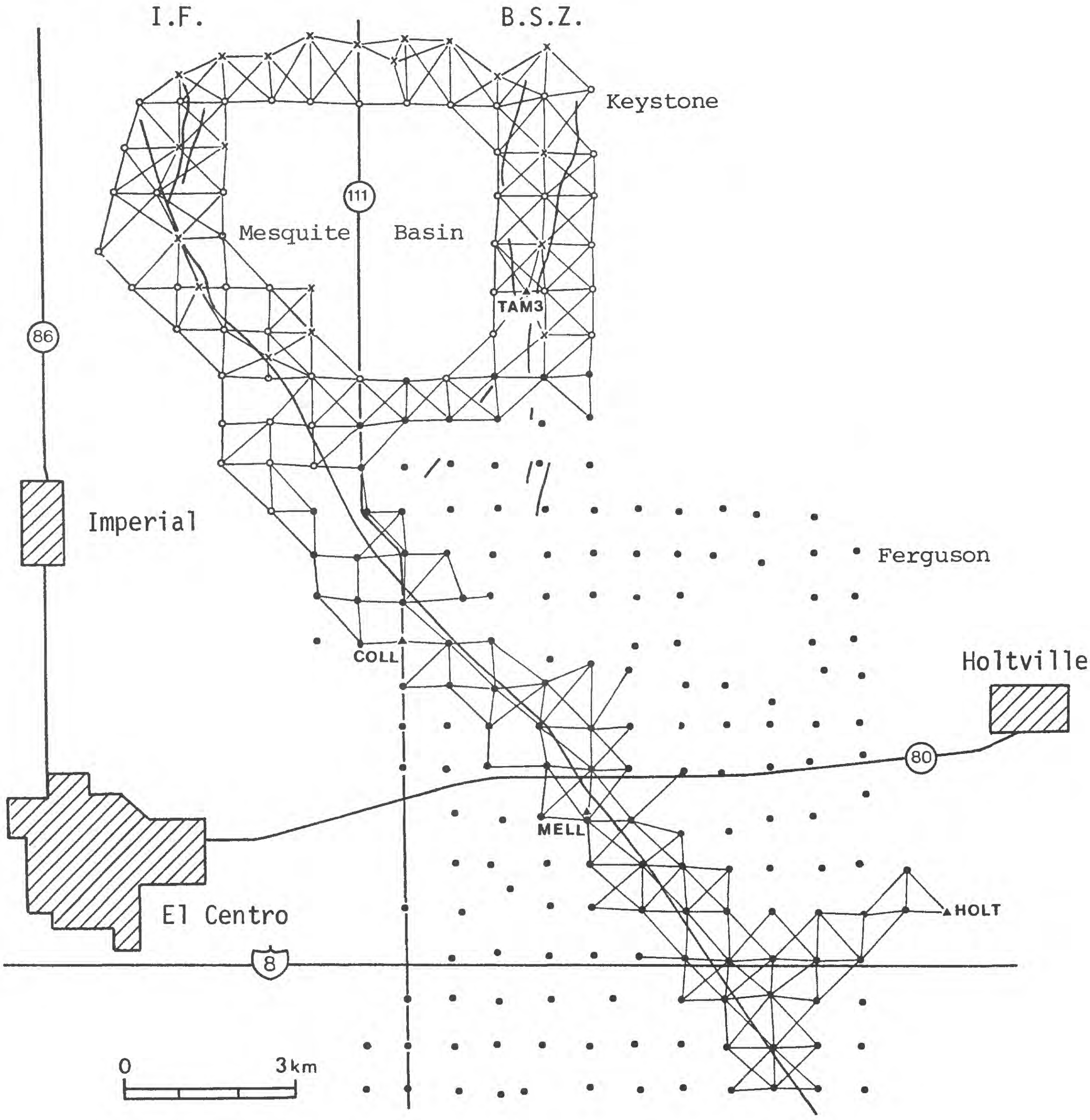

Figure 1. Lines measured in 1993. Solid circles are original stations connected previously in three dimensions, open circles are stations built and leveled in 1991 but not previously connected horizontally, crosses are new stations.

ACTIVE MARGIN TECTONICS, PACIFIC NORTHWEST REGION

9960-13416

P. A. McCrory

Branch of Earthquake Geology and Geophysics
U. S. Geological Survey
345 Middlefield Road, MS 977
Menlo Park, California 94025
(415) 329-5677
pmccrory@isdmnl.wr.usgs.gov
Program Element II

Investigations

This research project addresses the problem of how the Cascadia subduction margin of the Pacific Northwest responds tectonically to varying convergence angles and rates with the objective of understanding whether the timing, style, and rates of regional tectonic deformation can be attributed to plate kinematics. This problem can be approached both spatially and temporally in the Pacific Northwest as active convergence directions and rates vary along the margin. Current research utilizes the technique of forward modeling to reconstruct plate geometries and kinematics in the Pacific Northwest and the technique of geohistory modeling to discern the record of tectonism in late Cenozoic rocks and sediments along the southern Washington margin, along with more traditional geologic techniques to quantify rates of fault movement and tilting of strata.

Although current seismicity is low along the Cascadia margin, geodetic monitoring of interseismic strain accumulation reveals coupling between the Juan de Fuca plate and North American margin, and the Holocene paleoseismic record in the Pacific Northwest reveals cycles of widespread abrupt subsidence of coastal marshes attributed to release of interseismic strain accumulation. Upper Cenozoic rocks and sediments in this region also record a history of intense and episodic tectonism that reflects convergence between the Juan de Fuca and North American plates. Field investigations in coastal Washington have identified several sites with geomorphic and stratigraphic evidence of youthful folding, faulting, uplift or subsidence. Strata at these sites are being examined in detail to quantify recent tectonic deformation.

Field investigations during FY93 included reconnaissance of tilted and faulted Quaternary deposits at a new site and establishment of benchmarks for monitoring fault activity and active diapirism at two other sites.

Lab investigations during FY93 included microscope analysis of microfossils collected from Quinault Formation and tephra analysis of tuffaceous clasts from faulted Quaternary deposits from another site.

Results

1. Quaternary sand and gravel deposits overlying the Neogene Quinault Formation display minor folding with fold axes trending east-west and a fold wavelength of 2 to 5 km. These folds are superimposed on a major regional fold with an east-west trending synclinal axis near the Queets River. At certain sites along the southern Washington coast this general pattern of crustal shortening is interrupted by zones of more intense deformation. In particular, a number of sites with highly tilted or faulted sediments have been identified. Some fault zones, active during the Miocene, continue to transport fluids (diapirism) and in one area several reverse faults appear to break the soil surface. This regional deformation pattern suggests that the abrupt subsidence events recorded in marsh strata may reflect regional shortening due to crustal structures activated either during megathrust events or perhaps separate from megathrust events. This hypothesis is being addressed in southern Washington by this project (and in Oregon by other workers) by documenting young vertical movement (inelastic strain) along the coastline with the aim of determining whether the entire coastline subsides during seismic events or instead the coastline undergoes shortening with the intermarsh areas rising while marshes subside.

2. Established benchmarks at two of the diapir/shear zones that appear most active in order to quantify rates of vertical movement and address the hypothesis that these features may act as strain meters.

3. Continued investigation of highly tilted and reverse-faulted Quaternary strata adjacent to a diapir with the aim of determining whether this local crustal structure is seismogenic and whether paleoliquifaction features documented along the Copalis River ca. 11 ka can be attributed to a local seismic event.

4. Continued analyses of sedimentary rock samples collected in southern Washington in FY89 and FY91 for age and uplift data. Rock samples collected in FY92 have been processed for microfossil analyses.

Reports

McCrory, P. A., Ingle, J. C., Jr., Wilson, D. S., and Stanley, R. G., 1993, Neogene transfer of central California to the Pacific plate: Implications for evolution of the San Andreas transform: Eos, Transactions, American Geophysical Union, v. 74, p. 586.

McCrory, P. A., Ingle, J. C., Jr., Wilson, D. S., and Stanley, R. G., *in press*, Neogene tectonic evolution of Santa Maria Province, California and transfer of central California to the Pacific plate: U. S. Geological Survey Bulletin 1995 Series, 27 p.

BAY AREA DIGITAL SEISMIC NETWORK

T.V. McEvilly, P. Johnson, R. Clymer,
Seismographic Station, Dept. of Geology & Geophysics and
Earth Sciences Division, Lawrence Berkeley Laboratory
University of California, Berkeley, CA 94720
510-642-4494 (TVM); tom@perry.berkeley.edu

Award 14-08-0001-G2122; Element II.7

Goals

The purpose of the Hayward Fault Network (HFN) in the San Francisco East Bay is to provide high resolution, high frequency (1000 samples per second), wide dynamic range (24-bit digitization), 3-component, on-scale seismic data for earthquakes of magnitude 0 < M < 7.0 for detailed studies of the Hayward fault. From our experience managing the Parkfield High-Resolution Network, with similar dimensions to the HFN, we believe we can accomplish this goal even in a noisy urban environment, given carefully designed sensors and deep borehole emplacement.

The HFN is a joint effort with the USGS. The network as envisioned will consist ultimately of 24-30 stations, 12-15 each north and south of the San Leandro seismic gap, managed respectively by UCB and USGS. Other sites are being drilled by the State of California Transportation Department (CALTRANS) and instrumented by the Lawrence Livermore National Laboratory (LLNL) at the major Bay Area bridges. Sensors designed and constructed at UCB/LBL are being installed in the entire network. Recording and telemetry equipment will differ between north and south, but the resulting data will be shared in near real time and archived with CALNET data in common format in the Bay Area optical mass store facility at Berkeley, also operated jointly by UCB and the USGS, and will thus be made promptly available to the research community.

FY 93 Accomplishments

During the past fiscal year we have installed and operated a network of four borehole seismometers on the northern Hayward fault. As a temporary system, RefTek Model 72-A07 24-bit event recorders borrowed from the UCB Seismographic Station and Lawrence Berkeley Laboratory operate independently at each site, recording on DAT tape. The central-site acquisition and control workstation (SPARCstation 10) was delivered and installed, and successfully reads the DAT tapes from the field recorders. The permanent Quanterra recorders and communication software are on order and a prototype system is undergoing bench testing at Berkeley.

1. Sensor Installation and Data Collection.

Six-component borehole sondes, with three channels of acceleration and three of velocity, have been emplaced in four holes of opportunity at depths of up to 600 feet along the northern Hayward fault. Identical downhole sensor packages were provided to Malcolm Johnston of the USGS for colocation in dilatometer boreholes on the southern Hayward fault, and to Larry Hutchings at LLNL for installation in boreholes drilled by CALTRANS at three piers of the Dumbarton bridge. Site information is specified in Table 1.

We have experienced some problems with sonde leakage at the cablehead, resulting in a mid-course design change. In addition, noise spikes cause occasional false triggers, apparently due to induced voltage steps on the long cables carrying the low-level signals. Subsequent units will amplify the signals in the sonde if this problem cannot be reduced sufficiently by careful grounding.

We hope to install sensor packages in several more holes of opportunity in the coming year in cooperative efforts with CALTRANS, EPRI, LLNL and the California Division of Mines and Geology.

It should be noted that the BRIB borehole, drilled by the USGS, is multi-use: The UCB/HFN sensor package presently shares the borehole with a USGS dilatometer. These will eventually be joined by a broadband seismometer operated by the UCB Seismographic Station as part of the Berkeley Digital Seismic Network (BDSN). Continuous geodetic GPS measurements, begun in the fall of 1993, are archived by the Seismographic Station.

2. Central Site and Field Data Loggers.

The SPARCstation10, to be the central data acquisition and control platform, has been operational for a year. The Quanterra field recorders, once installed, will communicate with the Sparc10 computer over 38 kb ADN phone lines. There will then be central event detection and other network controlling decision-making.

At Berkeley, Quanterra Company and UCB personnel recently installed for in-house bench-testing the prototype acquisition software and central-to-site communication handshaking on a conventional Quanterra field data logger simulating those to be deployed on the network. Necessary software modifications were identified. We expect delivery of the final Quanterra data loggers during early 1994, with fully functional operation of the complete system by the end of the year.

3. Data

Earthquakes have been recorded on the array now for about one year with the temporary 24-bit event recorders. Many of the local earthquakes are located within an interesting cluster of events beneath Berkeley; others are elsewhere along the Hayward fault. We are evaluating noise reduction and bandwidth achieved with respect to surface sites, compared to similar borehole installations in non-urban areas (e.g., Parkfield, Anza, The Geysers, Long Valley). The slowly growing data base will be placed on the regional mass store system at Berkeley. The increased time resolution, dynamic range and bandwidth attained will be useful in refining our definition of crustal structure in the East Bay region, in delineating the spatial-temporal complexity of the clustered events along the fault, in our investigations of earthquake source dynamics, and in developing localized elements of the real-time earthquake warning systems presently under development using the northern California broadband network.

TABLE 1. Hayward Fault Network Station Information

Site	Latitude (deg N)	Longitude (deg W)	Surface Elevation (msl-meters)	Instrument Depth (m)
Northern sites (UCB):				
BBEB	37.82167	122.32867	0.7	182.9
UCSB	37.87202	122.25060	126.1	167.6
RFSB	37.91616	122.33502	4.2	91.4
BRIB	37.91894	122.15062	253.5	108.8
Southern sites (USGS)				
GARS	37.6458	122.0067	359.7	120.6
CHAS	37.7489	122.0958	263.7	118.5
MILS	37.5480	121.9000	268.2	155.3
SUNS	37.6422	121.9408	533.4	123.5
COYS	37.5521	122.0877	9.8	136.8
Dumbarton Bridge (LLNL/CALTRANS)				
PIER1	37.4977	122.1278	0	0, 71.6, 228.0
PIER27	37.5057	122.1145	0	182.9
PIER44	37.5107	122.1103	0	0, 62.5, 157.9

Notes:
- Latitude and longitude are with respect to 1927 North American Datum (NAD27).
- Elevations are with respect to mean sea level.
- Elevations and depths are with respect to local ground level at the well head.
- Locations of UCB sites were obtained by GPS measurements, accurate to ±1m or better.
- Locations of USGS and LLNL sites are preliminary, from 7.5' topographic maps.
- UCB site BRIBis colocated with USGS dilatometer site RRCS.
- The east and west ends of the Dumbarton Bridge are equiped with sensors at three depths. The deepest instrument at all three sites is 100 feet into bedrock.

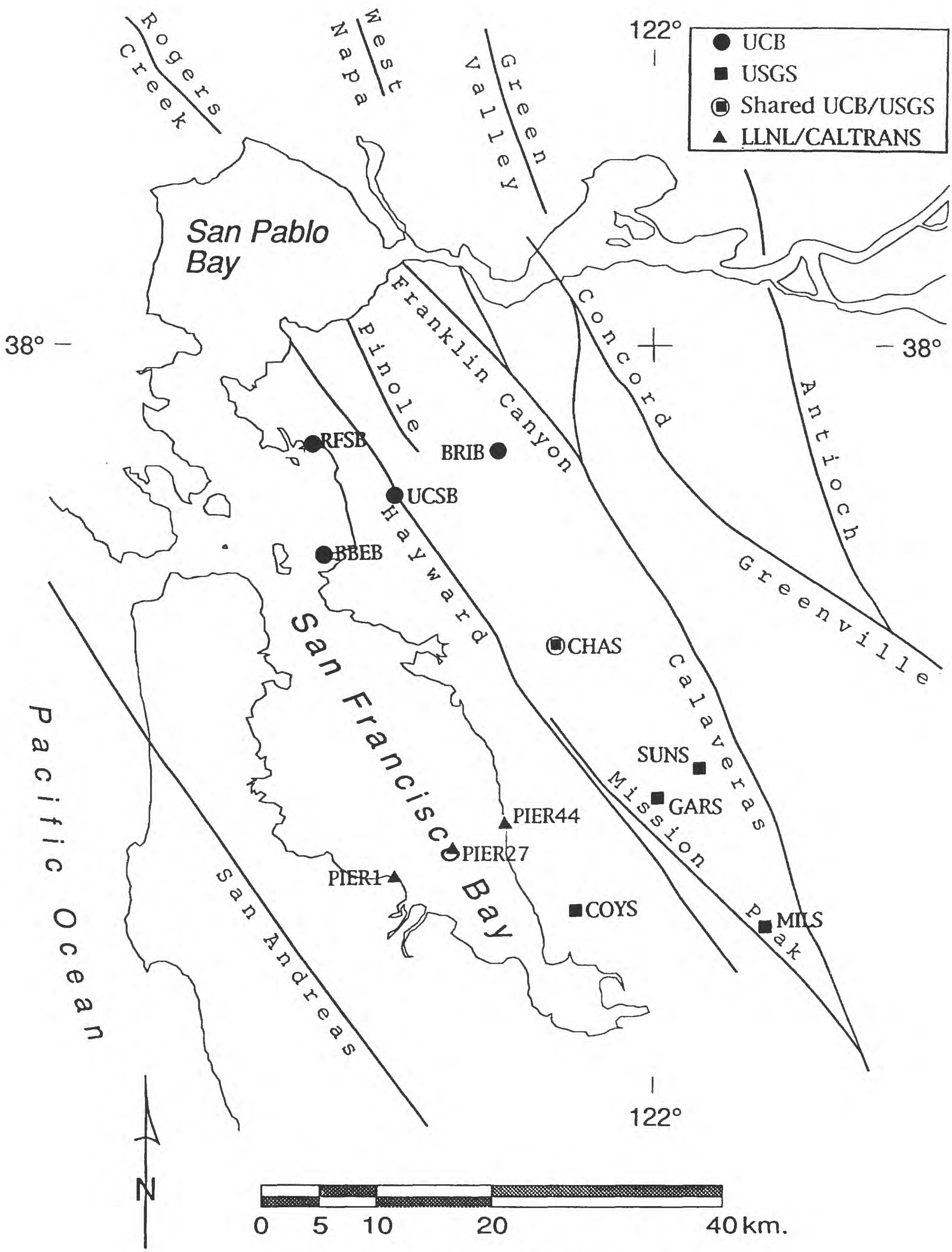

Figure 1. Hayward Fault Digital Network.

SEISMIC WAVE MONITORING AT PARKFIELD, CALIFORNIA

T.V. McEvilly, E. Karageorgi, R. Nadeau, P. Johnson, R. Clymer, W. Foxall
Seismographic Station, University of California, Berkeley, CA 94720
and
Earth Science Division, Lawrence Berkeley Lab, Berkeley, CA 94720
Phone: 510-642-4494 (TVM), E-Mail: tom@perry.berkeley.edu

Award 14-08-0001-G2160; Program Element: II.7

INTRODUCTION

Two programs of seismic wave analysis continue: Earthquake recording with the high-resolution seismic network (HRSN), begun in December, 1986, and controlled-source monitoring with HRSN begun in June, 1987.

The HRSN (Figure 1) consists of ten, 3-component, borehole seismometers surrounding the 1966 Parkfield epicenter. The data-acquisition system features digital telemetry with 125-Hz bandwidth and 16-bit resolution, and can operate in external-trigger (i.e., controlled-source) or event-trigger (earthquake) modes. Low-gain recorders with similar parameters, on loan from the IRIS PASSCAL instrument pool, are operating at five of the sites in parallel with the telemetry system. Network characteristics are summarized in Karageorgi *et al.*, 1992.

In a related effort (non-NEHRP funding), the UC Berkeley Seismographic Station has established a broadband seismometer at Parkfield called PKD1. The seismometer is presently in a temporary installation, and will be moved to a permanent site in the first half of 1994. This site is now an integral part of the Berkeley digital network, and data from it have contributed to a paper on real-time magnitude estimates (R. Uhrhammer) being readied for submission.

INVESTIGATIONS

1) Microearthquakes.

Local microearthquakes of magnitude about -0.5 to about +1.8 are routinely recorded on scale by the high-gain, telemetered system, extended to near M5 at the five low-gain sites. A 3-D velocity model (Michelini and McEvilly, 1991), a high-precision relative hypocenter location procedure for clustered events with similar waveforms, and other tools have been developed for high-resolution analyses of local earthquakes. Clustered events are being studied for evidence of temporal changes in fault zone processes and properties, including anisotropy. Studies are underway in source scaling, failure processes, fault zone structure, and material properties within the Parkfield nucleation zone.

2) Controlled-source monitoring with HRSN.

From June, 1987 through December, 1993, the HRSN has been illuminated 47 times with S-waves of three polarizations at seven source positions throughout the study zone, using a shear-wave Vibroseis source, in an on-going, long-term monitoring program (Figure 1). The resulting data are searched for temporal variations of wave propagation characteristics throughout the nucleation zone. Data reduction is accomplished at the Center for Computational Seismology (CCS) in the Earth Sciences Division of the Lawrence Berkeley Laboratory (LBL). This work was reported by Karageorgi, *et al.*, 1992.

DATA COLLECTED

Considerable progress has been made (R.N.) to put the 1987-1993 microearthquake data base into a consistent and correct format. Problems with channel assignments, amplitudes, time code interpretation, data gaps, and format are being dealt with. The final results are to be placed on the Berkeley regional mass-store by the end of 1994. A total of approximately 4000 events are presently in the archive.

Four vibrator data sets have been collected and the data reduced in this project year. Data after routine processing (edit, stack, correlation, gather by source site) are archived in SEGY format on magnetic tape.

RESULTS

Earthquake Studies:

Event analysis: Local Parkfield events are now picked and located with the 3-D model within a month of occurrence. This effort is presently current through December, 1993.

Characterization, Redefinition, and Preliminary Analysis of Similar Event Clustering, 1987-1992 (R.N): Using a modification of the similar event characterization method of Aster and Scott, 1993, we have characterized event similarity for the 1987-92 Parkfield HRSN data set, and reformulated our definition of similar event clusters at Parkfield based on three characteristics: 1) a bimodal distribution of correlation coefficients, defining clustered and unclustered events - see Figure 2, 2) cluster size stability, and 3) visual inspection of waveforms. Results are shown in Figure 3. The spatial, temporal, and relative size characteristics of the clustered and unclustered seismicity yield important information about fault zone dynamics during the earthquake nucleation process.

Preliminary results suggest:

1) Clustering is much more extensive at Parkfield than was previously believed, accounting for about 2/3 of all recorded events.
2) Clustering is concentrated at depths of less than 5km and on the creeping section of the fault NW of Middle Mountain.
3) Spatial distribution of clusters correlates with features of the velocity model of Michelini and McEvilly.
4) There is a bimodal distribution of correlation coefficients which we believe relates to a physical dichotomy in source processes and proximity.
5) Clusters can be unambiguously defined in terms of the bimodal correlation distribution.
6) The maximum characteristic cluster dimension is approximately 400 m.
7) A bimodal recurrence interval distribution suggesting two physical clustering processes, one of which imitates the lognormal behavior used in earthquake forecasting.
8) Clusters often contain events having magnitudes differing by over two orders.
9) The standard deviation of recurrence intervals within individual clusters seems to correlate with the range of magnitudes.
10) The existence of a characteristic recurrence interval for clusters.
11) That the characteristic recurrence interval is experiencing a temporally varying trend.

Fault-Zone Modeling (WF): We have carried out a detailed analysis and interpretation of the 3D V_p, V_s and V_p/V_s models of the San Andreas fault (SAF) zone at Parkfield first presented by Michelini and McEvilly (1991). The main feature of the V_p model is a deep high-velocity anomaly (Figure 4) that corresponds to the locked patch detected by Harris and Segall (1987) and to the 1966 rupture plane. This feature is similar to, but smaller than the high-velocity body (HVB) detected in our V_p model of the Loma Prieta segment of the fault zone at the opposite (NW) end of the central creeping section of the SAF. We proposed (Foxall et al., 1993) that the fault plane within the high-velocity body at Loma Prieta slips unstably (stick-slip) and acts as the barrier to stable fault slip at that end of the creeping section. Concentration of stress at the barrier under continuing tectonic loading causes it to evolve to the asperity which failed as the 1989 Loma Prieta earthquake. We propose that the same mechanics apply to the HVB at Parkfield: The HVB acts as the barrier that arrests slip at the SE end of the creeping section, and evolves to the asperity that fails during Parkfield earthquakes.

The main feature of the V_p/V_s model is an intense positive anomaly immediately NW of the HVB (Fig. 4). The amplitudes of the V_s and V_p/V_s anomalies indicate that this is a dilatant, saturated damage zone caused by the intense stress concentration in front of the barrier. Equivalently, this dilatant volume can be interpreted as the process zone at the crack tip of a stably propagating, ~150 km long megafracture corresponding to the central creeping section of the SAF. The 3-4 km length of the V_p/V_s anomaly provides an upper bound on the length of the process zone, and is consistent with published estimates of ~0.5-2.5 km for the lengths of process zones associated with earthquake nucleation. Figure 4 shows that this dilatant zone is presently aseismic. According to the hypocenter locations computed by Ellsworth et al. (1994), the 1966 foreshock and mainshock nucleated within the process zone in front of the barrier, although the mainshock hypocenter is located below the most intense V_p/V_s anomaly.

The coincidence of the V_p/V_s anomaly with the nucleation zone of the Parkfield earthquakes under Middle Mountain has important implications with regard to weak fault zone models that have recently been proposed. In one class of these models (Byerlee, 1993; Sleep and Blanpied, 1992) high fluid pressure is maintained within a sealed fault zone during the interevent interval by shear-related compaction. Therefore, the first characteristic that distinguishes the Parkfield nucleation zone (and perhaps other nucleation zones) is that it is dilatant rather than compacted during the interevent interval. The saturated condition of the zone indicates that it exists under drained conditions and is recharged from the surroundings at a rate comparable to the dilation rate. This implies that if the fault zone is sealed elsewhere, then the seals (lateral, vertical or both) must be broken at the nucleation zone. If recharge is through lateral hydraulic conductivity with the country rock, then this would suggest that the fluid pressure within the dilatant zone is low relative to the proposed overpressured fault zone elsewhere. In this case, the high V_p/V_s zone is undergoing dilatant hardening, consistent with nucleation of the Parkfield earthquakes there, the relatively low rate of interevent microseismicity within the zone, and the high stress drops that characterize events that occur in this vicinity (O'Neill, 1983).

Source Scaling (PJ): The earthquake sequences of October 1992 and November 1993, which produced the only two A-level alerts in the history of the Parkfield project, have provided a rich data set for investigating the scaling of earthquakes in the range M -0.7 to M 4.7, about 5 orders of magnitude. Earlier work involving spectral ratios of larger events to smaller events suggests that earthquakes with magnitudes in the range 0.5 to 1.0 have corner frequencies of about 100 Hz, near the upper end of our bandwidth (125 Hz).

We have been investigating the utility of a very simple technique for estimating source properties also. Following O'Neil and Healy (1973) and Frankel and Kanamori (1983), we computed rupture duration from the initial pulse widths (time from onset to the first zero crossing) on velocity recordings of Parkfield earthquakes. For several dozen earthquakes, we have measured pulse widths at five sites.

The study is complicated by the contrast in attenuation between the two sides of the San Andreas fault. The pulse widths show a clear path dependence, with sites to the southwest of the fault (where Salinian granite dominates the ray path) indicating rupture times which average roughly half those of sites at similar distances to the northeast, where waveform attenuation through a large thickness of Franciscan formation decreases the bandwidth. Pulse width decreases with moment and at the northeast sites appears to level off at the lower magnitudes.

To the southwest of the fault, the VCA station, for example, records waveforms whose rupture times as derived from the pulse widths continue to decrease linearly with magnitude, from a value of 0.040 s to 0.015 s over the magnitude range 4.7 to 0.2, the smallest earthquake studied for this site to date (moment = 3 x 10e18 dyne-cm). No bottoming out of pulse widths is observed over this magnitude range at this station.

The inferred rupture times for events recorded at VCA correspond to corner frequencies lower than those estimated from spectral ratios. We are now in the process of trying to separate the effects of attenuation and source processes.

Controlled-Source Studies (EK):

The final working data sets for analysis are "time gathers": one source into one receiver gathered across calendar time, producing 720 files, each containing, at present, 47 similar traces on most paths. The time gathers are then examined for variations in waveform parameters.

Most displays show only seasonal variations in various properties (travel time, amplitude, spectral properties). Seasonal variations are due to very near-surface moisture changes under the vibrator (Clymer and McEvilly, 1981).

However, paths in the vicinity of source site 2, south-west of the 1966 epicenter, show a prominent travel-time anomaly that began in mid 1988, and continues at least through October, 1992 (Figure 5). No significant change was found in the anomaly with special surveys run during the October, 1992 M4.7 sequence. But 1993 data show an apparent reversal of the anomaly for late arrivals on paths 2-MMN and 2-VCA. Note that these measurements were also made after an exceptionally rainy winter following several years of drought, raising the possibility that the anomaly was due to the drought. Measurements along 2-RMN continue to show the anomaly, and 2-SMN continues to show no significant variations. There is some indication of a return of the anomaly on 2-MMN and 2-VCA in mid-November, 1993. Continuing measurements will help to distinguish seasonal variations from any on-going long-term anomaly.

Present efforts are focused on the determination of the depth of penetration of the waves showing the anomaly, and verification of the anomaly using repeating, clustered microearthquakes as the sources of seismic waves.

References

Aster, Richard C. and Jennifer Scott, 1993. Comprehensive characterization of waveform similarity in microearthquake data sets, *Bull. Seis. Soc Am.*, **83,** 1307.

Byerlee, J, 1993, Model for episodic flow of high-pressure water in fault zones before earthquakes, Geology, 21, 303-306.

Clymer, R.W., and T.V. McEvilly, 1981. Travel time monitoring with VIBROSEIS, *Bull. Seism. Soc. Amer*, **71,** 1902-1927.

Ellsworth, W.L., A. Desai, and L.D. Deitz, 1994, The hypocenter of the 1966 Parkfield, California, earthquake and it relationship to recent activity, *Bull. Seismol. Soc. Am.* (submitted).

Foxall, W., A. Michelini, and T.V. McEvilly, 1993, Earthquake travel time tomography of the Southern Santa Cruz Mountains: Control of fault rupture by lithological heterogeneity of the San Andreas fault zone, *J. Geophys. Res.*, 98, 17691-17710.

Harris, R.A., and P. Segall, 1987, Detection of a locked zone at depth on the Parkfield, California, segment of the San Andreas fault,. *J. Geophys. Res.*, 92, 7945-7962.

Karageorgi, E., R. Clymer and T.V. McEvilly, 1992. Seismological studies at Parkfield. II. Search for temporal variations in wave propagation using Vibroseis, *Bull. Seism. Soc. Am.*, **82,** 1388-1415.

Michelini, A., and T.V. McEvilly, 1991, Seismological studies at Parkfield: I. Simultaneous inversions for velocity structure and hypocenters using cubic B-splines parameterization, *Bull. Seismol. Soc. Am.*, 81, 524-552.

O'Neill, M.E., 1984. Source dimensions and stress drops of small earthquakes near Parkfield, California, *Bull. Seismol. Soc. Am.*, 74, 27-40.

Sleep, N.H., and M.L. Blanpied, 1992, Creep, compaction and the weak rheology of major faults, Nature, 359, 687-692.

Publications:

Daley, T.M. and T.V. McEvilly, 1990. Shear wave anisotropy in the Parkfield Varian Well VSP, *Bull. Seism. Soc. Am.*, **80**, 857-869.

Michelini, A. and T.V. McEvilly, 1991. Seismological studies at Parkfield: I. Simultaneous inversion for velocity structure and hypocenters using B-splines parameterization, *Bull. Seism. Soc. Am.*, **81**, 524-552.

Karageorgi, E., R. Clymer and T.V. McEvilly, 1992. Seismological studies at Parkfield. II. Search for temporal variations in wave propagation using Vibroseis, *Bull. Seism. Soc. Am.*, **82,** 1388-1415.

Foxall, W., A. Michelini, and T.V. McEvilly, 1993, Earthquake travel time tomography of the Southern Santa Cruz Mountains: Control of fault rupture by lithological heterogeneity of the San Andreas fault zone, *J. Geophys. Res.*, 98, 17691-17710.

Nadeau, R., M. Antolik, P. Johnson, W. Foxall and T.V. McEvilly, Seismological studies at Parkfield. III. Microearthquake clusters in the study of fault-zone dynamics, *Bull. Seis. Soc. Am,* in press.

Ph. D. Theses:

Michelini, A., Fault Zone Structure Determined Through the Analysis of Earthquake Arrival Times, 1991.

Foxall, W., Fault-Zone Heterogeneous Slip and Rupture Models of the San Andreas Fault Zone Based upon Three-Dimensional Earthquake Tomography, 1992

Papers Presented on Parkfield Research in 1993.
1993 Fall AGU, San Francisco:

Aster, R., G.Slad, R.Nadeau, T.V.McEvilly, and M. Antolik, 1993. Coda Stability of similar earthquakes in seismic gaps, *EOS,* **74** (supplement), 397.

Johnson, P. A., and T.V.McEvilly, 1993. Wideband, high dynamic range, borehole networks: A window with a grand view into earthquake scaling, *EOS,* **74** (supplement), 406.

Nadeau, R., W.Foxall, and T.V.McEvilly, 1993. Comprehensive characterization, redefinition, and preliminary analysis of the 1987-1992 Parkfield HRSN similar event clusters, *EOS,* **74** (supplement), 416.

Foxall, W., A.Michelini, and T.V.McEvilly, 1993. Relationship of lithological heterogeneity to fault slip and rupture characteristics along the San Andreas fault zone at Parkfield, *EOS,* **74** (supplement), 612.

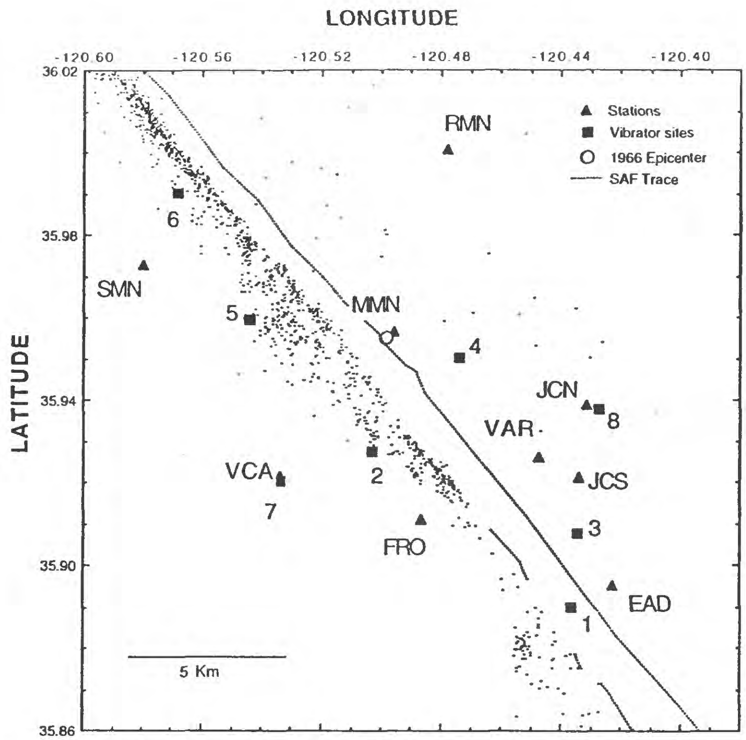

Figure 1. Location map showing the Parkfield borehole seismometer network, vibrator positions. and microearthquake seismicity for 1987-1992 (about 1700 events).

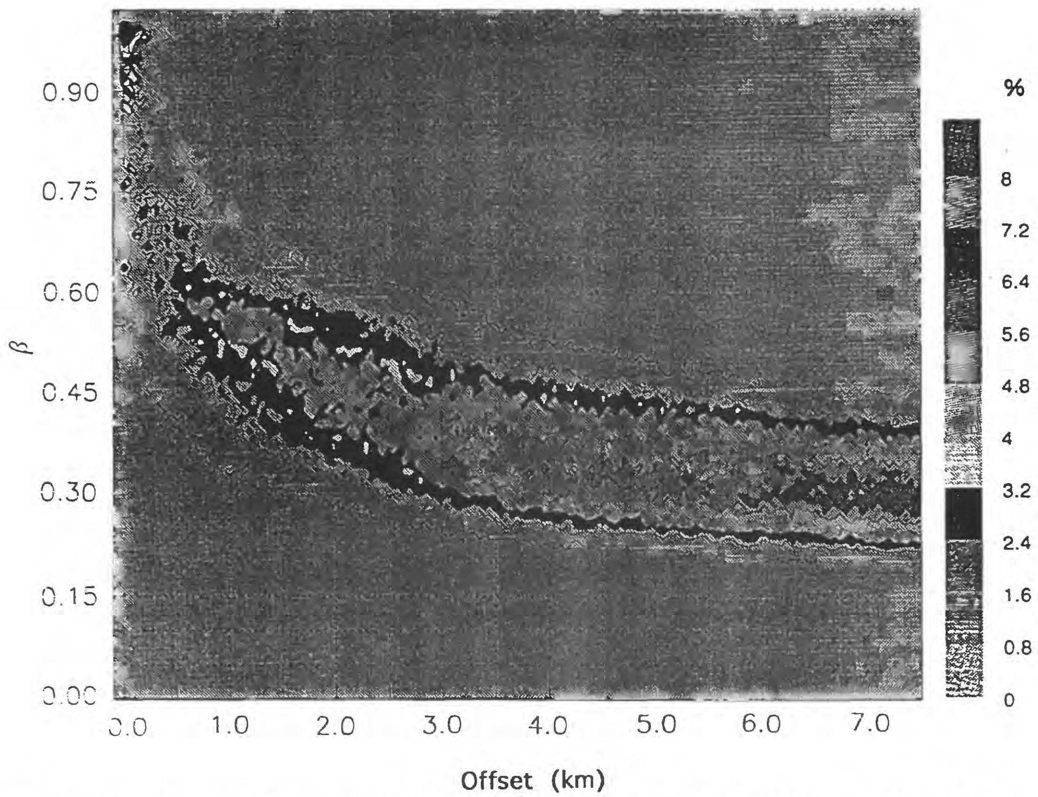

Figure 2. Event pair similarity (beta) vs. hypocenter separation (offset) in percent of events compared at each offset. Of special interest is the sudden rise in similarity at offsets less than 400-500 meters indicating a dramatic change in earthquake source processes at these near offsets. This discontinuous behavior is used as the basis for an unambiguous definition of clustering at Parkfield.

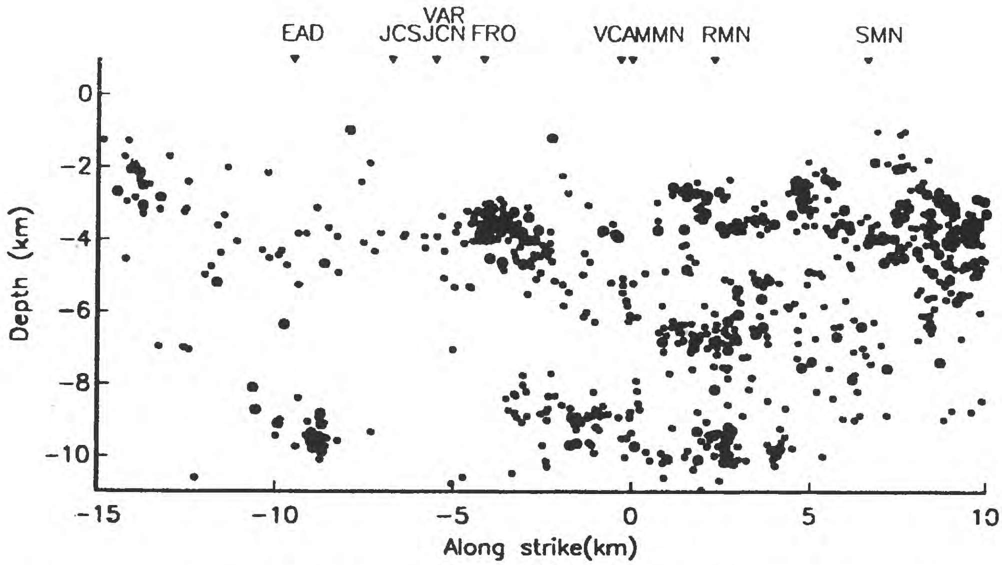

Figure 3. Cross-section with 1987-1992 seismicity along the San Andreas fault. Horizontal (y) axis shows distance from the epicenter of the 1966 Parkfield earthquake. Circles show the centroid location of clusters; dots show unclustered events. Locations of recording sites of the HRSN are shown as projected onto the fault plane.

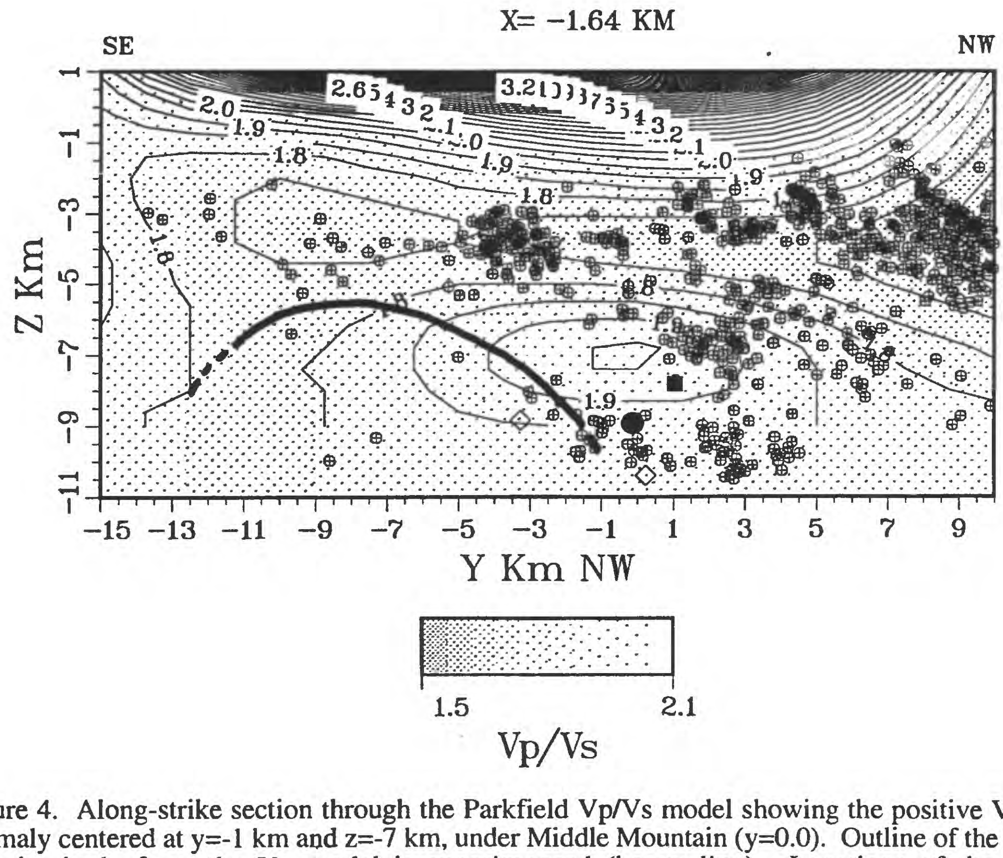

Figure 4. Along-strike section through the Parkfield Vp/Vs model showing the positive Vp/Vs anomaly centered at y=-1 km and z=-7 km, under Middle Mountain (y=0.0). Outline of the high-velocity body from the Vp model is superimposed (heavy line). Locations of the 1966 mainshock and foreshock are shown as filled circle and square, respectively.

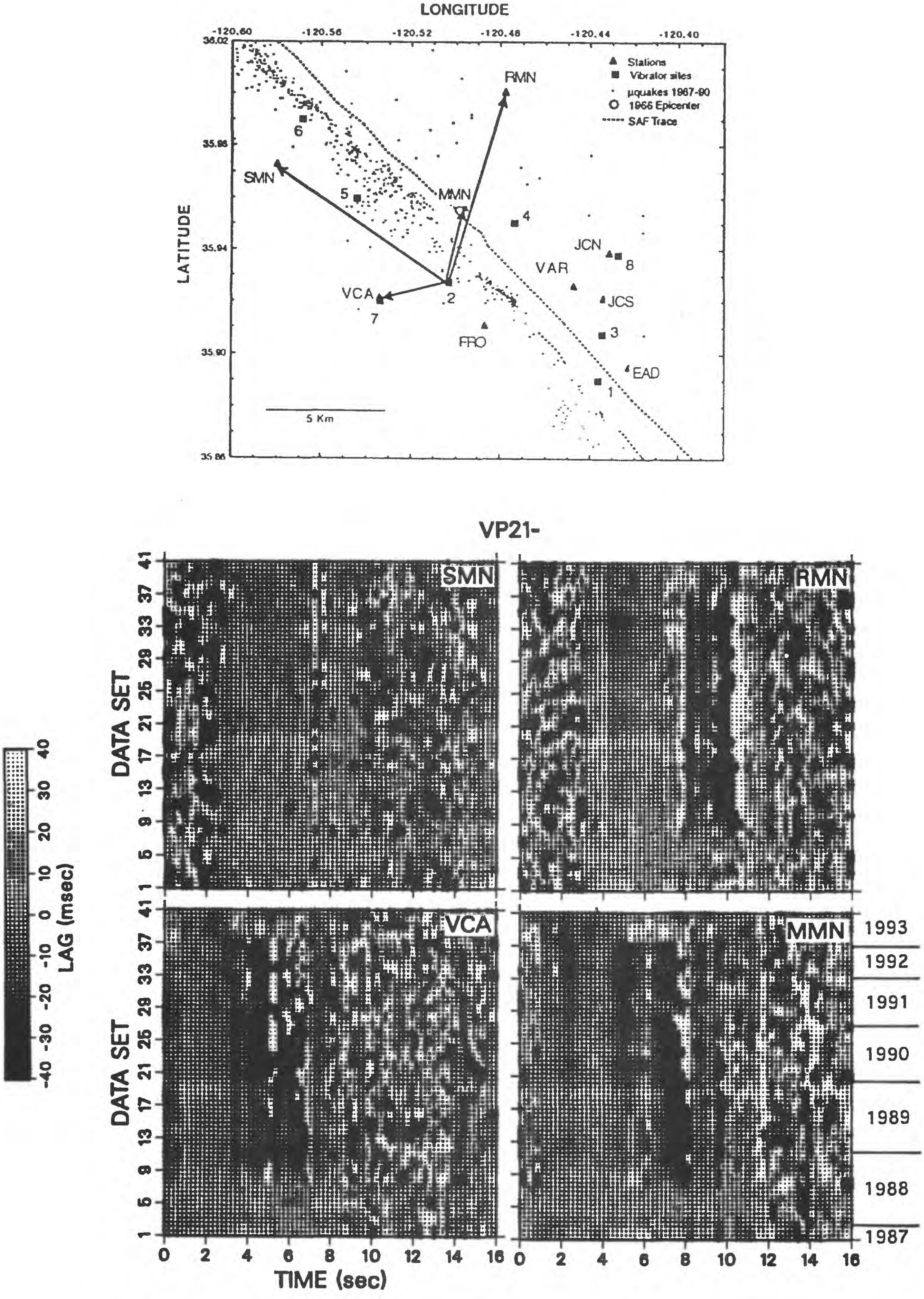

Figure 5. Travel-time variations relative to a reference trace (arbitrarily chosen, here in mid 1988) measured across the repeated 16-sec seismograms in a moving window for several paths from vibrator site two.

Program Element: II.1

Geologic and Tectonic Framework, Mendocino Triple Junction
9540-70420

Robert J. McLaughlin, (Principal Investigator), Kirsten Cyr, S.H. Clark, Jr.,
U.S. Geological Survey
Branch of Western Regional Geology
345 Middlefield Road, MS 975
Menlo Park, California 94025
(415) 329-4945

K.R. Aalto and G.A. Carver
Department of Geology, Humboldt State University
Arcata, CA 95221

Investigations:

(1) The primary objective of this project has been to produce a colored digital geologic data base for the Mendocino Triple Junction (MTJ) region. At the time of the Petrolia earthquake in April, 1992, a geologic mapping study of the region had been completed and the geology was compiled onto a greenline base at 1:100,000 scale. We proposed to digitize this data base in ARC-INFO and make it available in a timely manner for use in various anticipated geophysical and geodetic investigations. The digital compilation was begun in January 1993.

(2) At the invitation of K.R. Aalto (Humboldt State University) McLaughlin spent four days with him in the Cape Mendocino area, mapping and sampling a previously inaccessible part of the coast between False Cape and Bear River. Aalto had found some complexly deformed rocks there which were assigned to the Eocene Coastal terrane of the Franciscan complex. We suspected them to be a much younger, exhumed part of the offshore Cascadian accretionary complex.

Results:

(1) Digital compilation of the Cape Mendocino and Eureka 1° x 1/2° quadrangles was undertaken at the outset of calendar year 1993 in anticipation of the focus of post-Petrolia earthquake investigations. We especially wanted these maps to be useable for a planned deep seismic reflection and refraction study scheduled for 1993 and 1994 calendar years. In addition, a bathymetric base was added from offshore U.S. Coast and Geodetic Survey data, and structural data from the offshore work of D.H. McCulloch and S.H. Clarke, Jr., were also added to the map. Preliminary full-color digital geologic maps were presented at a GSA Cordilleran section meeting poster session in April, 1993. An interpretive text, including rock descriptions, paleontologic data, major onshore and offshore faults, structure sections, and a tectonic synthesis were prepared, and the maps were routed into

technical review late December 1993. Following the review process, we plan to release the maps to open file in CD-ROM, or in a similar rapid-release format, after their submittal to BWTR. Work on the Garberville 1:100,000 digital map begins in calendar year 1994.

(2) Mapping in the False Cape part of the MTJ region and micro-paleontologic data (diatoms, foraminifers, radiolarians) confirmed the presence of a part of the early Miocene Cascadian accretionary margin onshore north of Cape Mendocino. These rocks are exhumed from beneath the Eocene Coastal terrane of the Franciscan Complex along out-of-sequence thrusts, and are folded through the older accretionary complex, possibly in response to coupling between the Gorda and North American plates. These early Miocene deformed rocks were named the False Cape terrane and are assigned to the Franciscan Complex. The distribution of these rocks, to the the extent known was added to the Cape Mendocino-Eureka map base.

Reports published:

1. Clarke, S.H., Jr., McLaughlin, R.J., Carver, G.A.,Burke, R.M., and McPherson, R.C., 1993, Tectonic setting of the Mendocino triple junction region: Geological Society of America Abstracts with Programs, v. 25, no. 5, p. 21.

2. McLaughlin, R.J., and Underwood, M.B., 1993, Early Miocene transpression across the Pacific-North American plate margin; initiation of the San Andreas fault, and tectonic wedge activation: Geological Society of America Abstracts with Programs, v. 25, no. 5, p. 118.

3. Aalto, K.R., Carver, G.A., Dunklin, T., Barron, J., McDongall, K., and McLaughlin, R.J., in press, 1994, An uplifted Neogene accretionary wedge, Humboldt County, California: Geological Society of America Abstracts with Programs, v. 26, no. 5.

4. Stein, R.S., Marshall, G.A., and Murray, M.H., with contributions from other USGS staff and Humboldt State University, 1993, Permanent ground movement associated with the 1992 M=7 Cape Mendocino earthquake: Implications for damage to infrastructure and hazards to navigation: U.S. Geological Survey Open-File Report 93-383.

Report submitted to Branch Review, 12/93:

McLaughlin, R.J., Ellen, S.D., Aalto, K.R., and Carver, G.A., with contributions to offshore geology by S.H. Clarke, Jr., in review, 1993, Geology of the Cape Mendocino and Eureka 1:100,000 quadrangles, northern California: 2 map plates, scale 1:100,000 descriptive and interpretive text, 49 manuscript pages and 2 structure sections (plate 3).

Loma Prieta Data Archive Project

1434-92-G-2228
Program Element II.1

Jack P. Moehle and Katherine A. Frohmberg
Earthquake Engineering Research Center
University of California
1301 S. 46th Street
Richmond, CA 94804-4698
(510)-231-9401
e-mail: katie@eerc.berkeley.edu

Introduction

Under the general editorship of the U.S. Geological Survey (USGS), the National Earthquake Hazards Reduction Program (NEHRP) is issuing the official report to Congress describing the post-earthquake investigation of the October 17, 1989, Loma Prieta, California earthquake. That report will synthesize results of earthquake research funded and performed by a wide range of investigators. These investigators have produced or gathered a variety of data sets generated by the earthquake or produced as a result of research into the earthquake. Of necessity, the NEHRP report will not be a suitable medium for distributing this extensive data.

The nonprint data is extremely important to organize and preserve since it will not be published in the open literature and, unless preserved, will be lost to future scholarship. The Loma Prieta earthquake is the first major earthquake in the San Francisco Bay Area since 1906 and is the first to occur in a high populated, heavily instrumented area. The data will form an important baseline for research into future earthquakes in this area and elsewhere.

The National Information Service for Earthquake Engineering (NISEE) at the Earthquake Engineering Research Center (EERC) was charged by the National Science Foundation in 1971 to gather and disseminate information in earthquake studies particularly earthquake engineering. As a result of the Loma Prieta earthquake, NISEE founded the National Clearinghouse for Loma Prieta Earthquake Information in 1990. The clearinghouse has gathered data from a wide variety of sources and published the Loma Prieta Clearinghouse Catalogs, listing more than 2100 sources of information on or about the earthquake.

Investigations Undertaken

NISEE has established the Loma Prieta data Archive to gather, organize, and issue the raw data associated with the Loma Prieta earthquake in one coherent format. In particular, NISEE will

* **identify** the data sources produced as a result of the earthquake
* **gather** them together
* **organize and issue** the data on CD-ROM with a printed users' guide
* **deposit** the guide and CD-ROMs in selected national and university libraries throughout the country as well as distribute them at cost to anyone interested
* **publicize and disseminate** the archive to researchers worldwide

The data from the Loma Prieta earthquake is extremely important to preserve since this earthquake occurred in a heavily populated area where there were a great number of strong-motion instruments. There is more data available for study from this earthquake than for any significant earthquake in recent history. Therefore, experimental data will be used as a baseline for future research in the Bay Area and other locations. In addition, making this data generally available will allow for independent verification of results by other researchers.

Results Obtained

About 25 data sets have been obtained and about 25 more will be acquired. They range from seismological to engineering to social science data sets and include digital files, survey responses, text, videos and slides. These have been processed and copied to computer files where they are being stored til the completion of the project.

Reports Published

The U.S. Geological Survey (USGS) Professional Paper series which will constitute the NEHRP Report to Congress will be completed some time in 1995. At that time, the data sets will be written to CD-ROM. A printed guide to the data will be issued as an addendum to the Professional Paper series. The CD-ROMs themselves will be distributed by NISEE at cost.

ANNUAL REPORT
SOUTHERN CALIFORNIA EARTHQUAKE PROJECT
93-9902-11010

J. Mori, T. Heaton, L. Jones, D. Eberhart-Phillips, D. Wald,
D. Given, R. Dollar, C. Koesterer, L. Wald, S. Perry, L. Curtis

Branch of Seismology, Office of Earthquakes, Volcanoes, and Engineering
U.S. Geological Survey
525 S. Wilson Ave. Pasadena CA 91106

818-405-7821
mori@bombay.gps.caltech.edu

INVESTIGATIONS

This project encompasses the USGS personnel that work together on the Southern California Seismic Network to ensure that earthquakes are well-recorded and archived in southern California, and that reliable seismic information is communicated to goverment agencies, scientific groups, media, and the public. The routine analyses and archiving of data involves close cooperation with Caltech and the Southern California Earthquake Center (SCEC). With the recent emphasis on providing rapid information, the project provides the necessary coordination of developing automated computer systems and organizing people that quickly respond to significant earthquakes. The project also includes the scientists' individual research topics that are closely tied to seismic data collected by the network. Tasks for FY1993 were divided into 3 categories.

- Seismic Data Collection
- Earthquake Hazards Monitoring and Public Information
- Earthquake Research

Seismic Data Collection
(Elements II.2, II.7, III.1, IV.1)

A major responsibility of the project is to maintain and operate the large seismic network, thus a substantial part of the project's resources are used for instrument maintenance. The network consists of over 300 channels of data from 225 sites and provides the primary data for hazard monitoring in southern California and data for much of the research done by the project scientists. Responsibilities for hardware (instrument sites, radio telemetry, microwave and telephone links, computer cluster) and software (on-line recording system, off-line data processing, real-time earthquake information systems) are shared jointly with Caltech.

In addition to maintaining the network, we continue to try and improve our seismic recording capabilities by installing new sites in sparsely instrumented areas, adding Force-Balance-

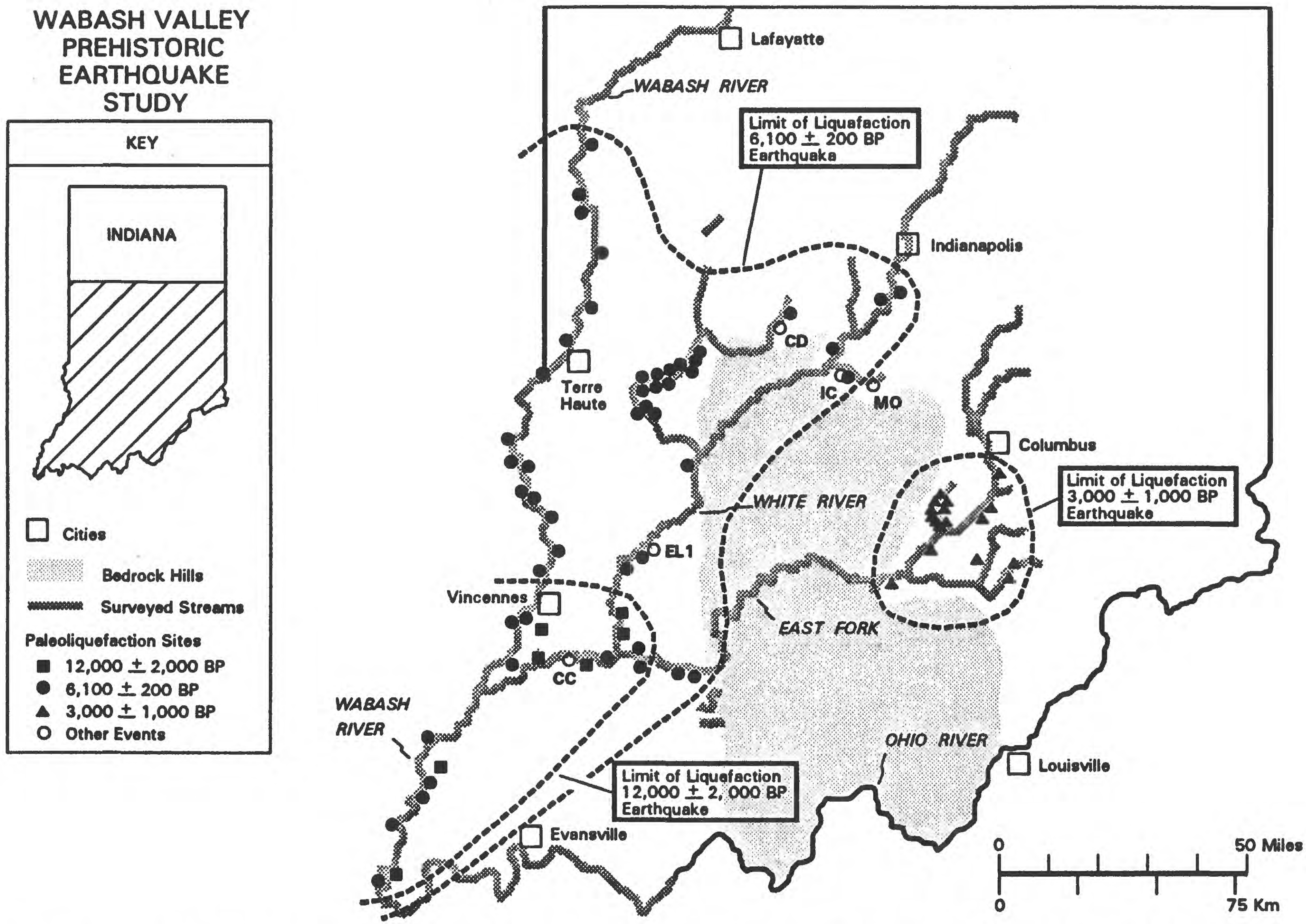

Figure 1. Map showing areas searched, locations of paleoliquefaction sites, and estimated limits in Indiana of liquefaction from three large prehistoric earthquakes.

PALEOSEISMOLOGY AND QUATERNARY DEFORMATION OF COASTAL OREGON

9950-04180

ALAN R. NELSON and STEPHEN F. PERSONIUS

Branch of Earthquake and Landslide Hazards
U.S. Geological Survey, MS 966
Box 25046, Denver, CO 80225
(303) 273-8592; anelson@gldvxa.cr.usgs.gov

INVESTIGATIONS

The project consists of two components: Nelson's study of coseismic changes in late Holocene sea level as revealed by tidal-marsh stratigraphy, and Personius' study of fluvial terrace remnants along major Coast Range rivers to determine styles and rates of late Quaternary deformation. Both components will help define the potential hazard from great subduction earthquakes in the U.S. Pacific Northwest.

RESULTS

Coseismic changes in late Holocene sea level

Has subduction of the Juan de Fuca plate beneath the North America plate in the Pacific Northwest produced great (M>8) earthquakes during the late Holocene? Records of the past 200 years yield no evidence of great plate-interface earthquakes in the Cascadia subduction zone. But along the coasts of Oregon and Washington peaty, tidal-wetland soils are interbedded with mud in estuarine stratigraphic sequences, and the submergence (relative rise of sea level) of some of these soils seems too widespread (>100 km), too large (>1 m), and too sudden (<10 years) to be attributed to any process except coseismic subsidence. How large were the Cascadia plate-interface earthquakes that produced coastal subsidence and how often did they occur? Such questions are critical for earthquake hazard assessment in the Pacific Northwest (PNW).

Nelson's research in FY93 focused on the following two questions:

Objective 1: *Were the peaty units interbedded with estuarine mud in late Holocene tidal-marsh stratigraphic sequences in the Pacific Northwest submerged and buried during the same 50- to 300-yr-long periods?*

Peaty stratigraphic units may have been submerged and buried during great (M>8) subduction earthquakes, smaller upper-plate earthquakes, or by nonseismic processes. Precise

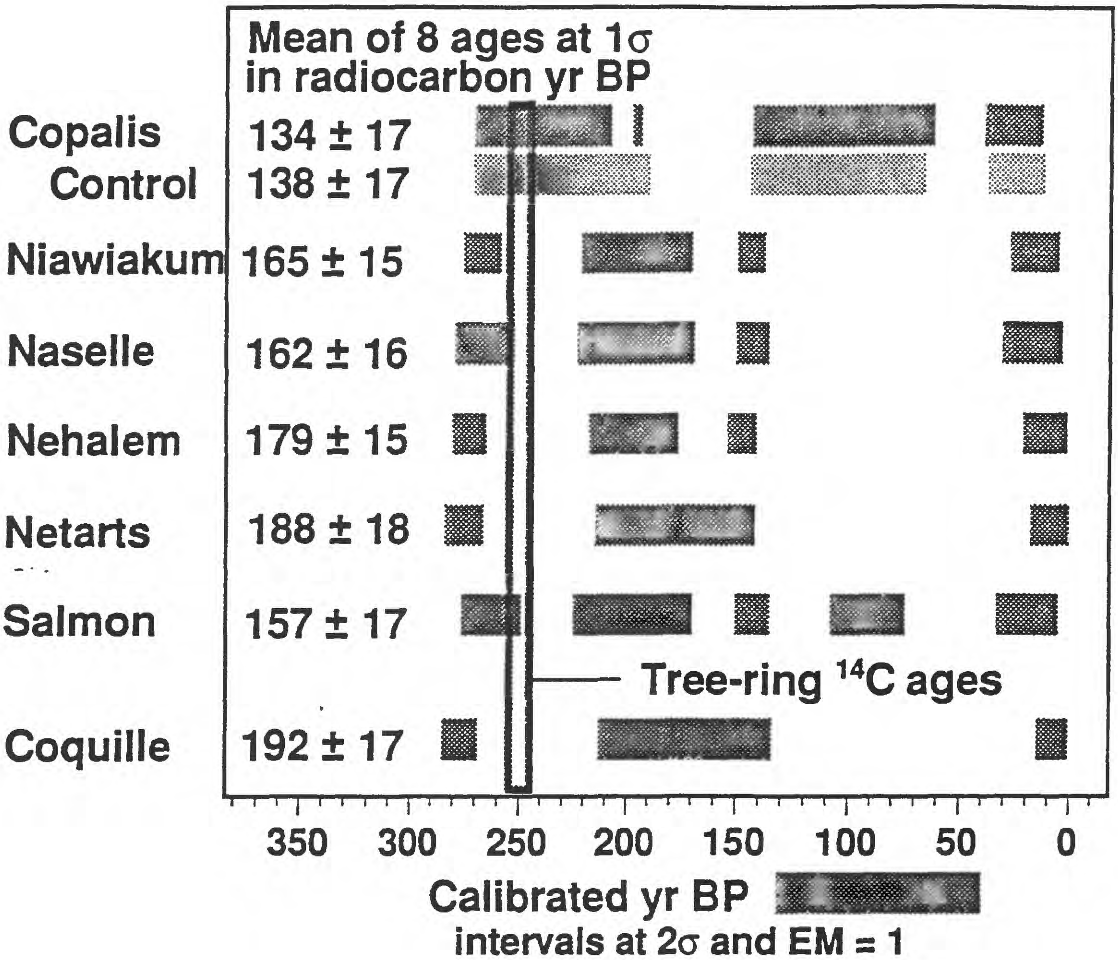

Figure 1. Mean ages (in radiocarbon years at one standard deviation) and corresponding calibrated-age time intervals (at two standard deviations) for sites where we have analyzed marsh plant fossils rooted in the top of the marsh soil that was suddenly submerged about 250 BP. The control sample of wood from the outer ring of a tree killed by submergence at the Copalis River allowed us to estimate the error multiplier for all samples at <1. Because of the wide variation in the ^{14}C calibration curve in the past 300 years the ^{14}C ages correspond to several time intervals during the past 300 years. History does not record sudden submergence of the PNW coast, such as caused by great earthquakes, in the past 200 years. This suggests that the oldest of the time intervals corresponds to the true age of the samples. Because the oldest intervals of all samples overlap, we cannot conclude that any samples differ in age. The apparent small age difference between the more precise tree-ring ages of Atwater and others (width of vertical bar) now available from three sites (Copalis, Niawiakum, and Nehalem) and some AMS ages may be due to a systematic difference in young ages between laboratories.

Analysis of the 1992 M6.1 Joshua Tree Earthquake Sequence and Its Relation to the Southern San Andreas Fault, California

Craig Nicholson
Institute for Crustal Studies, University of California, Santa Barbara, CA 93106-1100
Phone: (805) 893-8384 email: craig@quake.crustal.ucsb.edu
and Jonathan M. Lees
Department of Geology and Geophysics, Yale University, New Haven, CT 06511-8130
Phone: (203) 432-6947 email: lees@lamb.geology.yale.edu

Program Element II.2

Investigations Undertaken

Two deployments of portable digital instruments were made in 1992 following the April M6.1 Joshua Tree event and again in June following the M7.4 Landers and M6.5 Big Bear events. Both deployments were successful, largely because of the tremendous cooperation between the various participating SCEC institutions involved, including Caltech, UCSB, UCSD, USC, USGS, IRIS/PASSCAL, and SDSU.

22 April M6.1 Joshua Tree Earthquake

Five SCEC instruments were initially deployed within 6.5 hours of the April 22 M6.1 Joshua Tree mainshock. UCSB assisted in the deployment and maintenance of these sites. Six PASSCAL recorders were added to the deployment in the following days. The array was maintained until early June and collected about 5-6 Gbytes of raw digital data. At ICS, we corrected timing and performed event association on 3-4 Gbytes of data left after initial data processing and reduction. Over 10,700 events were associated, and the data were made available to the SCEC Data Center at Caltech.

28 June M7.4 Landers and M6.5 Big Bear Earthquakes

Nine PBIC DAS's were deployed for this aftershock sequence. PASSCAL supplemented the SCEC array with 10 DAS's in the days following the mainshock. SCEC member institutions, including UCSB, worked together to deploy and maintain the array. Once fully deployed, the array consisted of 18 sites including 3 STS-2 and 2 CMG-3 broadband sensors. A prototype field computer was used to perform initial field quality control of the data. Over 8 Gbytes of raw data were collected. Data processing, event association and timing corrections were performed at UCSD. Over 8,000 events were associated, and the data made available to the SCEC Data Center at Caltech.

FY1993 Research Results

1. Changes in Attitude - Changes in Latitude: What Happened to the Faults in the Joshua Tree Area Before and After the M7.4 Landers Mainshock?

Craig Nicholson, Ruth A. Harris, and Robert W. Simpson

The M6.1 Joshua Tree earthquake of 23 April 1992 occurred about 8 km northeast of the southern San Andreas fault and about 20 km south of the Pinto Mt fault. It was followed by over 6,000 M>1 aftershocks. No surface rupture for this sequence was found; although ground fractures were discovered in this area after the Landers earthquake on June 28. From the distribution of aftershocks and directivity effects, the mainshock ruptured unilaterally to the north along a fault about 15 km long. The focal mechanism indicated right-slip on a plane striking N14°W, dipping 80°W, with a rake of 175°. We relocated 10,570 events between 23 April and 24 July using the data from the regional network; and determined 3,030 single-event focal mechanisms with 15 or more first-motions. A large number of aftershocks occurred off the mainshock rupture plane on adjacent secondary structures that strike either sub-parallel to the Joshua Tree mainshock plane or on relatively short, left-lateral faults that strike at high angles to the mainshock plane. Aftershocks continued to migrate to the north and south following the mainshock, and ultimately extended from the southern San Andreas fault near the Indio Hills to the Pinto Mt fault. The northern 15-km section of the aftershock zone had a strike more nearly N10°E. Seismicity on this fracture network ceased in the hours prior to the 28 June M7.5 Landers event, and has not yet resumed. Instead, the Landers mainshock appears to have caused the activation of a new fracture network located farther west, that intersects the previous Joshua Tree activity in the area of the Joshua Tree mainshock, and is oriented more nearly N15°W. We investigate possible explanations for this change in the pattern of earthquake activity as a result of inferred stress changes induced by the Landers mainshock and some of its larger aftershocks.

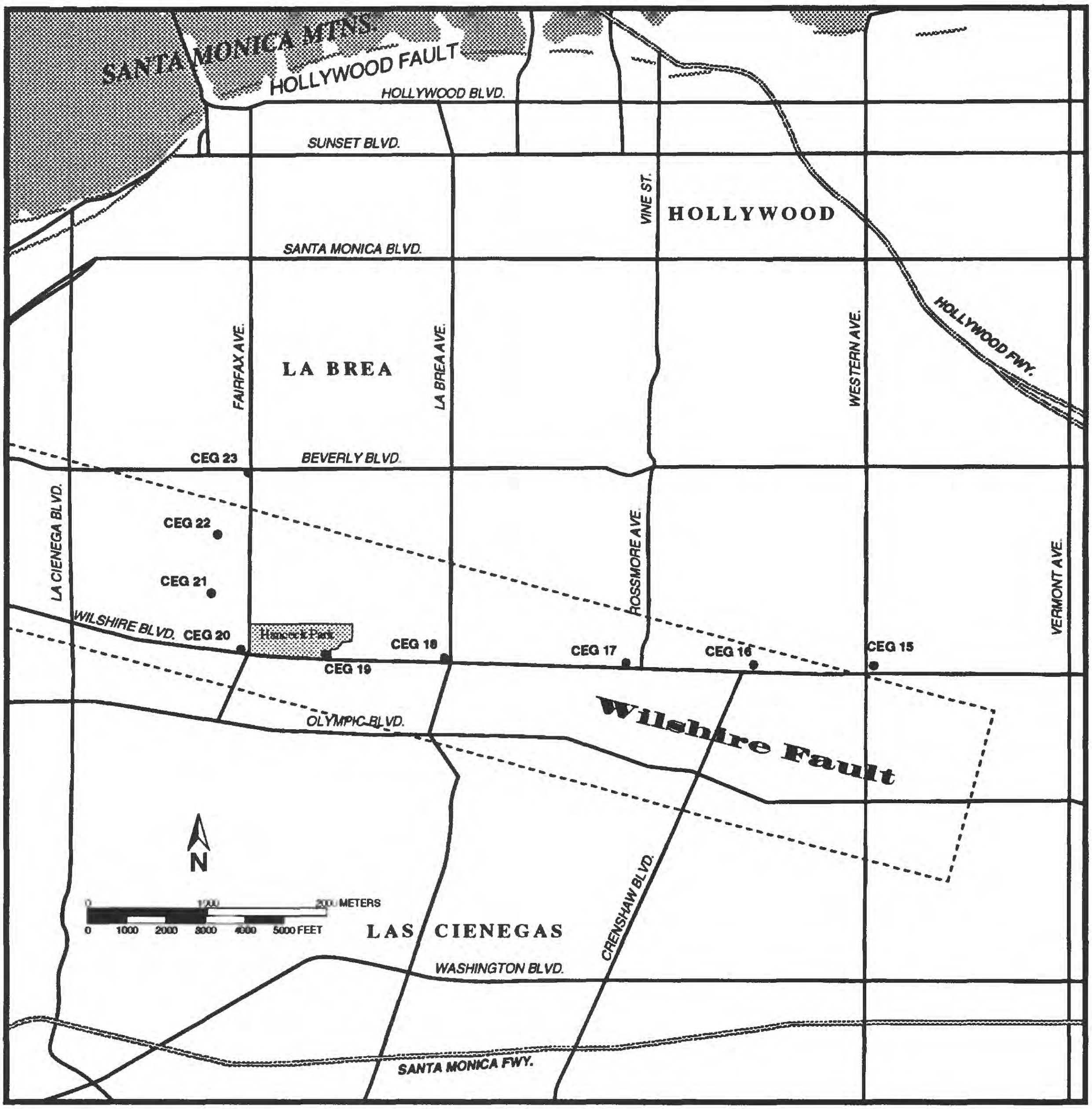

Figure 1. Map of the Wilshire area in the northern Los Angeles basin, showing location of MetroRail borings used in the current study (dots) and the approximate location of the surface projection of the "blind" Wilshire fault (dashed rectangle).

Not only is the "Pico" here older than its foram assemblage indicates, but sediments in other parts of the basin that contain younger ashes (~3.4-4.4 Ma) are locally associated with biostratigraphically "older" (Repettian and Delmontian) fauna. The MetroRail data provide a way to quantify the time-transgressive nature of benthic foram stage boundaries and show that they are not, by themselves, reliable age indicators.

These data increase the uncertainty of our age assignment for the deformed marine gravels, and consequently increase the uncertainty of slip rate estimates for the Wilshire fault. However, the implications of these data for the seismic hazard evaluation of blind thrust faults reach far beyond the Wilshire fault. Most recent structural interpretations and models of blind thrusting depend on oil well data that rely almost exclusively on benthic foraminiferal stages for age and stratigraphic control. Not only are derived fault slip rates based on foram stages potentially more uncertain than we currently recognize, but without other corroborating data, inferred faults and unconformities marked by missing faunal zones and abbreviated stratigraphic section may have little tectonic significance. Even the inferred geometry of subsurface folds could be misinterpreted where the local biostratigraphic stage boundaries diverge widely from geochronologic horizons. As we do not know how localized these problems are, the need for additional independent age control is evident.

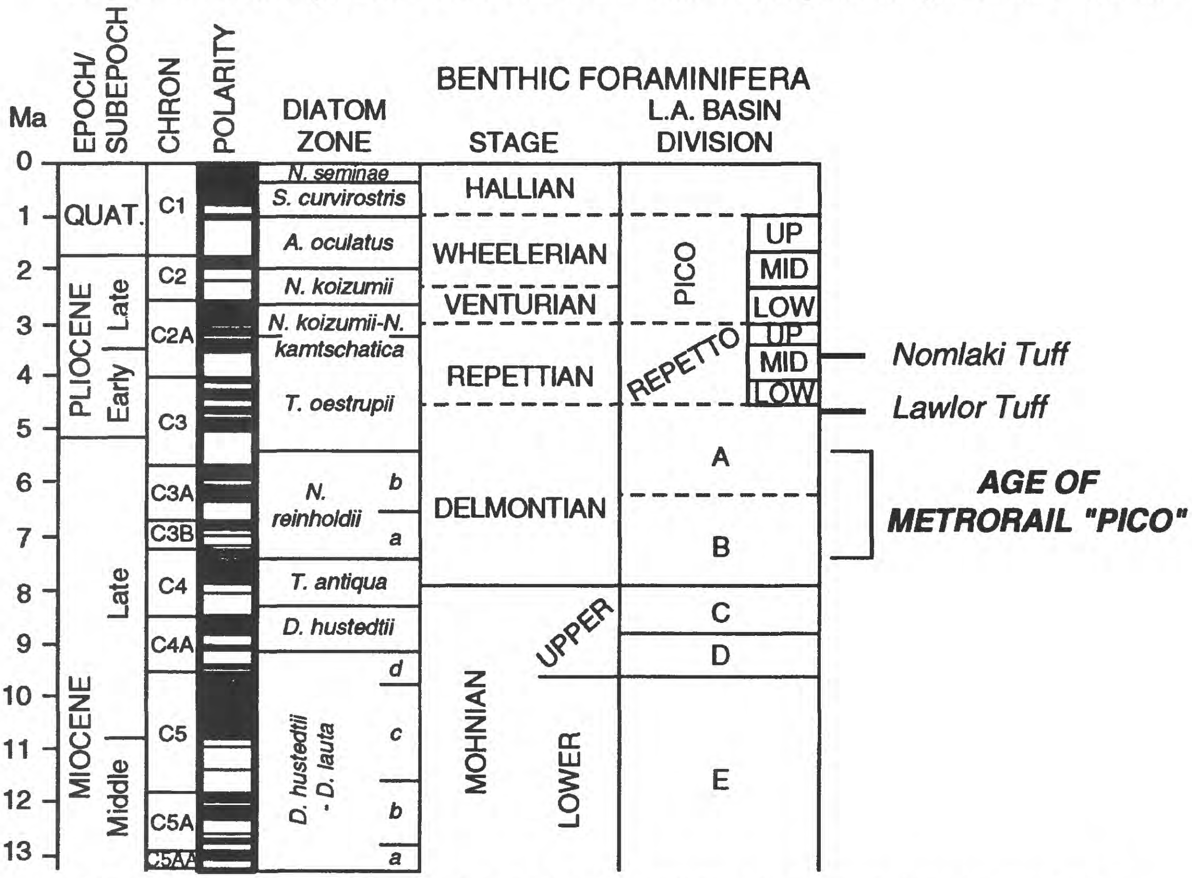

Figure 2. Chronostratigraphic framework for the middle Miocene through Pleistocene of California, showing correlation of diatom zones to the benthic foraminiferal stages of the L.A. basin. The MetroRail "Pico" Formation contains benthic foraminifera belonging to the Wheelerian and Venturian stages, but diatoms belonging to the *Nitzchia reinholdii* zone, which falls within the late Miocene. This age is confirmed by tephrochronology. The Nomlaki and Lawlor tuffs, which occur in Repettian and Delmontian sediments on the Palos Verdes peninsula, post-date the ashes found in the Wilshire area. Figure modified from Blake (1991), using the geomagnetic polarity time-scale of Cande and Kent (1992).

2. Historical investigations of the 1906 earthquake in the southern Santa Cruz Mountains allow us to compare effects of the 1906 earthquake to effects of the 1989 earthquake, and provide context for interpreting the nature of coseismic ground deformation in the region. In both 1906 and 1989, many large ground cracks occurred in the Summit Road and Skyland Ridge areas. Three specific localities in the Summit Road area were documented well enough in 1906 to make detailed comparisons with 1989: 1) the Wright's tunnel, 2) the Morrell Ranch, and 3) the Blacksmith shop at Burrell. Published surveys of Wright's tunnel indicate a broad zone of deformation extending SW from the San Andreas fault for more than 1.5 km; this survey forms the basis for interpreting the fault zone to be very broad in this region. However, recently discovered documents related to the Wright's tunnel show that if the tunnel was tectonically offset in 1906, the deformation was distributed over a zone not more than

made each day at 6 stations in the network (Figure 1). The observations were designed to facilitate integration with recent GPS campaigns organized by the Southern California Earthquake Center (SCEC) following the Joshua Tree-Landers-Big Bear earthquakes, and by NGS in the Imperial Valley. In addition, observations in Northern Mexico compliment and extend coverage for the NASA/DOSE Northern Baja, California survey completed during April 1993. A complete set of the GPS observations have been archived at the University Navstar Consortium (UNAVCO).

Participants in the GPS field campaign included Lamont-Doherty Earth Observatory (L-DEO), Riverside County Flood Control and Water Conservation District (RCFCWCD), Centro de Investigacion Cientifica y de Educacion Superior de Ensenada (CICESE), Lawrewnce Livermore National laboratory, Scripps IGPP, and the U.S. Army (Yuma) Optical Development and Integration Branch. Both the US and Mexico field work were fully supported by UNAVCO.

2. We continue to concentrate on reduction, analysis, and interpretation of the 1986-1993 GPS observations in collaboration with USGS (Pasadena), L-DEO, NGS, SCEC, and CICESE. Crustal deformations derived from the 1986-1990 observations have been used to investigate coseismic deformation for the 1987 Superstition Hills earthquake (Larsen et al., 1992), regional strain accumulation (Larsen and Reilinger, 1992), and active tectonic processes in the complex transition zone from spreading in the Gulf of California to continental transform faulting along the San Andreas fault (Reilinger and Larsen, 1993).

   GPS observations for the period 1990-1992 are being used in conjunction with USGS EDM measurements to investigate the slip distribution of the 23 April 1992, M=6.1 Joshua Tree earthquake (Bennett et al., 1993). Measurements at 19 sites (6-GPS 13 EDM) before and after the event have been corrected for secular deformation in order to estimate coseismic movements. The coseismic motions are used to invert for fault slip with the strike, dip and location of the fault determined by the earthquake and aftershock locations. The resulting slip distribution is shown in Figure 2B and the comparison between observed and calculated motions in Figure 2A. Our results suggest a moment of 1.7 x 10^{25} dyne-cm, generally consistent with seismic estimates. The slip distribution is consistent with the hypocentral location, seismic evidence for unilateral rupture to the north, and correlates remarkably well with the aftershocks; most aftershocks occurring where the main shock caused large stress increases. Using the largest aftershock as an empirical Green's function, we also estimate the relative source time function from which we obtain a rupture duration of 5 sec consistent with the approximately 12-15 km rupture diameter. We are currently investigating the implications of these results for stress changes on nearby faults and at the hypocenter of the Landers main shock.

PUBLICATIONS

Larsen, S., R. Reilinger, H. Neugebauer, and W. Strange, GPS measurements of deformation associated with the 1987 Superstition Hills earthquakes, Imperial Valley, California: Evidence for conjugate faulting, *J. Geophys. Res., 97,* 4885-4902, 1992.

Larsen, S., and R. Reilinger, GPS measurements of strain accumulation across the Imperial Valley, California: 1986-1989, *J. Geophys. Res., 97*, 8865-8876, 1992.

R. Reilinger and S. Larsen, Present-day crustal deformation in the Salton Trough, Southern California, (in) D.E. Smith and D.L. Turcotte (eds), *Contributions of Space Geodesy to Geodynamics: Crustal Dynamics,* American Geophysical Union, Washington, DC, 177-192, 1993.

Bennett, R.A., Y. Li, R. Reilinger, W. Rodi, N. Toksoz, and K. Hudnut, Slip distribution of the 23 April 1992 Joshua Tree earthquake, Southern California from Global Positioning System determination of static ground displacements, *EOS, Trans. Am. Geophys. Union, 74,* 183, 1993.

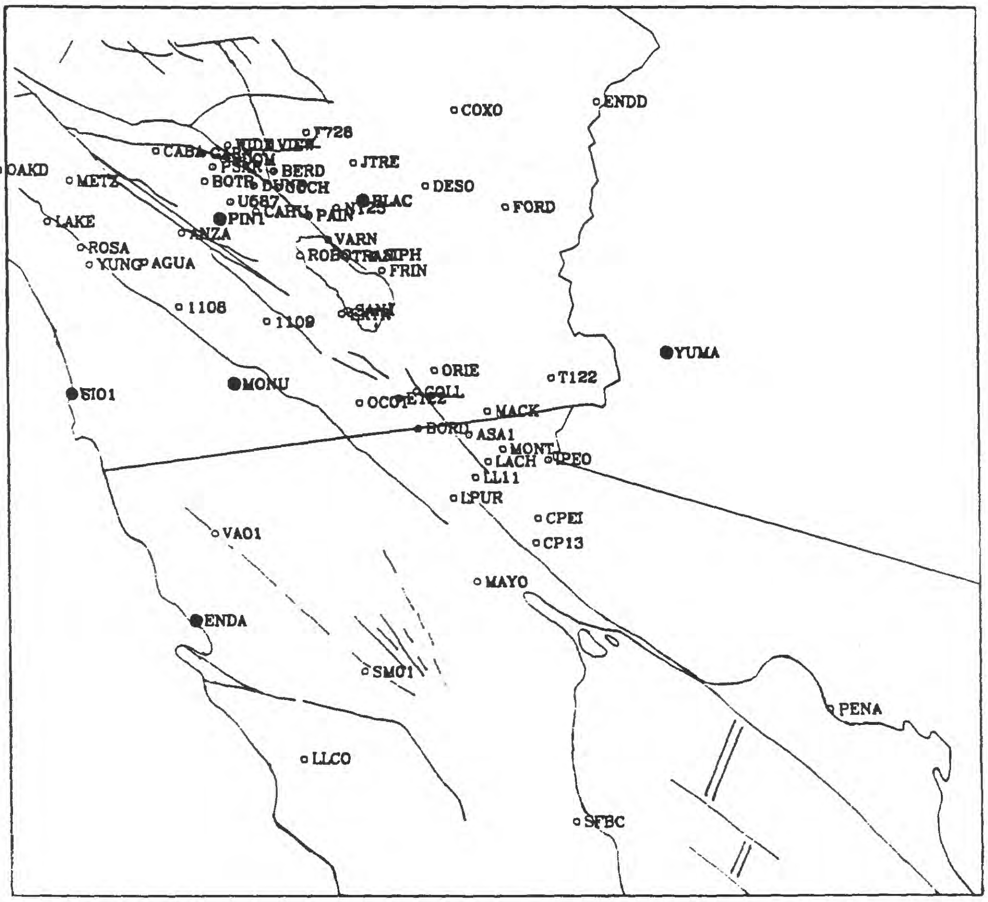

Figure 1. GPS stations observed during the 1993 Salton Trough-Riverside County/Northern Baja California campaign. Large dots show sites occupied throughout the survey.

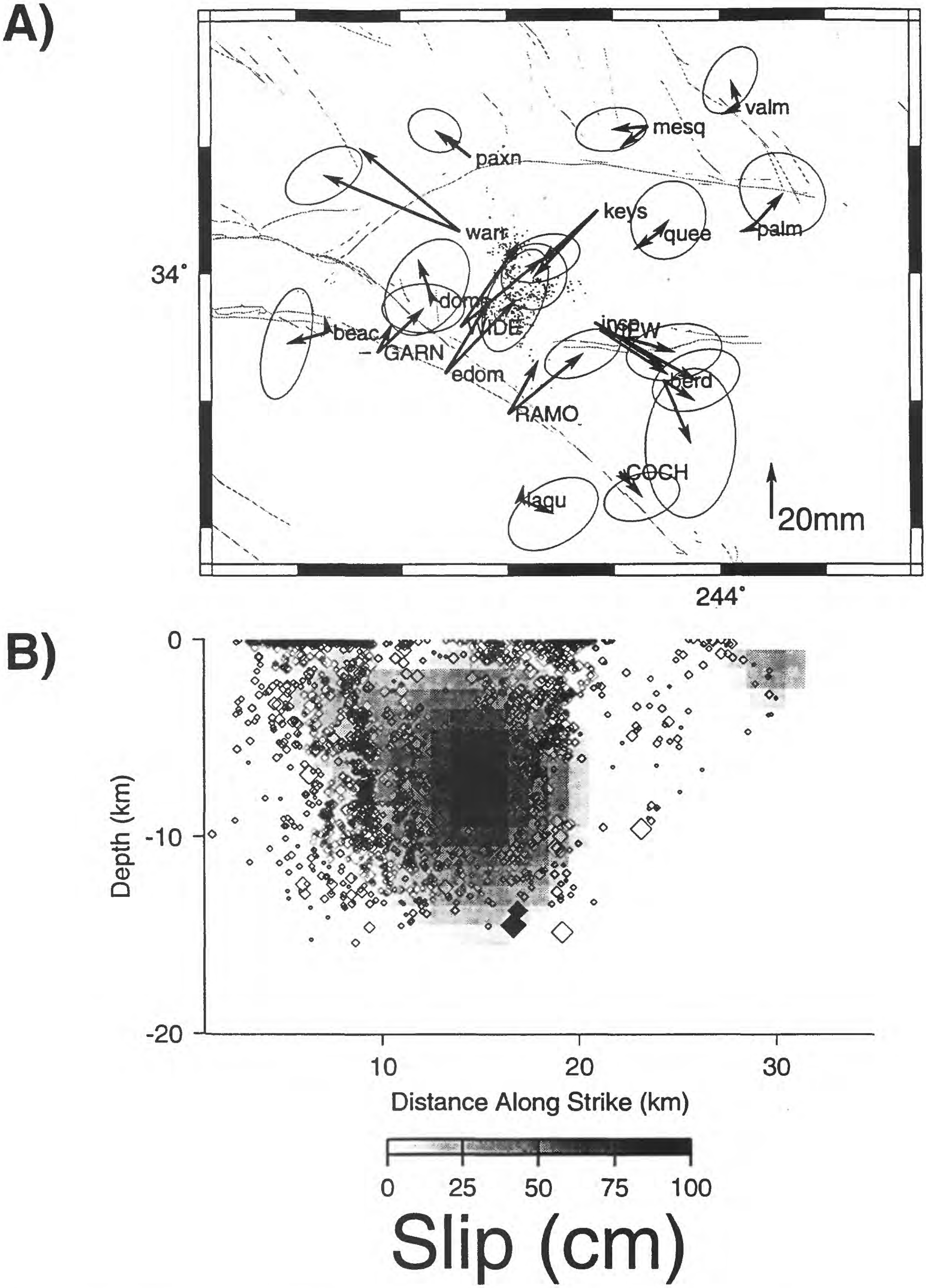

Figure 2. A) Observed (with 1 sigma error ellipses) and modeled static surface deformation for slip distribution shown in Figure 2B. Capitalized sites are GPS, others are EDM. B) Modeled slip distribution for the M=6.1, 23 April 1992 Joshua Tree earthquake. Solid diamonds are main shock and foreshock hypocenters, open diamonds are aftershocks. Earthquake hypocenters courtesy of Egill Hauksson.

FLUID PRESSURE AND EARTHQUAKE GENERATION

9960-10216, 9960-11216, 9960-12216

Evelyn Roeloffs, Eddie G. Quilty
Branch of Earthquake Geology and Geophysics
U.S. Geological Survey
5400 MacArthur Blvd.
Vancouver, WA 98661
Tel. (206)696-7693 Internet:evelynr@io.wr.usgs.gov
Program Element II

Investigations

1. The project carried out real-time monitoring and processing of water level data from two areas of California: Parkfield, and the Mojave Desert. Water level data were processed in real time to remove tidal and barometric fluctuations, and the processed data were automatically screened for anomalous signals.

2. Water level measurements were made in two wells in the east San Francisco Bay area in order to determine whether these wells would be suitable for long-term monitoring.

3. Finite element calculations were made of stresses and pore pressure beneath an axisymmetric reservoir impounded on a porous elastic half space in order to investigate the mechanism of reservoir-induced seismicity.

Results

Parkfield Water Levels

In cooperation with the USGS Water Resources Division, water level data from a network of 11 sites near Parkfield, California, were collected throughout the reporting period. Site locations are shown in Figure 1. Raw water level, barometric pressure, and rainfall data are shown in Figures 2a-d.

Water levels in many wells rose beginning in January due to seasonal recharge.

In the Middle Mountain (MM) well near Parkfield, water level changes associated with fault creep on the San Andreas fault continue to be observed, as they have been at this site since recording there began in 1987 (Roeloffs et al., 1989). No other signals due to fault motion were identified in the Parkfield water level data during FY93.

Mojave Water Levels

Water level data recording was resumed in the Hi Vista and Crystallaire wells. The well locations are shown in Figure 3 and the data are shown in Figure 4. Water level in the Crystallaire well rose beginning in February, presumably in response to seasonal recharge. A smaller water level rise took place in the Hi Vista well beginning in late August. This rise may be due to recharge, which would be expected to occur later in the Hi Vista well because of its greater distance from elevated recharge areas. Data quality from both wells continues to be good.

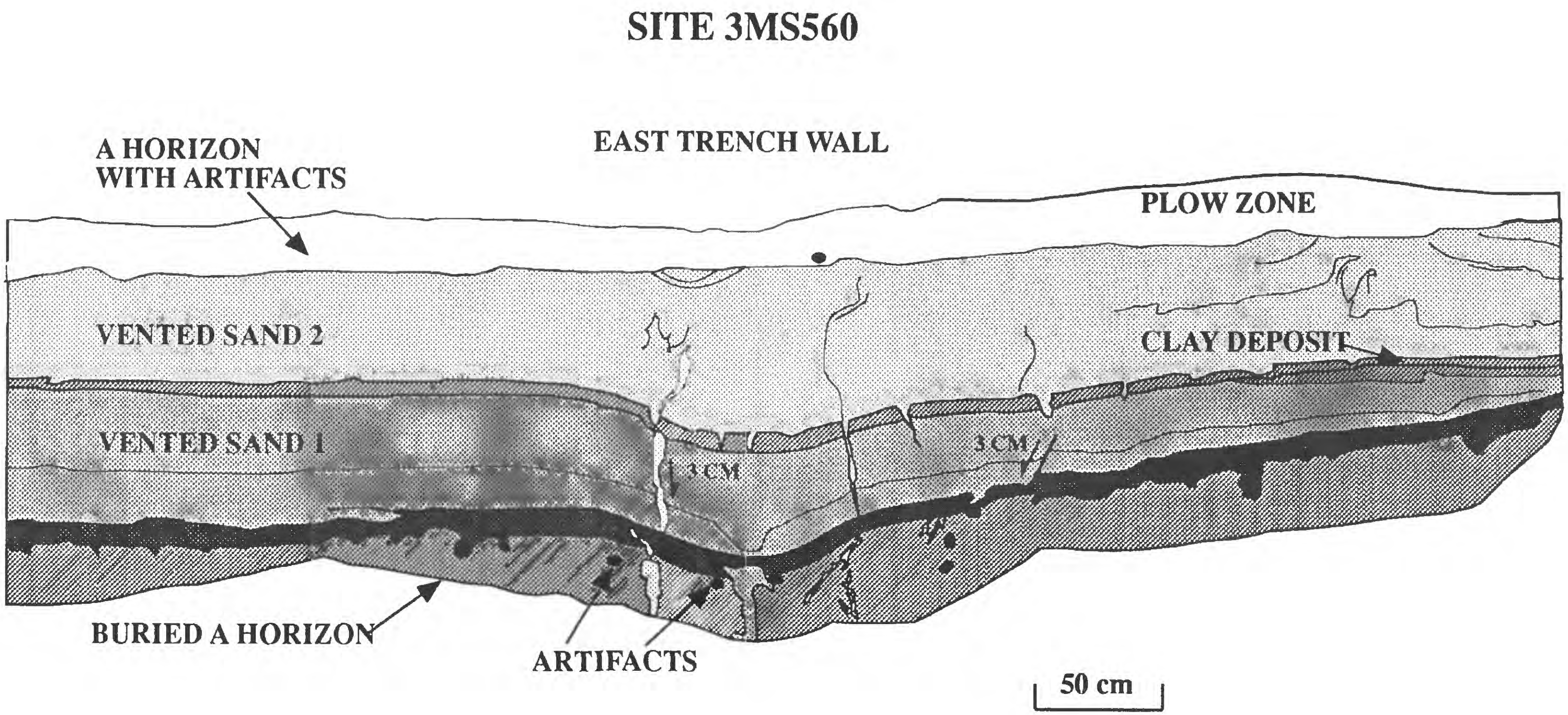

Figure 2: Site 3MS-560, at Eaker Air Force Base, Arkansas (site A in Figure 1). Two sand blows are present, separated by a laterally continuous clay layer. Archeological and carbon-14 data suggest the sands were vented between A.D. 700 and A.D. 1,600. Although the lower vented sand appears more weathered than the upper sand, we have not yet determined if they are significantly separated in age.

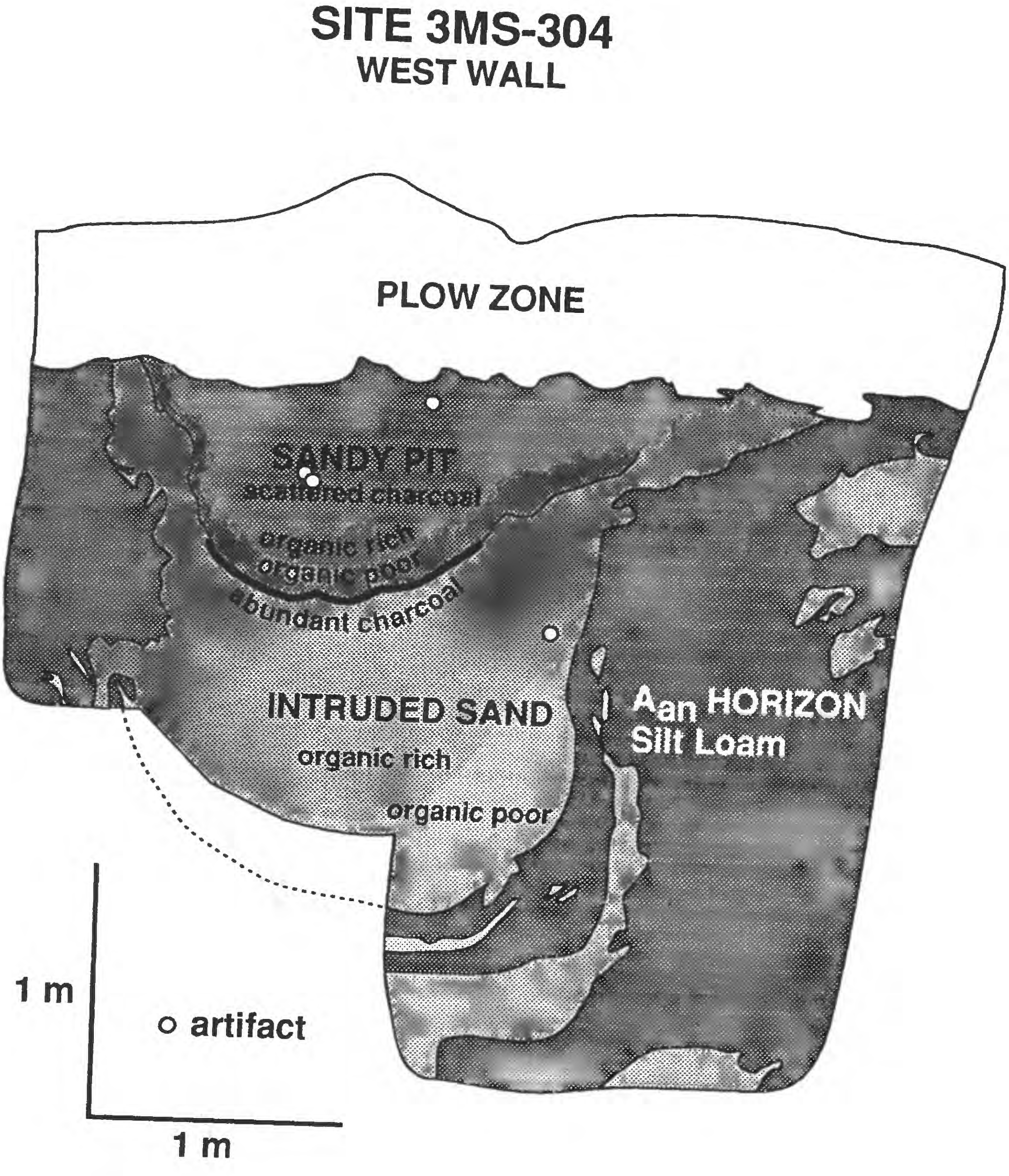

Figure 3: West wall of site 3MS-304, just north of Eaker Air Force Base (site A in Figure 1). Archeological and carbon-14 data suggest the sand was vented between A.D. 700 and A.D. 1,600.

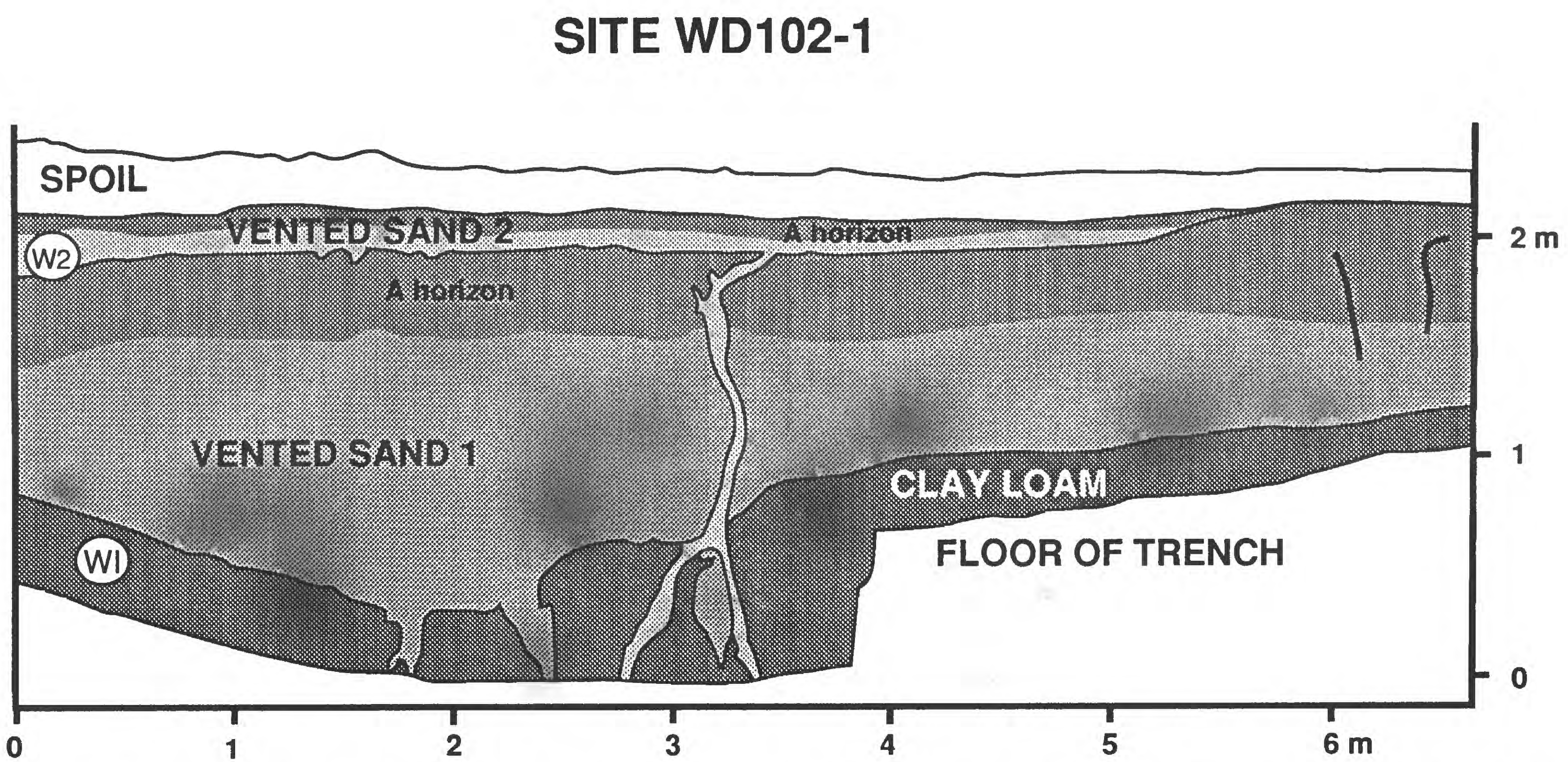

Figure 4: Site WD102-1, about 20 km northeast of New Madrid, Missouri (site C in Figure 1). Although the ages of the two sand blows is unknown, the well-developed A horizon on the lower sand suggests it is perhaps a few perhaps a few thousand years older than the upper one. This site is within 35 km sites D, E, and F, all of which show evidence for two pre-1811 earthquakes within the past 2,000 years.

We have used 3D-DEF to explore two fundamental questions about active deformation in the New Madrid seismic zone (Gomberg and Ellis, in press): 1) what is the underlying driving mechanism causing deformation, and 2) how is the deformation accommodated? A variety of reasonable models were used to calculate 3-dimensional surface displacement fields; we model displacements because all other descriptions of the deformation can be derived from them and because they are directly observable, either from geomorphic or geodetic analyses. We find that these fields cannot distinguish between either a far-field simple or a pure shear strain field, or one that involves a deep shear zone coplanar with the upper crustal faults. Thus, neither geomorphic nor geodetic studies are expected to reveal the ultimate driving mechanism behind the present-day deformation. However, predicted surface displacements provide strong constraints on how strain is accommodated in the central step-over (Figure 1). We find that the topographic data favor the existence of two southwest dipping faults, the geometry of which are inferred from micro-earthquake data. The modeling results indicate that, over the long-term, the central shallow dipping cross-fault acts as a reverse fault but that the steeper cross-fault acts as a normal fault. Horizontal displacement fields for models with and without cross-faults differ significantly, suggesting that geodetic surveys should further constrain the existence and geometry of these inferred faults.

Processing and Interpretation of Shallow Seismic Reflection Data over the Crittenden County Fault Zone — In collaboration with Kaye Shedlock (USGS/BELH), Roy Van-Arsdale (University of Arkansas), Lisa Kanter (Memphis State University) and Gene Luzietti (formerly USGS), shallow seismic reflection data (Mini-SOSIE) were collected in 1990 and 1991 along the Bootheel lineament, Crowley's Ridge, the Crittenden County fault zone, as well as several other targets in northeastern Arkansas, southeastern Missouri, and western Tennessee. As part of this project and for his M.S. thesis, David Nicholas has processed and interpreted the 1991 Crittenden County data (Nicholas et al., 1992; Nicholas, 1993). The Crittenden County fault zone, along the southeastern boundary of the Reelfoot rift, is only 40 km west of Memphis, Tennessee. Although nearly aseismic, earlier studies have documented Cenozoic deformation on this structure. Thus, it is significant for regional seismic-hazard analyses. When combined with data previously collected, we now have imaged 30 km of the fault zone with lines spaced approximately every 4 km. The new lines confirm a maximum of 60-70 m of southeast-side-down displacement of Cretaceous through lower Eocene rocks across a monoclinal flexure that contains some minor high-angle reverse faulting. Most of the deformation occurred between deposition of the upper Paleocene-lower Eocene Flour Island Formation and Quaternary/Eocene unconformity. The youngest clear reflector (Quaternary/Eocene unconformity) has only minor relief that we interpret as due to fluvial erosion, but is not imaged well enough to determine if minor Quaternary faulting is present.. Throw across the fault zone decreases to near zero directly west of Memphis. The northeastern end of the fault zone is not yet defined.

Analysis of Growth Structures and Syntectonic Sedimentation: Implications for Timing, Slip Rates and Future Earthquakes along Buried Thrust Faults, Santa Barbara Channel

1434-92-G-2192
Program Element II.5

John Suppe, Karl Mueller, John Shaw, Enrique Novoa and Maribeth Price
Princeton University
Princeton, NJ 08544
(609) 258-4100
john@wanda.princeton.edu

Investigations Undertaken

Research undertaken in 1993 by the Princeton Structural Geology and Neotectonics Group has focused primarily on hazard analysis of major active blind thrust faults in the Santa Barbara Channel (Shaw, 1993; Shaw and Suppe, 1994; Mueller et al., 1994; Novoa et al., 1994). We have mapped active folds caused by displacement on non-planar blind thrusts along the Oakridge, Pitas Point, Blue Bottle and Dos Cuadras trends and their western extensions in the eastern Santa Barbara Channel. Map patterns derived by analysis of these growth structures (e.g., Suppe et al., 1992; Shaw and Suppe, in press) allow us to: 1) define the lateral distribution of dip slip along blind thrusts; 2) evaluate the recency of faulting and folding along them; 3) calculate their long-term slip rates and potential for future damaging earthquakes and, 4) complete kinematic analyses of their progressive development. Comparison of these growth structures with recent seismicity has also revealed important relations between active folding and microseismicity (Shaw, 1993).

Results

Southeastern Channel Region: Axial surface mapping, balanced cross section construction and kinematic analysis of fault related folds along the Pitas Point and Blue Bottle trends have constrained the location and geometry of a south vergent thrust system contained above the north-dipping Channel Islands Thrust (Figure 1; Shaw, 1993). Analysis of syntectonic (growth) sediments yields a combined Quaternary slip rate of 1.3 mm/yr on the thrust system (Pitas Pt and Montalvo blind thrusts; Shaw, 1993; Shaw and Suppe, in press). The coincidence of active axial surfaces developed above these thrusts with the bathymetric expression of the active folds on the seafloor show that these faults are active and pose a seismic risk to the region. Comparison of the 1984 Santa Barbara Channel earthquake swarm (Henyey and Teng, 1985) with growth structure associated with the Channel Islands thrust show that small scale faulting is a dominant deformation mechanism associated with active fault bend folding (Figure 2; Shaw, 1993). In addition, the Channel Islands thrust is the dominant blind thrust in the Santa Barbara Channel; maximum future earthquakes likely to occur along it may have M = 7.2 to 7.3.

Northeastern Channel Region: We have expanded our work to the northern Channel and Santa Ynez Mountains, because the highest deformation rates exist here. Balanced cross section construction and kinematic analysis of thrust faults and fault related folds along the Dos Cuadras trend were completed using a grid of oil industry seismic reflection profiles and well data. (Figure 1). Results of this work suggest a complex pattern of north and south vergent thrust faulting and fault bend folding, dominated by wedge structures. The timing of development and geometry of these structures determined by application of growth fold theory suggests a link between blind wedge structures beneath the Dos Cuadras trend and the active, north-vergent Red Mountain and Rincon Creek thrusts (Jackson and Yeats, 1982). Other active blind thrust faults mapped in this region include the Santa Ynez thrust (new name - Novoa et al., 1994) , a south vergent, blind thrust displaying approximately 20 km of shortening. Integration of historic

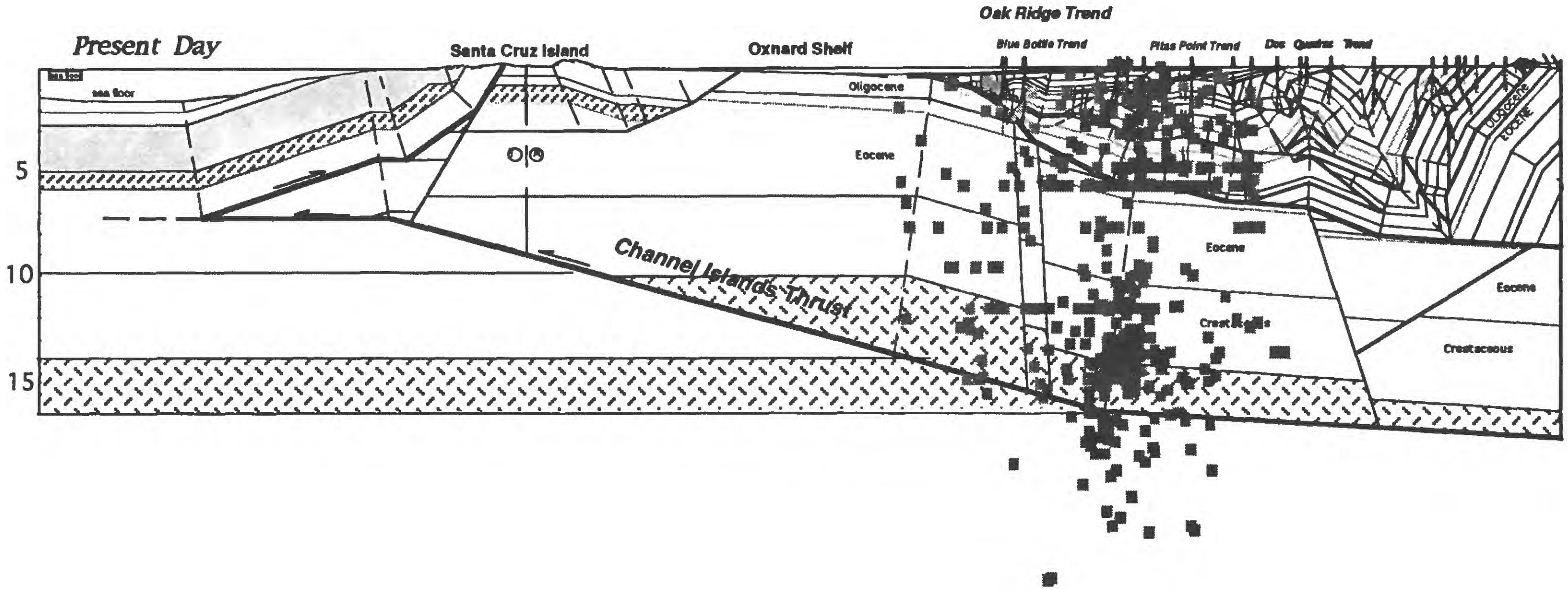

Figure 1. A balanced, retrodeformable cross section across the offshore Oakridge, Blue Bottle, Pitas Pt and Dos Cuadras trends that combines subsurface seismic reflection and well log data (note trace of section on Figure 2). Note the different levels of blind thrust faulting. Section adapted from Shaw, 1993 and Novoa, unpublished mapping.

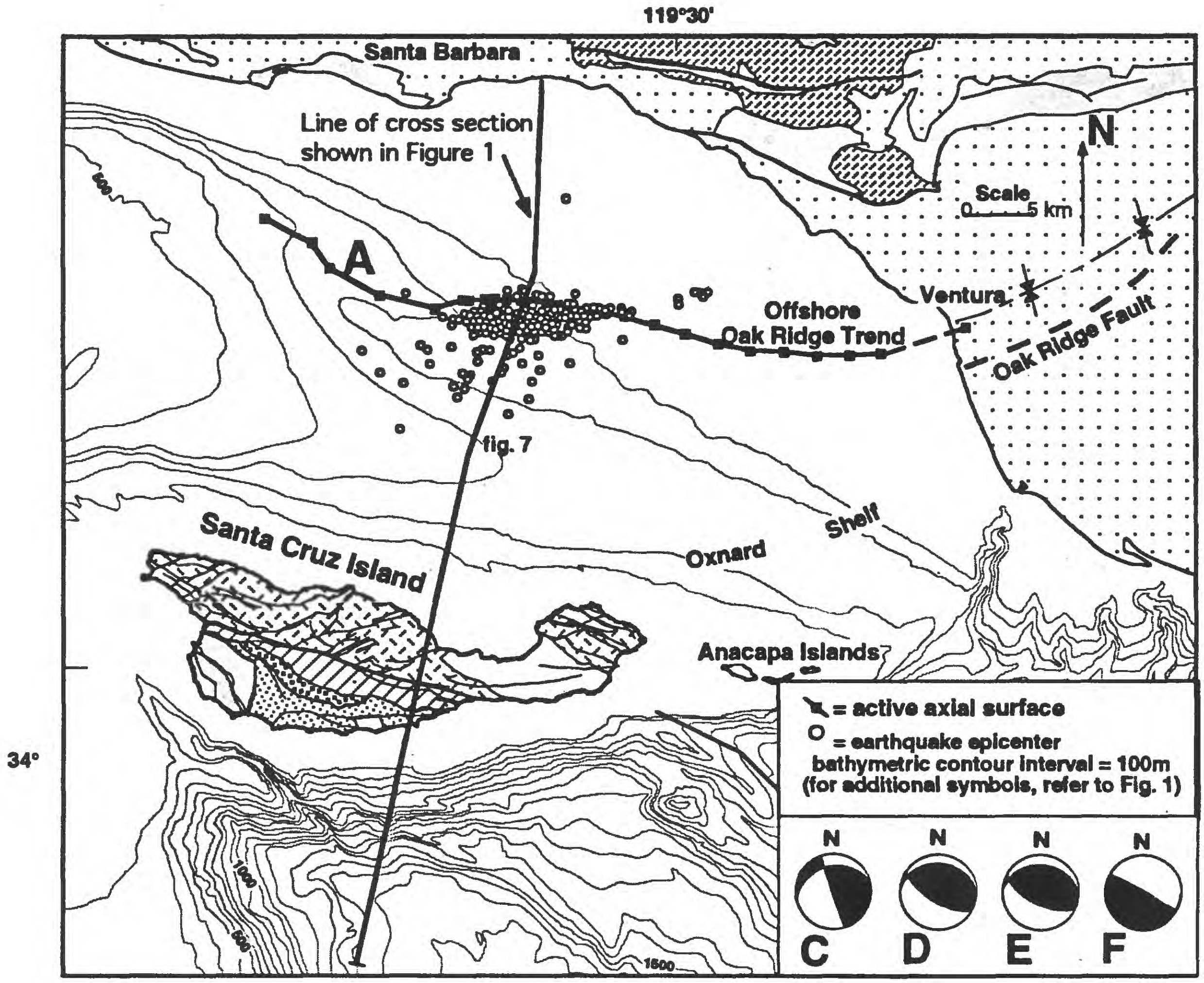

Figure 2: Epicenters from an earthquake swarm in 1984 (Henyey and Teng, 1985) define the active axial surface (A) of the Offshore Oak Ridge trend. Single event (C, D) and composite (E, F) focal mechanism solutions from the 1984 seismicity show gentle north dipping (C, D, E) and horizontal (F) preferred nodal planes (Henyey and Teng, 1985) consistent with folding through the active axial surfaces by bedding parallel slip. Note the location of the cross section line shown as Figure 1.

seismicity data indicates that the 1978 Ml 5.1 Santa Barbara earthquake occurred along a ramp segment of the Santa Ynez blind thrust.

Western Santa Barbara Channel: Preliminary mapping in the Western Santa Barbara Channel using 135 newly acquired seismic reflection profiles indicates that the Channel Islands Thrust (Shaw, 1993; Shaw et.al., 1994; Mueller, et.al., 1994) extends westward to at least midway between the longitudes of the city of Santa Barbara and Point Conception. Additional mapping of axial surfaces in the western Santa Barbara Channel has defined the location of an active, structurally higher, south vergent thrust fault . This fault extends completely across the western channel to Point Conception and may be the westward continuation of a thrust fault located beneath the Blue Bottle trend to the east (Shaw, 1992; Shaw and Suppe, 1994). In addition a dip panel associated with the preexisting Channel Islands Thrust limits the updip extent of the ramp developed in the active, structurally overlying thrust, effectively controlling the maximum size of future earthquakes along it.

Arc/Info data base: We have input shot point locations of over 220 seismic reflection profiles from 6 separate industry surveys located throughout the Santa Barbara Channel into the Arc/Info format. This, combined with the development of a spreadsheet database has allowed us to accurately record the results of out axial surface mapping of fault related folds. We have also downloaded the entire USGS/CIT data base of instrumented earthquake locations and magnitudes in this region for comparison with the mapped location of active structures. In the upcoming year we will continue to integrate our ongoing mapping with recent seismicity, high-resolution bathymetry and newly acquired seismic reflection data (Sparker and Uniboom).

Future work

Upcoming work will focus on further defining the rates of blind thrust faulting and fault related folding in the Santa Barbara Channel. We are currently extending our existing balanced cross sections in the western Channel region onto the northern shelf and onland to evaluate the kinematic evolution and timing of crustal shortening across the entire Western Transverse Ranges . We will also be conducting a high resolution seismic reflection survey (Sparker and Uni-Boom) this winter in the north-central and western Santa Barbara Channel to evaluate the likelihood of determining Late Quaternary coseismic folding events. We will focus acquisition along active axial surfaces associated with the Channel Islands thrust in an attempt to constrain the record of late Quaternary blind thrusting along it.. In addition, we will be continuing to map growth structure associated with active blind thrust faults on 135 newly acquired seismic reflection profiles located between Santa Barbara and Pt. Conception.

References

Henyey, T., and Teng, T., 1985, Seismic studies of the Dos Cuadras and Beta offshore oil fields, Southern California OCS, *A final technical report submitted to the Dept. of the Interior, Mineral Management Service*, by the Center for Earth Sciences, Univ. Southern California, California.

Jackson, P., and Yeats,. R., 1982, Structural evolution of Carpinteria Basin, western Transverse Ranges, California: *American Association of Petroleum Geologists Bulletin*, V. 66, p 805-829.

Suppe, J., Chou G.T. and Hook, S.C., 1992, Rates of folding and faulting determined from growth strata, in: *Thrust Tectonics*, K.R. McMclay ed., Unwin Hyaman, Publisher, pp. 105-121.

Stanley, W.D., Finn, Carol, and Plesha, J.L., 1987, Tectonics and conductivity structures in the southern Washington Cascades: Journal of Geophysical Research, v. 92, p. 10,179-10,193.

Stanley, W.D., Mooney, W.D., and Fuis, G.S., 1990, Deep crustal structure of the Cascade Range and surrounding regions from seismic refraction and magnetotelluric data: Journal of Geophysical Research, v. 95, p. 19,419-19,438.

Stanley, W.D., Gwilliam, W.J., Latham, Gary, and Westhusing, Keith, 1992, The southern Washington Cascades conductor—a previously unrecognized thick sedimentary sequence?: American Association of Petroleum Geologists Bulletin, v. 76, p. 1569–1585.

Swanson, D.A., 1989, Geologic maps of the French Butte and Greenhorn Buttes quadrangles, Washington: U.S. Geological Survey Open-File Report 89-309, scale 1:24,000, 25 p.

____, 1990, Trends of middle Tertiary dikes in and north of the Dark Divide Roadless area, southern Washington Cascades: Eos, Transactions of the American Geophysical Union, v. 71, p. 1144.

____, 1991, Geologic map of the Tower Rock quadrangle, southern Cascade Range, Washington: U.S. Geological Survey Open-File Report 91-314, scale 1:24,000, 26 p.

____, 1992, Geologic map of the McCoy Peak quadrangle, southern Cascade Range, Washington: U.S. Geological Survey Open-File Report 92-336, 36 p., map scale 1:24,000.

____ 1993, Geologic map of the Blue Lake quadrangle, southern Cascade Range, Washington: U.S. Geological Survey Open-File Report 93–297, scale 1:24,000, 34 p.

____1994, Geologic map of the East Canyon Ridge quadrangle, southern Cascade Range, Washington: U.S. Geological Survey Open-File Report (in preparation).

Weaver, C.S., and Malone, S.D., 1987, Overview of the tectonic setting and recent studies of eruptions of Mount St. Helens, Washington: Journal of Geophysical Research, v. 92, p. 10,149-10,154.

Weaver, C.S., and Smith S.W., 1983, Regional tectonic and earthquake hazard implications of a crustal fault zone in southwestern Washington: Journal of Geophysical Research, v. 88, p. 10,371-10,383.

Winters, W.J., 1984, Stratigraphy and sedimentology of Paleogene arkosic and volcaniclastic strata, Johnson Creek-Chambers Creek area, southern Cascade Range, Washington: Portland, Oreg., Portland State University, M.S. thesis, 162 p.

Zollweg, J.E., and Crosson, R.S., 1981, The Goat Rocks Wilderness, Washington, earthquake of 28 May 1981: Eos, Transactions of the American Geophysical Union, v. 62, p. 966.

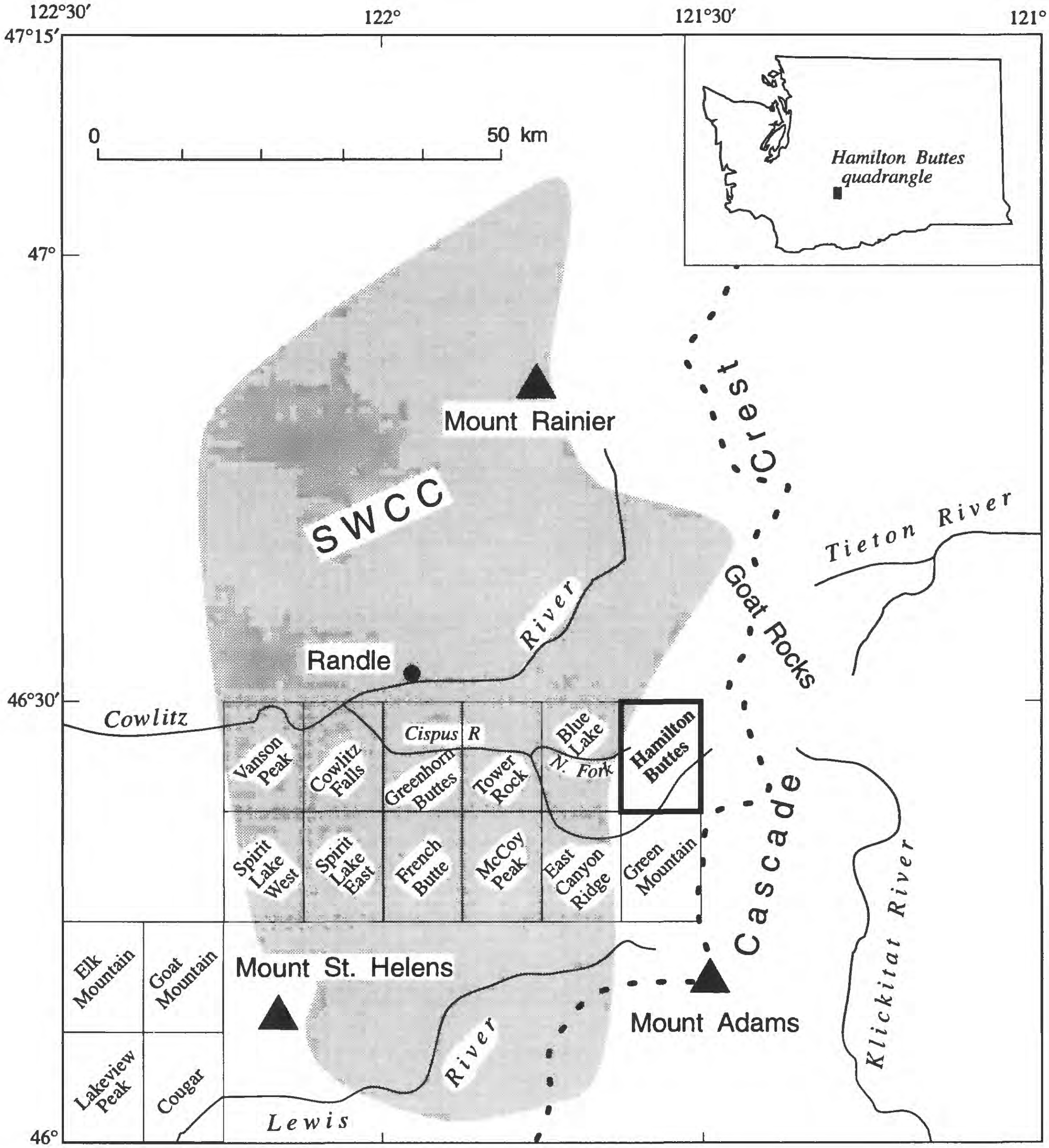

Figure 1. Map showing locations of Hamilton Buttes quadrangle and other quadrangles being mapped in the southern Washington Cascades relative to the Southern Washington Cascades Conductor (SWCC). The quadrangles west of longitude 122° are being mapped by Russ Evarts and Roger Ashley (U.S. Geological Survey, Menlo Park), and those east of longitude 122° by me.

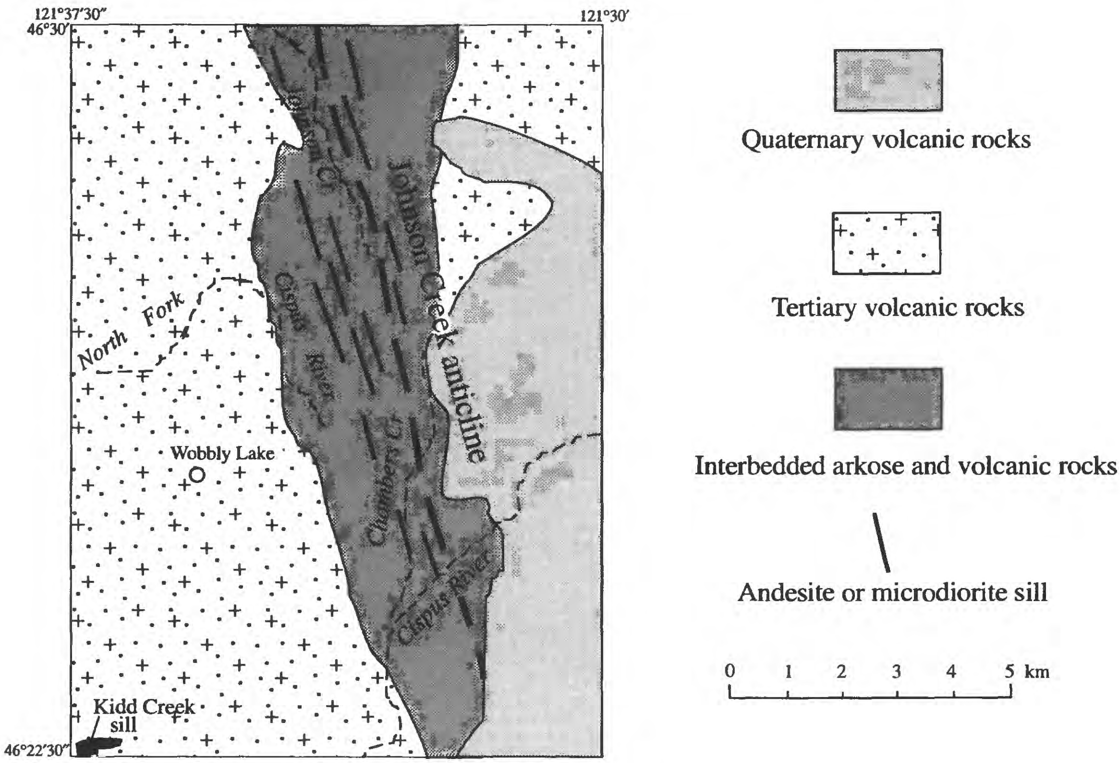

Figure 2. Generalized geologic map of the Hamilton Buttes quadrangle, showing relations among the Tertiary volcanic and volcaniclastic rocks, arkose, and Quaternary basalt and andesite. Note concentration of sills in the interlayered, well-bedded section of volcanic sandstone, mudstone, and micaceous arkose in the core of the Johnson Creek anticline. Note also the small sill of hornblende microdiorite of the Kidd Creek intrusive suite in southwest corner of quadrangle, the farthest northwest occurrence of the Kidd Creek and almost exactly along the eastern edge of the SWCC (fig. 1) as mapped by Stanley and others (1987).

Intermediate and Long-term Seismic Precursors to Large Earthquakes in California

Lynn R. Sykes
Program Element II

Lamont-Doherty Earth Observatory of Columbia University
Palisades, New York 10964
(914) 365-8880
sykes@ldeo.columbia.edu

Objective:

For the past several years we have been studying premonitory changes before large earthquakes along the San Andreas fault system in California. Moderate earthquakes prior to the 1868 Hayward, 1906 San Francisco, and 1989 Loma Prieta earthquakes in central California, most or all of which are outside the ensuing rupture zone, show a pattern of accelerating moment release. In light of this precursory change in seismicity in a region of complex fault interaction, we have begun re-examining seismicity of moderate-to-large earthquakes in southern California to establish if such changes also occur before large earthquakes on the San Andreas system in southern California. We have also examined changes in the occurrence of moderate earthquakes in the San Francisco Bay region in the context of stress changes generated by the occurrence of the large earthquakes of 1868 and 1989, and the great 1906 earthquake. We find that $M \geq 5.5$ earthquakes in the few tens of years before 1906 and 1989 preferentially occur in regions expected to be more highly stressed before those earthquakes, and the moderate earthquakes after 1906 and 1989 occur in regions moved towards failure by coseismic stress changes.

Results:

The rate of seismic activity of moderate-size ($M \geq 5.5$) earthquakes in the San Francisco (SFB) region has varied considerably during the past 150 years. As measured by the rate of seismic moment release, seismic activity in the SFB region is observed to accelerate prior to $M \geq 7.0$ earthquakes in 1868, 1906, and 1989, and then decelerate following them. We examine these seismicity changes in the context of stress changes in the SFB region by modeling the $M \geq 7.0$ earthquakes as dislocations in an elastic

Thus, data recorded by this network will fill an information gap left by standard strong-motion accelerographs installed in Memphis many years ago which have never been triggered. Useful information on Memphis ground motion will come from the frequent events of nearby seismic zones, many of which drive local high-gain seismographs off-scale without triggering the strong motion stations. Project instrumentation is designed to cover the dynamic range between these two existing types of seismographs. We expect to fill this gap with earthquake data directly relevant to seismic hazards of the urban area.

Current Investigations

Meanwhile, we have analysed seismograms and modeled the surface wave dispersion of the magnitude 4.6 Risco, Missouri earthquake of May 3, 1991 (Figures 2 and 3). Being the largest event ever recorded locally on broad-band and long-period instruments, the Risco earthquake produced low-frequency Love waves lasting for 6 minutes at Memphis. A manuscript by Dorman and Smalley is in review. The results show the effect of a shallow waveguide on three low modes of surface waves (Figure 4), and in particular the critical role of the shallowest unconsolidated deltaic sediments in determining the amplitude and frequency characteristics of these seismic arrivals. Similar effects should apply to higher mode (overtone) propagation to be investigated next.

Shallow refinement of the model waveguide (Figure 5) which adequately represents the characteristic low-frequency dispersion is expected in turn to explain with fair accuracy the higher-frequency features of the complex and strong Risco S-wave group. The Risco S-wave drove regional high-gain seismographs off-scale, but did not trigger standard strong-motion accelerographs in Memphis. However, S was well-recorded by strong-motion stations at shorter epicentral distances. These data are to be analysed and modeled in a thesis project at CERI. We are therefore approaching an understanding of the propagation effects which will facilitate deterministic waveform modeling of the elastic response to hypothetical New Madrid earthquakes.

Publication

James Dorman and Robert Smalley, *Low-frequency seismic surface waves in the Upper Mississippi embayment,* in review, Seismological Research Letters.

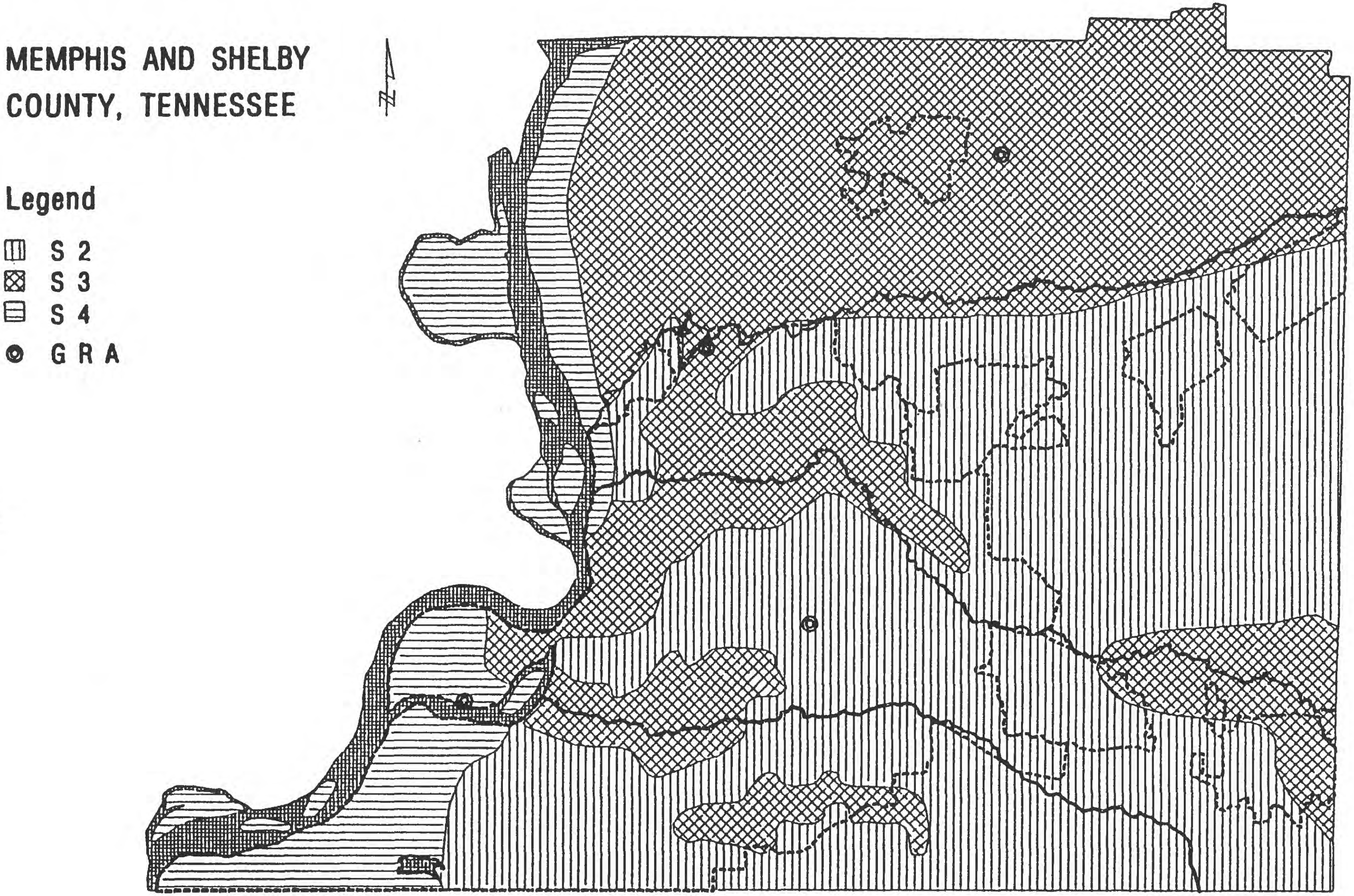

Figure 1. Sites for four high-dynamic-range seismograph stations in Memphis-Shelby County. Engineering soil classifications S2, S3, and S4 denote areas of moderate to poor soil conditions with respect to potential earthquake damage.

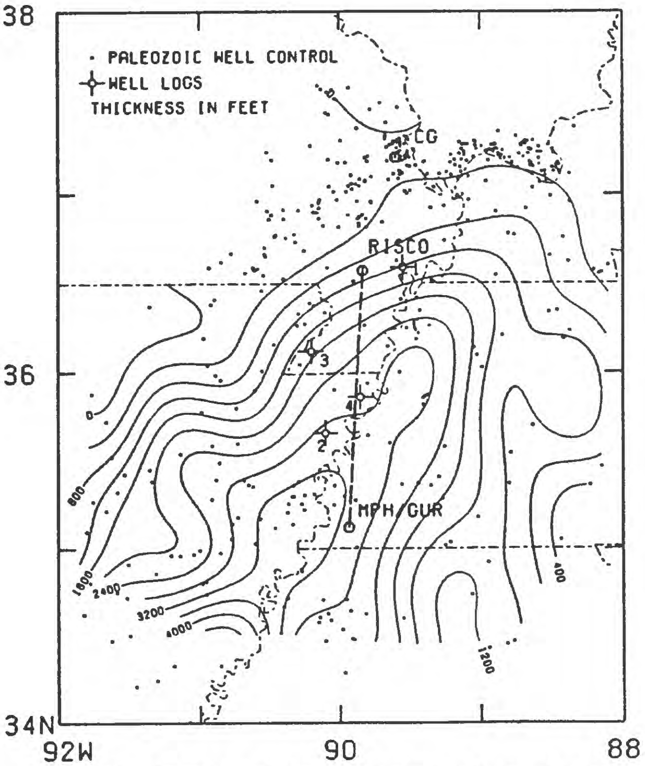

Figure 2. Epicenter of the magnitude 4.6 Risco, Missouri earthquake of May 4, 1991, and 159 km path to the broad-band and long-period stations at CERI. Isopach contours give the thickness (in feet) of the low-velocity Cretaceous-Tertiary-Quaternary embayment clastics layer.

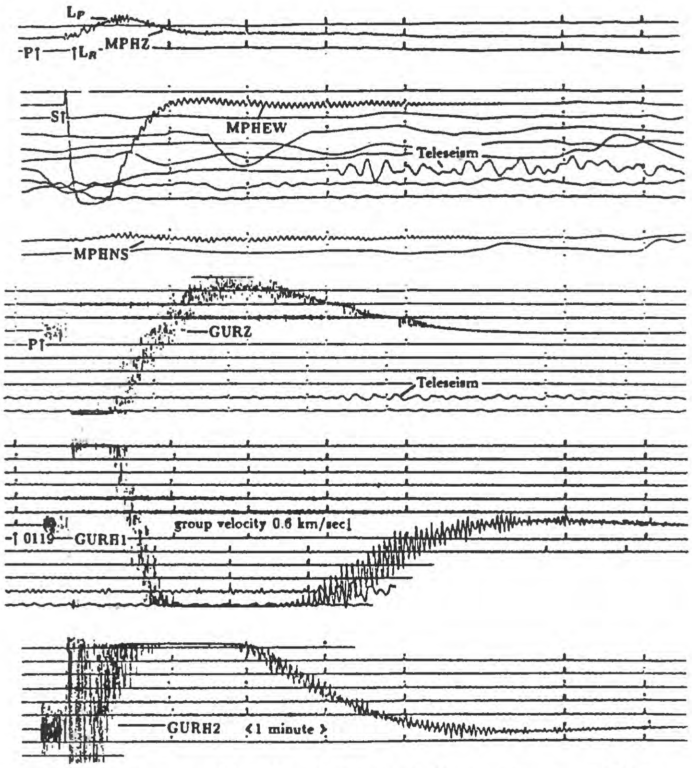

Figure 3. Broad-band and long-period seismograms of the Risco earthquake recorded at CERI. As at other high-gain seismograph stations, the S-wave drives the traces off-scale. The long Love wave train, well-recorded on the LPEW and GURH1 components, lasts for about 6 minutes. For larger magnitude earthquakes, the strength of the low-frequency Love waves will increase relative to the strength of S.

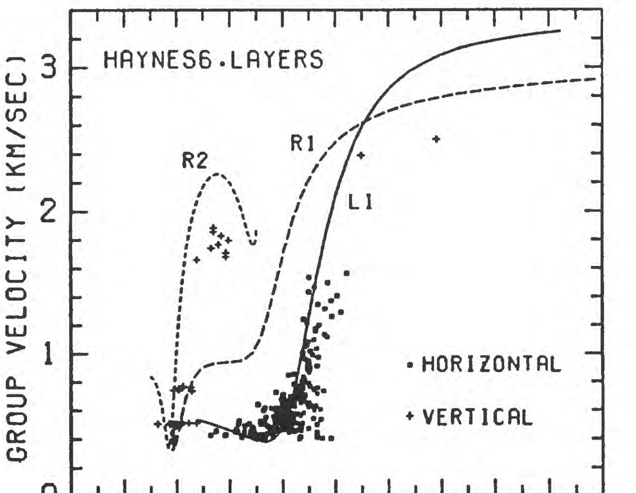

Figure 4. Points represent group velocity dispersion analysis of the low-frequency wave groups of Figure 3. The model curves (solid lines) which fit the Risco wave groups reasonably well govern the frequency and travel time relationships of waves traversing paths within the New Madrid seismic zone.

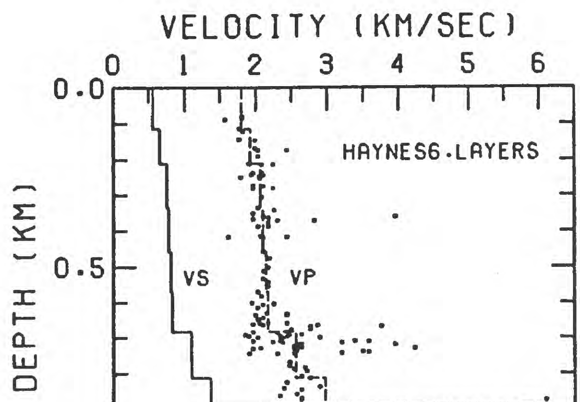

Figure 5. Compressional and shear velocity model for the embayment path of Figure 1. This layered velocity structure fits the sonic log velocities at the Haynes well and also fits the characteristic surface wave dispersion of Figure 4. These physical properties define the hazard of amplified low-frequency shaking from a regional earthquake.

Analysis of Digital Waveforms in the Northeastern U.S. for Source Depth and Strong Ground Motion Information

John E. Ebel
Weston Observatory
Department of Geology and Geophysics
Boston College
Weston, MA 02193
(617) 552-8300
EBEL@BCVMS.BC.EDU

Program Element III.2

Investigations

The purpose of this research is to analyze the waveforms of locally recorded earthquakes in the northeastern U.S. to better determine the source depth and the propagation of strong ground motions across the region. The investigation involves three tasks: (1) searching for free-surface reflections in the local waveforms to help constrain the earthquake focal depths, (2) studying the amplitudes of P and S phases at about 100 km distance from the sources to see if any amplification due to post-critical Moho reflections may be present, and (3) studying the distance attenuation of the spectral components of the ground motions in the region with application to spectral seismic hazard maps. This research uses data from the New England Seismic Network operated by Weston Observatory of Boston College.

Data Analysis

Thus far the primary effort has been put forth toward the first two tasks. These tasks are related in that some identification of post-critical Moho reflections is necessary in the local seismograms before the free-surface reflections can be sought (i.e., one does not want to misidentify a Moho reflection as a free surface reflection). The method of analysis has been to follow several processing steps on the data from several earthquakes. The first is to assemble all of the available waveforms in the distance range from 50 km to about 300 km from the events. For each waveform beyond 90 km an estimate is made of the expected arrival time of the PmP phase, and the record is then examined to see if the PmP phase can be identified. Next the individual stations are put on a single plot and aligned along the first P wave arrivals. This plot is then investigated to see if any free-surface reflections can be identified. Finally, these aligned waveforms are processed by having their absolute values taken (to ensure

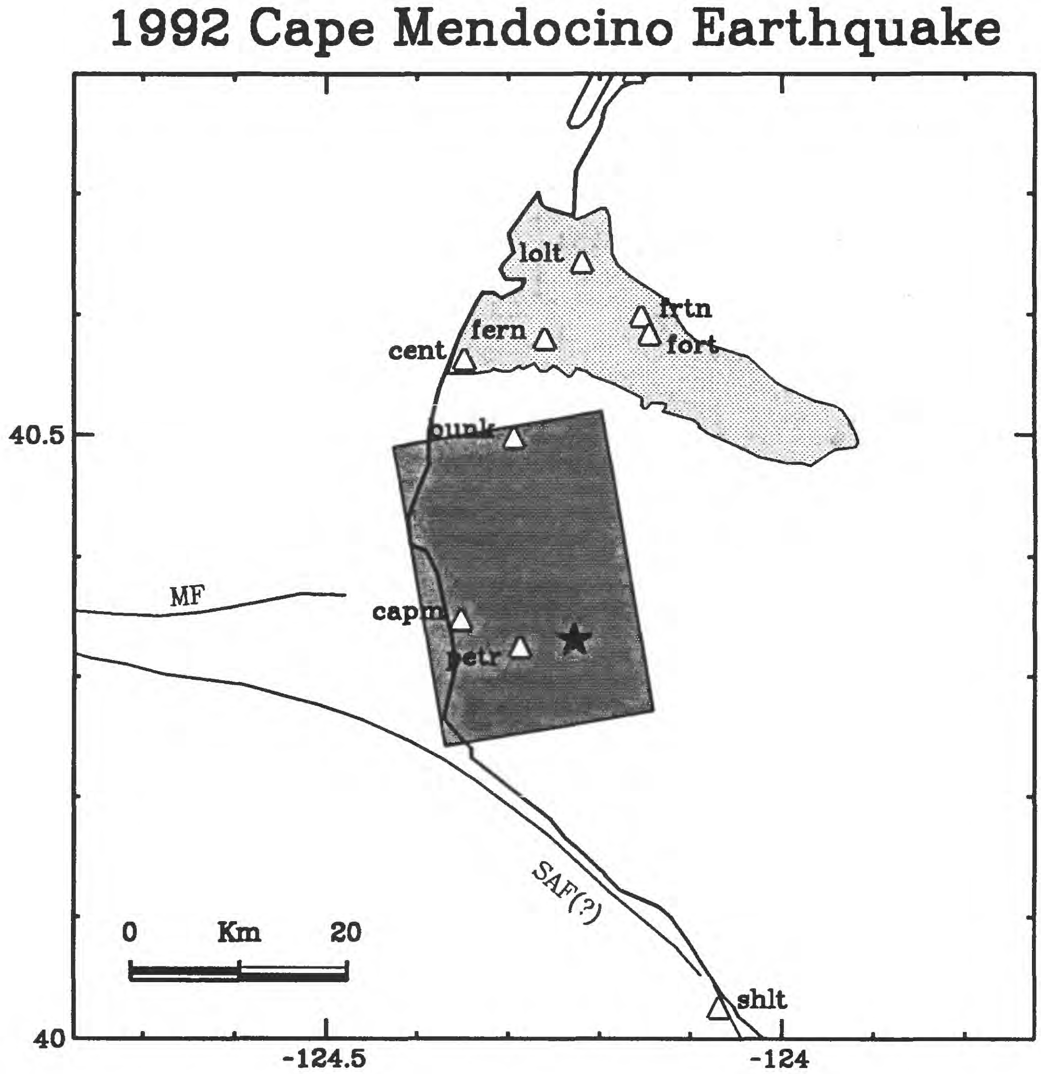

Figure 1. Map of the epicentral region of the 1992 Cape Mendocino earthquake. The star indicates the epicenter and the dark shaded region is the assumed rupture plane as inferred from aftershock distribution and geodetic modeling (Oppenheimer et al., 1993). The light shaded region to the north of the fault plane indicates the location of the Eel River basin.

Hartzell, S. H. and T. H. Heaton (1983). Inversion of strong ground motion and teleseismic waveform data for the fault rupture history of the 1979 Imperial Valley, California earthquake, Bull. Seis. Soc. Am., 73, 1553-1583.

Saikia, C. K. (1992). Characteristics of simulated ground motions in the central United States, Final report to U.S. Geological Survey under contract - 14-08-0001-G1994.

Somerville, P. G., J. P. McLaren, L.V. LeFevre, R. W. Burger and D. V. Helmberger (1987). Comparison of source scaling relations of eastern and western North American earthquake, Bull. Seis. Soc. Am., 77, 322-346.

Somerville, P. G. and N. A. Abrahamson (1991) . Characterizing earthquake slip models for the prediction of the strong ground motion, EOS, no 72, p341.

Somerville, P. G., M. K.Sen and B. Cohee (1991). Simulation of strong ground motions recorded during the 1985 Michoacan, Mexico, and Valparasio, Chile earthquakes, Bull. Seis. Soc. Am., 81, 1-27.

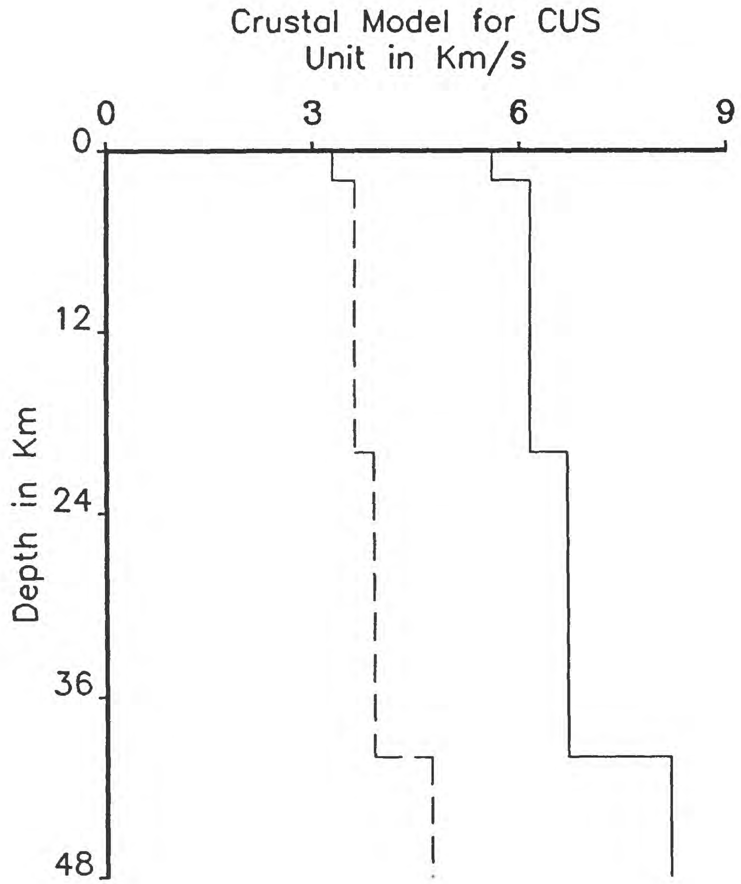

Figure - 1

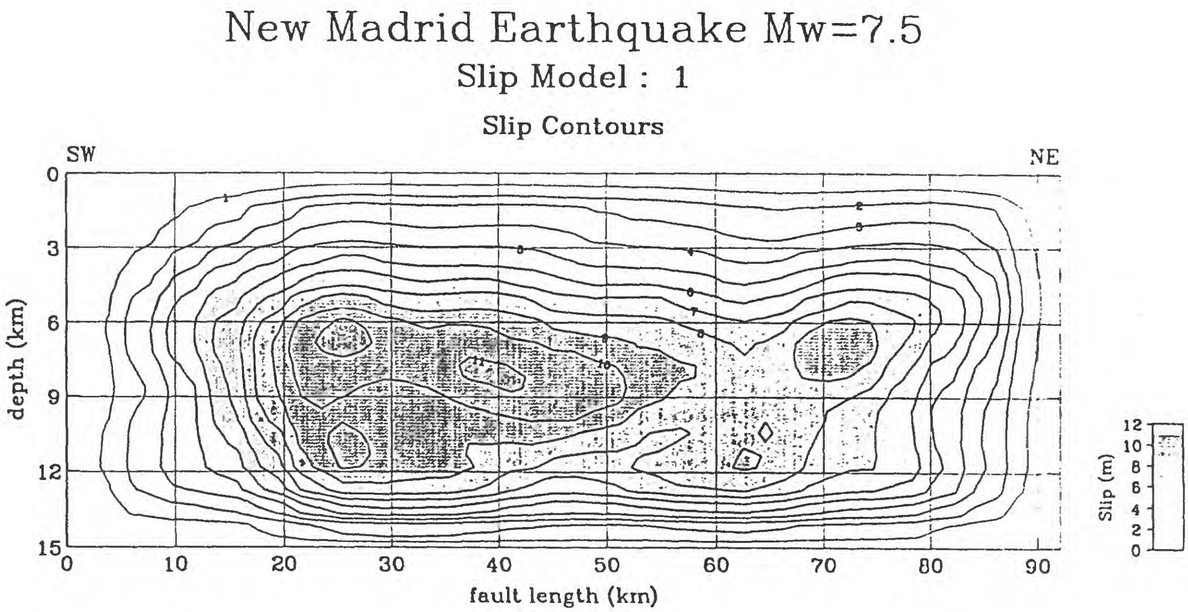

Figure 2. Slip Models

New Madrid Earthquake Mw=7.5

Slip Model : 2

Slip Contours

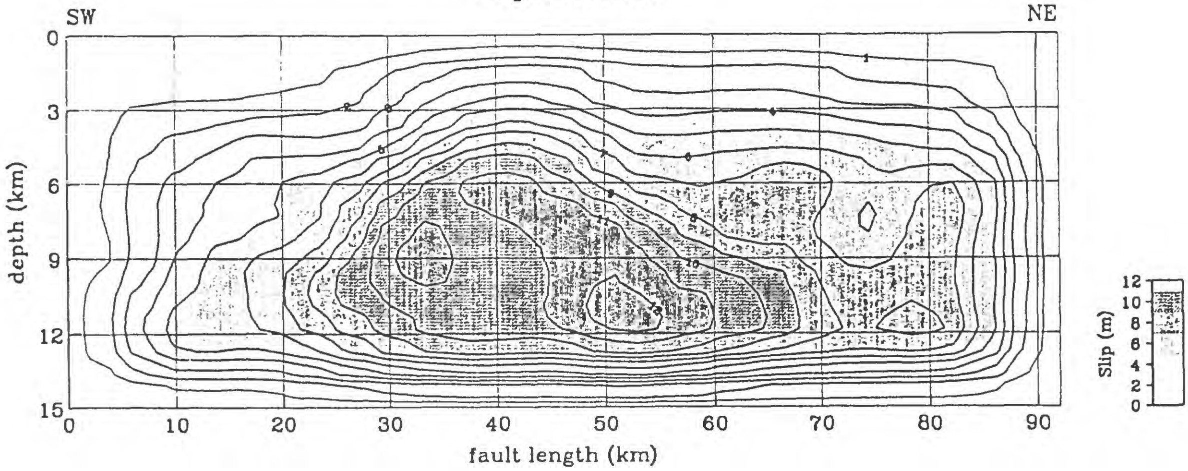

Slip Model : 3

Slip Contours

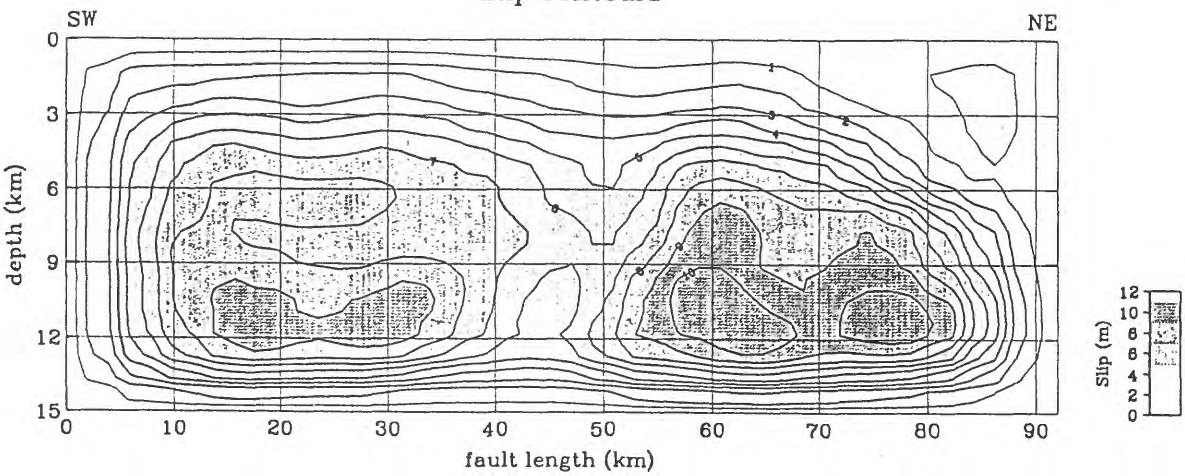

Slip Model : 4

Slip Contours

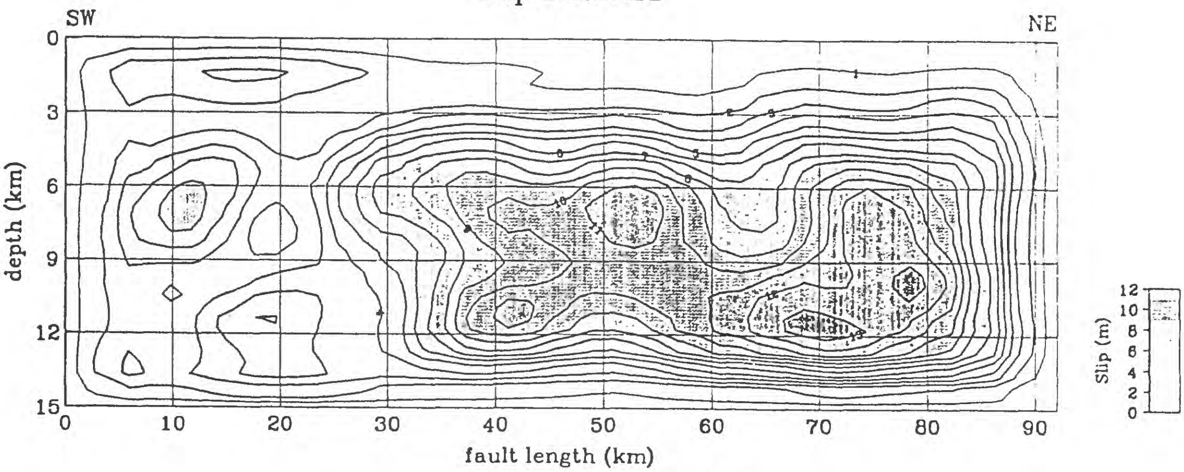

Figure 2(Contd).

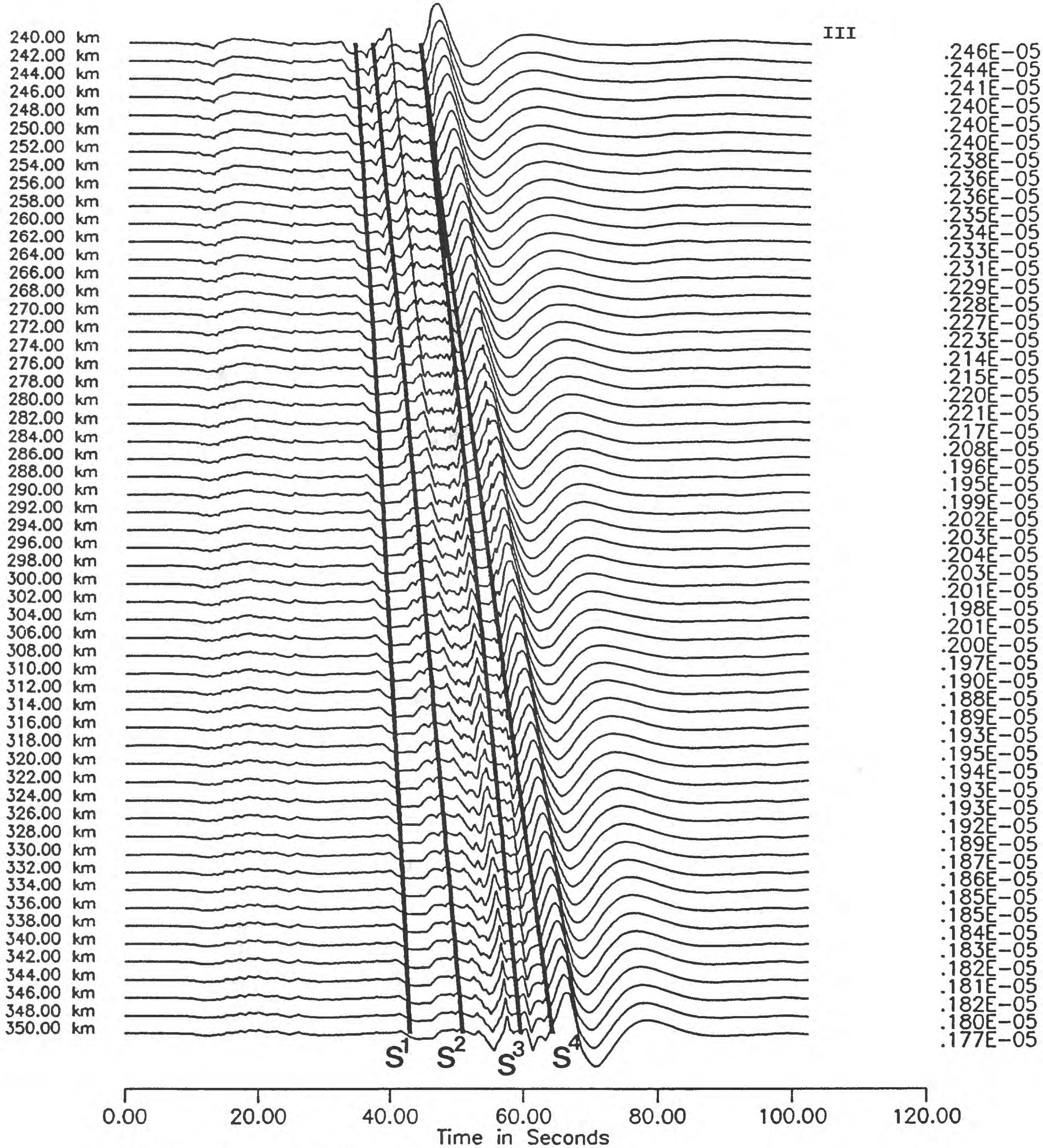

Curve – 1: V_r=3.75km/s 4.04km/s

Curve – 2: V_r=3.60km/s 3.70km/s

Curve – 3: V_r=3.25km/s 3.39km/s

Curve – 4: V_r=3.25km/s 3.24km/s

Figure 3

EAST GREAT SALT LAKE BASIN MODEL

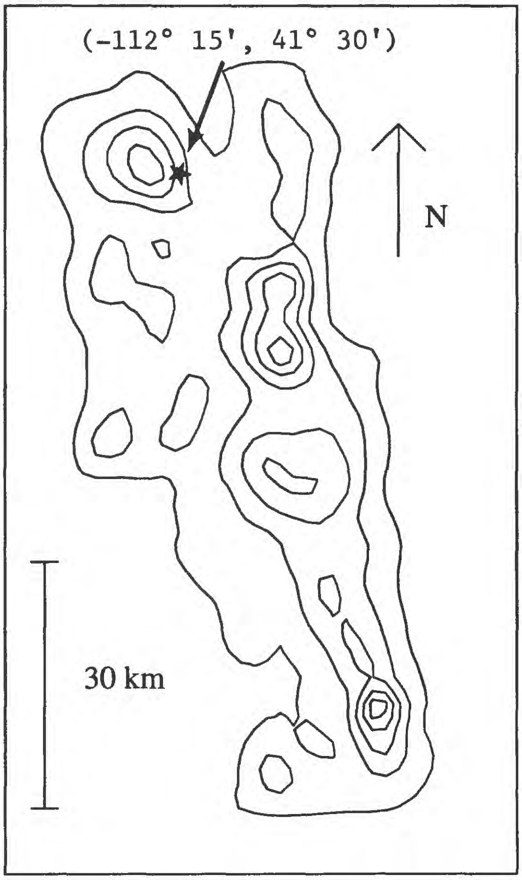

Figure 1. Depth to bedrock model of East Salt Lake Basin obtained from 3-D gravity inversion (McNeil, 1991). Contour interval is 1000 m.

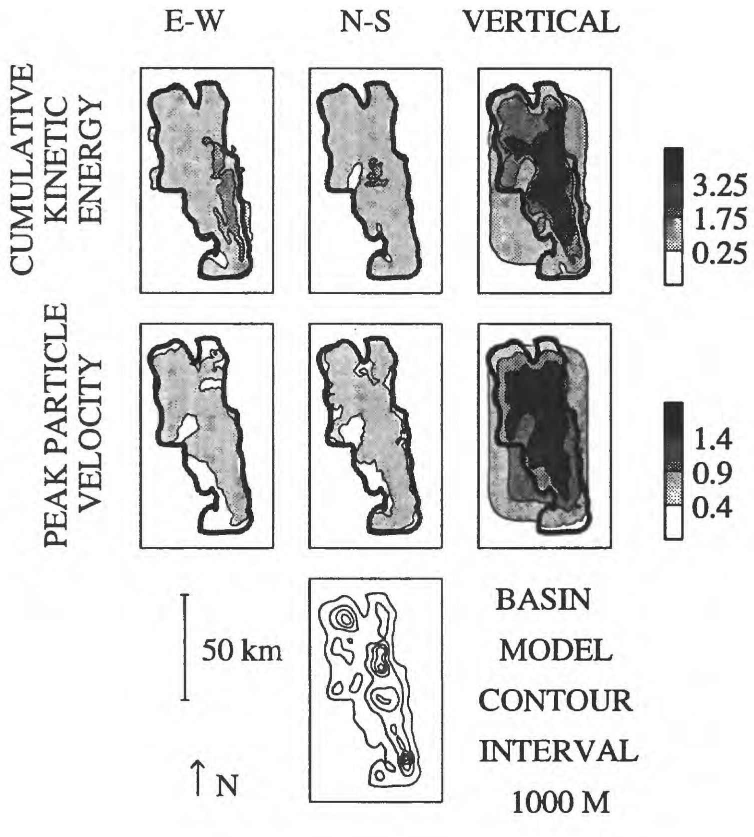

Figure 2 Maps of peak particle velocity ratios and accumulated kinetic energy ratios in the East Great Salt Lake Basin on the E-W, N-S and vertical component seismograms for a simulation with a vertically incident plane P wave. The values calculated for the vertical component at a rock site are used as reference. Contours shorter than approximately 16 km are considered beyond the resolution of the model and have been discarded from the plot. The contour map at the bottom shows the depth to the bedrock interface at 1000 m contour interval; the shallowest contour at 320 m is superimposed on the ground motion plots (thick line) for reference. The simulation parameters are listed in Table 1.